

## Osteoporosis: Limitations of current antiresorptive treatments

Jürg Andreas Gasser, PhD

*Novartis Institutes for BioMedical Research, Basel, Switzerland*

**Status quo and medical need:** The introduction of novel therapeutic options has resulted in substantial progress in the treatment of osteoporosis-related vertebral fractures. Various bisphosphonates, the bone anabolic N-terminal hormone fragment of parathyroid hormone (PTH, Forsteo<sup>®</sup>) and the more recently introduced RANKL-inhibitor Denosumab (Prolia<sup>®</sup>) have all been demonstrated to reduce the risk for vertebral fractures by 50-70%<sup>1-3</sup>. In contrast, the rate of success in the prevention of hip and other non-vertebral fractures is modest. The most powerful antiresorptive treatments which are available to date, the bisphosphonate Aclasta/Reclast<sup>®</sup> and the RANKL-inhibitor Prolia<sup>®</sup>, achieve a relative risk reduction for hip fractures of 40%. Robust data regarding the effects of the bone anabolic agent Forsteo<sup>®</sup> on hip-fractures is lacking but available evidence suggests an anti-fracture efficacy which is similar to the antiresorptive agents.

Considering the high medical need for effective prevention of non-vertebral fractures, the situation is not satisfactory. The life-time risk for a women over age 50 to endure a hip fracture is 18%. There is a gender-independent risk of 10% for hip-fracture patients to die within one year following the event, and an even much larger risk for them to lose their independence.

**Antiresorptive treatments:** From the mechanistic point of view, the effect of BPs and Prolia<sup>®</sup> is limited to the reduction of pathologically increased bone turnover to or below premenopausal 'normal' levels. This can be accomplished within approximately 6 months, and the reduction of the bone remodelling space can, depending on the initial rate of bone turnover and anatomical location, lead to an increase in bone mineral density of 4-8%. The reduction in accelerated bone turnover also delays, or at best stops the structural deficits resulting from the perforation and subsequent elimination of trabecular elements, reduces the age-related trabecularisation of the endocortex and diminishes cortical porosity. However, it seems likely that the most important contribution of antiresorptive agents to mechanical stability is their effect on stress-concentrators<sup>4,5</sup>. Bone resorption events on a trabecular surfaces act as stress concentrators which are able to reduce the mechanical competence of a trabecular element to a larger degree than would be predicted from the small amount of bone that is missing. Antiresorptive agents reduce the number of stress-concentrators by up to 90%, which may help to explain how a 'modest' 8% increase in bone density can lead to a 70% reduction in vertebral fractures.

The fact that antiresorptive agents can merely stabilise and conserve the available cortical and cancellous bone structures but not improve them, limits their clinical effectiveness, especially in patients at advanced stages of the disease. Available clinical data seems to suggest, that this class of agents does not offer room for improvement for lowering vertebral fracture rates below 70% and hip-fractures below 40%. Anti-fracture efficacy is achieved via a very pronounced suppression of bone remodelling of up to 90% raising fears that the long-term suppression beyond this level may interfere negatively with two essential functions, namely tissue renewal and micro-damage repair.

**Bone anabolic treatments:** In contrast to antiresorptive therapy which targets the osteoclast, PTH affects to main mechanisms which lead to the thickening of existing trabecular and cortical bone structures<sup>6</sup>. 1) Activation of bone modelling drifts

(activation of bone lining cells (activation of resting osteoblasts leading to direct bone formation without prior bone resorption) and 2) Increase in the number of bone remodelling cycles with positive bone balance. The activation of bone modelling is predominantly seen during the early response to PTH-treatment (<6 months) while, based on blood based bone resorption markers, the remodelling based bone gain is initiated around 3 to 6 months after the onset of treatment.

Given the knowledge about the detrimental effects of surface based remodelling events (stress raisers), the increase in bone turnover under PTH-treatment may partially offset the positive effect on mechanical competence resulting from trabecular thickening. It thus seems logical to propose the combination of PTH with an anti-resorptive agent, in order to prevent the increase in bone turnover and its negative mechanical consequences with a possibility to achieve a stronger reduction in vertebral and non-vertebral fractures<sup>7</sup>. Unfortunately there is very limited

clinical evidence in favour of such a co-treatment option and no fracture efficacy data has been reported to date<sup>8</sup>.

An alternative and perhaps more promising route may be offered by the anabolic treatment of osteoporotic patients with anti-sclerostin antibodies, a novel treatment option which is undergoing clinical testing. Inhibition of sclerostin, a bone formation inhibitory protein which is released by osteocytes, results in a strong anabolic response in rodents, primates and in man<sup>9,10</sup>. In contrast to PTH, the treatment with anti-sclerostin antibodies does not appear to activate bone remodelling and was even shown to reduce bone resorption. If confirmed in long-term studies, this novel bone anabolic treatment may prove superior to PTH and antiresorptive agents with regard to its ability to reduce vertebral-, and more importantly also non-vertebral fractures.

Last but not least, the improvement of muscle function and thus the reduction in the number of falls remains an essential goal in the prevention of non-vertebral fractures in osteoporotic patients and the maintenance of their independence. Ultimately, the combination of exercise to increase fitness, balance and coordination, together with the use of novel bone- and muscle anabolic treatments can be expected to reduce non-vertebral fracture rates to a more acceptable level.

<sup>1</sup>Neer RM, *NEJM* 2001;344:1434. <sup>2</sup>Black DM, *NEJM* 2007;356:1809. <sup>3</sup>Cummings SR, *NEJM* 2009;361:1. <sup>4</sup>Riggs & Parfitt, *JBMR* 2005;20:177. <sup>5</sup>van der Linden, *JBMR* 2001;16:457. <sup>6</sup>Lindsay R, *JBMR* 2006;21:366. <sup>7</sup>Canalis E, *NEJM* 2007;357:905. <sup>8</sup>Cosman F, *JBMR* 2011;26:503, <sup>9</sup>Ominsky MS, *JBMR* 2010;25:948. <sup>10</sup>Padhi D, *JBMR* 2011;26:19.

## **Biology and Pathology of Subchondral Bone**

Salter DM

*[Osteoarticular Research Group](#), Centre for Molecular Medicine, MRC IGMM, University of Edinburgh, Scotland*

Subchondral bone is the zone of epiphyseal bone just beneath the articular cartilage. It includes the subchondral bone plate and the underlying trabecular bone. It is intimately associated with calcified zone of articular cartilage. Subchondral bone has a number of important roles in normal joint protection, exerting important shock absorbing and supportive functions in addition to being a source of nutrients to cartilage and facilitating removal of metabolic waste products.

The anatomy of the subchondral bone is highly variable with variations in its thickness and density and the number of vascular perforations in the subchondral bone plate within and between joints. Differences are also recognised in the trabecular structure and mechanical properties of weight-bearing and non-weight-bearing areas. The close association between articular cartilage and subchondral bone suggests that these may act as a functional unit and abnormalities of one predisposes to abnormalities in the other.

Pathological changes in subchondral bone in established osteoarthritis such as vascular invasion of the calcified zone and tidemark multiplication duplication of the tide mark (Fig 1), bone sclerosis, cysts and marrow oedema are well recognised but abnormalities in the subchondral bone may in themselves be a cause of osteoarthritis. These include subtle changes in the mechanical properties of the subchondral bone or more severe pathological changes that are seen as a result of trauma, osteochondritis dissecans, or ischaemia, avascular necrosis. Increasing knowledge of the basic biology and pathological changes in the subchondral bone is highlighting new strategies for management of diseases such as osteoarthritis.

## The role of glutamatergic signalling in bone formation and arthritis

K Brakspear<sup>1</sup>, C Bonnet<sup>1</sup>, P Parsons<sup>2</sup>, BAJ Evans<sup>3</sup>, DJ Mason<sup>1</sup>,

<sup>1</sup>Division of Pathophysiology and Repair, School of Biosciences, Cardiff University, Wales. <sup>2</sup>Smith and Nephew, York, <sup>3</sup>IMEM, School of Medicine, Cardiff University, Wales.

**INTRODUCTION:** The observation that the glutamate transporter (EAAT1) is mechanically regulated in bone *in vivo* (1) led to the notion that glutamate could be an osteogenic signal, with potential for therapeutic manipulation. However, EAAT function and role in controlling human osteoblast differentiation and activity has not previously been reported. This study investigates EAAT expression, EAAT function and the influence of EAAT inhibition on osteoblast differentiation and activity. EAAT expression in rat arthritic bone *in vivo* was investigated to determine physiological relevance.

**METHODS:** EAAT expression was quantified by RT-qPCR and confirmed by immunofluorescence (GLAST11-S, 1:500, Alpha Diagnostics) in human primary and SaOS-2 osteoblast-like cells grown under standard conditions. EAAT function was measured using a radiolabelled glutamate uptake assay. The effect of (i) EAAT inhibition (using chemical inhibitors, t-PDC, TBOA) and (ii) EAAT splicing (antisense oligonucleotides [AONs] complementary to splice sites) on osteoblast number (LDH assay Cytotox96, Promega), gene expression (RT-qPCR), alkaline phosphatase (ALP) activity (*p*-nitrophenol release from *p*-nitrophenyl phosphate, Sigma) and mineralization (bound alizarin red) was determined. EAAT1 protein was immunolocalised in arthritic tissues from rat antigen induced arthritis (AIA).

**RESULTS:** EAAT1 and its splice variants (EAAT1a and EAAT1ex9skip), EAAT2 and EAAT3 mRNAs are expressed in human bone, human primary osteoblasts and SaOS-2 cells. EAAT1 (Fig 1a) and EAAT3 proteins are expressed in human primary and SaOS-2 osteoblasts. SaOS-2 cells exhibited Na<sup>+</sup>-dependent glutamate uptake (1-250 μM) with a V<sub>max</sub> of 48,510 ± 1,700 pmol/hr/mg and a K<sub>M</sub> of 7.4 ± 1.2 μM (Fig 1b). EAAT inhibitors (t-PDC and TBOA) significantly increased SaOS-2 cell number (10 μM t-PDC/TBOA, p<0.01; 100 μM t-PDC, p<0.001; 100 μM TBOA, p<0.05). EAAT inhibitors also reduced SaOS-2 alkaline phosphatase activity (10 μM, p<0.01, 100 μM, p<0.05, Fig 1c) and significantly reduced mineralisation in both SaOS-

2 cells and human primary osteoblasts (100 μM t-PDC/TBOA, p<0.001, Fig 1d).

Overexpression of EAAT1a or EAAT1ex9skip using respective AONs significantly reduced Na<sup>+</sup>-dependent glutamate uptake in SaOS-2 cells (p<0.001). Ex3skip AON significantly decreased osteocalcin mRNA expression (p=0.008) and ex9skip AONs significantly increased ALP activity (p=0.006) in SaOS-2 cells. EAAT1 and EAAT3 staining was extensive in areas of bone remodeling in rat AIA.

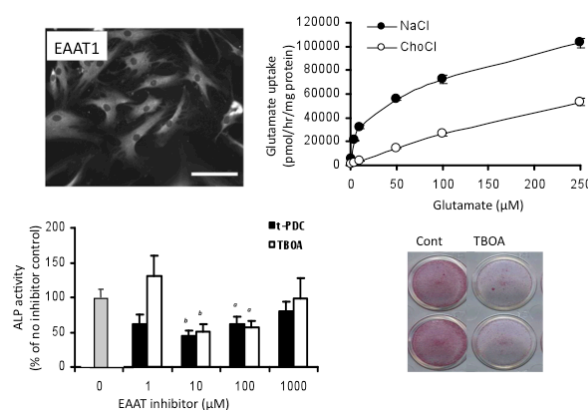


Fig. 1: EAAT1 protein is expressed in SaOS-2 cells (a) and these cells show Na<sup>+</sup>-dependent glutamate uptake (b). EAAT inhibition with t-PDC or TBOA reduces ALP activity (c) and inhibits mineralization of human primary osteoblasts (d).

**DISCUSSION & CONCLUSIONS:** We have shown for the first time that EAATs are functional in human osteoblasts and that chemical inhibition of EAATs reduces ALP and mineralisation in SaOS-2 and human primary osteoblasts. Furthermore, manipulation of EAAT splicing reduces glutamate uptake and influences ALP in a splice variant-specific manner. This, combined with the high expression of EAATs in remodelling bone in arthritis supports an important role for EAATs in bone formation.

**REFERENCES:** <sup>1</sup> D.J. Mason, L.J. Suva, P.G. Genever, et al (1997) *Bone* **20**:199-125.

**ACKNOWLEDGEMENTS:** We thank Carole Elford for human primary osteoblast culture and mineralisation.

## **Osteoblast/ Osteocyte Interactions**

Lynda Bonewald,  
*University of Missouri, Kansas City, USA*

Osteocytes have been found to be multifunctional cells. Osteocytes appear to be mechanosensors, regulators of mineral homeostasis, and orchestrators of bone modeling and remodeling sending signals to both osteoclasts and osteoblasts.

Osteocytes appear to be descendants of matrix generating osteoblasts. Osteoblast differentiation into osteocytes is accompanied by a dramatic change in morphology from a plump, polygonal collagen generating cell on the bone surface to a dendritic cell with 40-100 dendrites encased within the mineralized bone matrix.

Before embedding in the unmineralized osteoid, the cell starts to express markers such as Dmp1, Phex, and E11/gp38. At this stage the cell begins to regulate the mineralization process insuring that the encased cell will remain viable with connections to a vascular supply and connections with cells on the bone surface. Osteocytes can communicate with osteoblasts on the cell surface to provide signals of support for and signals to reduce or stop bone formation.

In response to mechanical load, osteocytes send signals in the form of small molecules such as ATP, nitric oxide, and prostaglandin which stimulate bone formation. Under conditions of immobilization and disuse, osteocytes send signals such as sclerostin to inhibit new bone formation and to osteoclasts such as RANKL to increase bone resorption. Not only are osteocytes sensitive to mechanical load, but also to hormonal stimulation in response to PTH or estrogen to titrate their signals to cells on the bone surface.

As osteocytes make up over 90-95% of all bone cells in the adult skeleton, it is important to consider their role in bone formation and regeneration.

## **The interface between angiogenesis and osteoclastogenesis/osteoblastogenesis during bone remodeling**

Erik Fink Eriksen,

*Dept. of Endocrinology, Oslo University Hospital, Norway*

Bone remodeling takes place in specialized vascular structures, the so called Bone Remodeling Compartments (BRCs). The boundaries of these structures are comprised by the denuded bone surface and a dome of flattened cells, displaying a predominant osteoblast/lining cell phenotype with some pericytes in between. The formation of the BRC is dependent on angiogenesis in the vicinity of remodeling sites, and the initial step in BRC formation most likely involves contact between a vessel and the bone surface. The BRC may have several important functions in bone:

It constitutes a dome, creating a space where osteoclast/osteoblast interactions are separated from the very active growth factor environment of hematopoiesis in the marrow space. If the access to the marrow space were open, the very high levels of growth factors in the marrow microenvironment would interfere with the local regulatory effects by these growth factors, crucial to osteoclast and osteoblast differentiation and the remodeling process. Recent studies on glucocorticoid induced osteoporosis suggest that the BRC may play a crucial role in the transition from the resorptive to the formative phase of bone remodeling.

It is the structure where coupling between osteoclasts and osteoblasts take place. Due to the timing and sequence of bone resorption and bone formation, the two processes rarely occur within the same area, which makes the needed cell to cell contact between osteoclast precursors and osteoblasts highly unlikely. The dome cell layer of the BRC are more likely candidates. The cells exhibit positive immuno-reactivity for RANKL and OPG, and might therefore be responsible for the cell to cell contact to osteoclast precursors.

The BRC may also be the structure through which mechanosensory signals from the osteocyte network are translated into changes in osteoclast and osteoblast activity via gap junctions between

lining cells on quiescent surfaces and osteocyte canaliculi

The BRC may also play a crucial role in the formation of bone metastases. It is the only place on the bone surface where tumor cells can interact with denuded bone surfaces. The growth of metastatic cells in bone is enhanced by the so called "vicious cycle", driven by PTHrp and cytokines. The existence of a closed compartment would make vicious cycle formation easier due to absence of potential interference with cytokine and growth factors from the marrow space. Also recent research has shown that break down of the dome structure occurs during advanced myeloma spread in bone.

## Wnt/ $\beta$ -catenin signalling pathway involved in the dual effects of desmethylcaritin on promotion of osteogenesis and inhibition of adipogenesis

Xin-Luan Wang<sup>1</sup>, Nan Wang<sup>1</sup>, Li-Zhen Zheng<sup>2</sup>, Peng Zhang<sup>1</sup>, Ling Qin<sup>1,2</sup>

<sup>1</sup> Translational Medicine R&D Center, Shenzhen Institutes of Advanced Technology China

<sup>2</sup> Department of Orthopaedics & Traumatology, The Chinese University of Hong Kong, Hong Kong

**INTRODUCTION:** *Epimedium*, a traditional Chinese Herbal Medicine, was found to be able to promote osteogenesis and inhibit adipogenesis, and thus to treat osteoporosis<sup>1</sup>. Recently, desmethylcaritin was identified as one of the active metabolites of *Epimedium*. In this study, we investigated the dual effects and mechanisms of desmethylcaritin on osteogenesis and adipogenesis.

**METHODS:** Osteoblastic-like UMR 106 cells were used to evaluate the osteogenic effects of desmethylcaritin. Alkaline phosphatase (ALP) activity and Alizarin Red S staining was performed according to established protocols<sup>2</sup>. Oil Red O staining in 3T3-L1 cells were used to demonstrate the effects of desmethylcaritin on adipogenesis. Real time PCR was used to quantify the mRNA expressions of related genes. All quantitative data were presented as means  $\pm$  SD of three experiments.

**RESULTS:** Desmethylcaritin promoted ALP activity dose-dependently (Fig 1A). Compared with the control group, more calcium nodules were formed in the desmethylcaritin group (Fig 1B). Compared to the adipogenic induction group (ctl+), desmethylcaritin decreased the adipocytes (Fig. 2A), as well as down-regulated the mRNA expression of adipogenic transcription factors, CCAAT/enhancer binding protein  $\alpha$  (*Cebpa*) and Peroxisome Proliferator-Activated Receptor  $\gamma$  (*Pparg*) (Fig. 2B,C). As for Wnt/ $\beta$ -catenin signaling pathway, desmethylcaritin increased *Wnt10b* expression (Fig. 3A) and decreased the *Lrp5* expression (Fig. 3B). In addition, desmethylcaritin significantly increased the mRNA expression of  $\beta$ -catenin (*Ctnnb1*) (Fig. 3A).

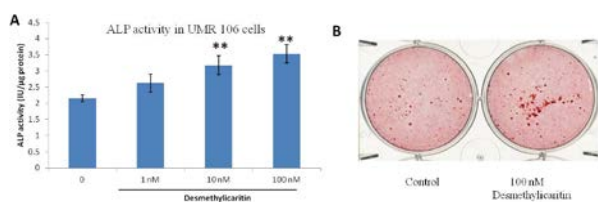


Fig. 1: Desmethylcaritin promoted osteogenesis in osteoblastic UMR 106 cells. (A) ALP activity, (B) calcium nodules. \*\*  $P < 0.01$  vs control.

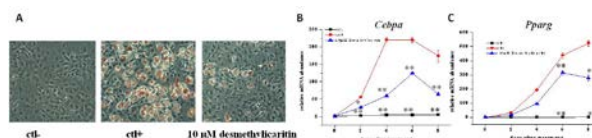


Fig. 2: Desmethylcaritin inhibited adipogenesis in 3T3-L1 cells. (A) Oil Red O staining, (B) mRNA expression of *Cebpa* and (C) *Pparg*. \*  $P < 0.05$ , \*\*  $P < 0.01$  vs adipogenic positive control.

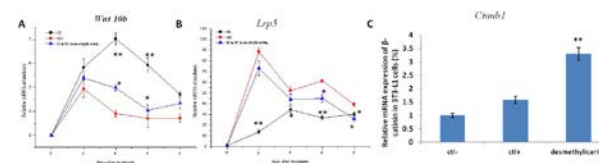


Fig. 3: The mRNA expression of *Wnt10b*, *Lrp5* (B) and *Ctnnb1* (C) in 3T3-L1 cells. \*  $P < 0.05$ , \*\*  $P < 0.01$  vs adipogenic positive control.

**DISCUSSION & CONCLUSIONS:** *Wnt10b*, increased by desmethylcaritin, is found the key factor to promote osteogenesis and inhibit adipogenesis. *Wnt10b* binds to *Lrp5* co-receptors and leads to hypophosphorylation of  $\beta$ -catenin, which activates WNT target genes and inhibit adipogenesis by suppressing *Cebpa* and *Pparg*<sup>3</sup>. Based on our results, Wnt/ $\beta$ -catenin signaling pathway involved in the dual effects of desmethylcaritin on promoting osteogenesis and inhibiting adipogenesis.

**REFERENCES:** <sup>1</sup> Peng, SL, Zhang G, He YX, et al., (2009) *Bone*, 2009. **45**: 534-44. <sup>2</sup> Wang, XL, Zheng LZ, Zhang G, et al., (2011) *Phytomedicine*, 18:868-72. <sup>3</sup> Bennett, CN, Longo, KA, Wright, WS, et al., (2005) *Proc Natl Acad Sci*, 102: 3324-9.

**ACKNOWLEDGEMENTS:** This work was supported by "12.5 Major New Drug Creating" Special Projects (Reference: 2011ZX09201-201-01).

## *In vitro* 3D osteoblast-osteocyte co-culture model

M Vazquez<sup>1</sup>, BAJ Evans<sup>2</sup>, JR Ralphs<sup>3</sup>, D Riccardi<sup>3</sup>, DJ Mason<sup>3</sup>

<sup>1</sup>Arthritis Research UK Biomechanics and Bioengineering Centre, School of Biosciences, Cardiff University, Wales. <sup>2</sup>Institute of Molecular and Experimental Medicine, School of Medicine, Cardiff University, Wales. <sup>3</sup>Division of Pathophysiology and Repair, School of Biosciences, Cardiff University, Wales.

**INTRODUCTION:** Normal mechanical loading potently induces bone formation via effects on osteocytes. Current investigations of mechanical loading of bone do not reflect the interactions of the cells within it, mostly focusing on mechanical loading of osteoblasts in monolayers. Existing 3D models do not elucidate the osteoblast-osteocyte interactions that regulate mechanically-induced bone formation. We developed a novel *in vitro* 3D co-culture model of bone [1] to investigate osteoblast-osteocyte interactions.

**METHODS:** MLO-Y4 cells ( $1.5 \times 10^6$  cells/ml) were incorporated into acid-soluble rat tail tendon type I collagen (2mg/ml in MEM, pH7.4) gels and MC3T3-E1 ( $1.5 \times 10^5$  cells/well) layered on top and cultured at 37°C in DMEM (5% dialysed FBS) for 1 week (Fig.1A&B). Co-cultures were fixed with 1% paraformaldehyde, infiltrated with OCT, cryosectioned and labelled with 1) toluidine blue or phalloidin and DAPI to assess cell morphology, 2) ethidium homodimer and DAPI to assess cell viability, 3) immunostained using anti-connexin 43 antibody to assess cell connectivity, or 4) immunostained with antibodies against osteoblast and osteocyte markers to assess phenotype. Cell phenotype was also determined by RT-qPCR of RNA extracted (Trizol) separately from surface osteoblasts (surface zone) and encased osteocytes (deep zone) (Fig. 1A).

**RESULTS:** Data show co-cultures survive, for at least one week, with osteocyte cell death, within gels, averaging  $16.86 \pm 3.56\%$  at day 1 and  $14.11 \pm 2.69\%$  at day 7 comparable to monolayer cultures [2]. MC3T3-E1 and MLO-Y4 cells maintain their morphology (Fig.1D&F), express Runx2, osteocalcin, ColI, ALP and RANKL mRNA and E11 (Fig.1C) and connexin 43 (Fig.1E) protein. Data were obtained from 3 independent experiments of n= 3 or 4. Conditions for mechanical loading of these cultures are being optimised.

**DISCUSSION & CONCLUSIONS:** We have established a mouse osteoblast-osteocyte 3D co-

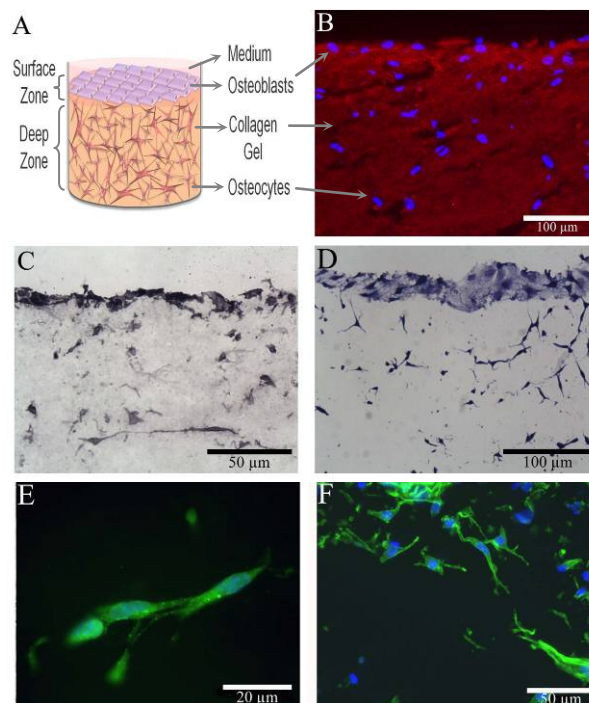


Fig. 1: A) Diagram of the 3D co-culture model. B) Staining of type I collagen gel (red) and cell nuclei (blue). C) E11 expression across the model. D) Toluidine blue staining showing osteoblast and osteocyte morphology. E) Osteocyte expression of connexin 43. F) Actin filament staining showing osteocyte morphology.

culture system where MLO-Y4 cells form an interconnected network of dendritic cells throughout the gel, overlaid with surface osteoblasts that express type I collagen. We are using this system to investigate mechanically-induced signals in osteocytes and osteoblasts.

**REFERENCES:** <sup>1</sup> D.J. Mason, C.H. Dillingham, B. Evans, et al (2009) Bio reconstruction de l'os a la peau. Saraumps Medical. pp35-39. <sup>2</sup> A. Bakker, J. Klein-Nulend, E. Burger (2004) Biochem. Biophys. Res. Comm. **320**:1163-68.

**ACKNOWLEDGEMENTS:** We thank Prof. Lynda Bonewald for providing MLO-Y4 cells, Carole Elford and Karen Brakspear for their contribution.

## Mechanical loading and how it affects bone cells

J Klein-Nulend<sup>1</sup>, RG Bacabac<sup>2</sup>, AD Bakker<sup>1</sup>

<sup>1</sup> Department of Oral Cell Biology, ACTA-University of Amsterdam and VU University Amsterdam, Research Institute MOVE, Amsterdam, The Netherlands. <sup>2</sup> Department of Physics, Medical Biophysics Group, University of San Carlos, Cebu City, Philippines

**OSTEOCYTES AND MECHANOTRANS-  
DUCTION:** Osteocytes are stellate cells that form a network within the calcified bone matrix, and play a pivotal role in the regulation of skeletal mass. Under physiological loading conditions, the matrix strains drive a flow of interstitial fluid through the lacuno-canalicular porosity. This flow is thought to mechanically activate the osteocytes [1]. Mechanically activated osteocytes produce signaling molecules like BMPs, Wnts, PGE<sub>2</sub> and NO, which modulate the activity of the bone forming osteoblasts and the bone resorbing osteoclasts, thereby orchestrating bone adaptation to mechanical loading.

In single osteocytes *in vitro*, mechanical stimulation of both cell body and cell process results in upregulation of intracellular NO production, indicating that both cell body and cell process play a role in mechanosensing. However, interstitial fluid is driven to flow within the canaliculi over osteocyte processes only *in vivo*. How interstitial fluid flow activates the osteocyte processes, i.e. via shear stress, hoop strains, or other mechanisms is still unknown. Using an ultra high voltage electron microscope (UHVEM) we constructed a realistic 3D image-based model of a single osteocyte cell process within a canaliculus in human bone, and analyzed the fluid dynamics of Newtonian fluid flow within the canaliculus (Fig. 1). The canalicular wall showed a highly irregular surface causing highly inhomogeneous flow patterns, which may induce deformation of cytoskeletal elements in the osteocyte process, thereby amplifying mechanical signals.

**THE CYTOSKELETON:** The cytoskeleton provides the structural scaffold that mechanically supports cell shape and viscoelastic properties. The cytoskeletal morphology varies in relation to the surrounding extracellular matrix (ECM), and therefore the ECM affects cell stiffness. Interestingly, osteocytes with round-suspended morphology are an order of magnitude more elastic compared to flat-adherent cells, and require lower force stimulation to show an increase in NO production. Apparently, elastic osteocytes seem to require less mechanical forces in order to respond than stiffer cells [2]. The motion of the nucleus

through the cell body during vibration stress application is a possible cytoskeleton-related mechanism for bone cells to sense high-frequency loading and might relate to the osteogenic benefits of vibration-related stimulation.

Inflammatory factors such as TNF- $\alpha$  and IL-1 $\beta$  modulate F-actin levels in osteocytes, and decrease cell stiffness. TNF- $\alpha$  and IL-1 $\beta$  also reduce calcium influx in mechanically stimulated cells, possibly because opening of stretch-activated ion channels is dependent on cytoskeletal integrity. Moreover TNF- $\alpha$  and IL-1 $\beta$  reduce NO production in mechanically stimulated osteocytes. This suggests that during inflammation, cytokines may affect the response of osteocytes to mechanical stimuli via an effect on the osteocyte cytoskeleton [5].

**CONCLUSION:** The osteocyte cytoskeleton, which ultimately determines cell shape, is a key factor in determining how osteocytes sense stresses, whether it is a local or bulk deformation, or whether it is a transfer of forces inside of the cell. As osteocytes orchestrate bone remodelling, any factor affecting the osteocyte cytoskeleton and thereby the osteocyte response to mechanical stimuli, potentially affects bone mass.

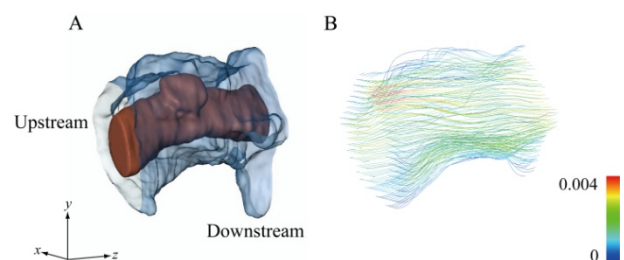


Fig. 1: A) 3-D model of canaliculus containing an osteocyte process. B) Distribution of absolute fluid velocity on stream lines. Fluid flow in pericellular space is generated by uniform external force directed from minus to plus direction of z-axis.

**REFERENCES:** <sup>1</sup> J. Klein-Nulend et al. (1995) FASEB J 9:441-5. <sup>2</sup> R.G. Bacabac et al. (2008) J Biomech 41:1590-8. <sup>3</sup> D. Mizuno et al. (2009) Phys Rev Lett 102:16802. <sup>4</sup> R.G. Bacabac et al. (2006) FASEB J 20:858-64. <sup>5</sup> A.D. Bakker et al. (2009) Arthr Rheum 60:3336-45.



## Modelling the fracture environment in computational models of bone healing

P.J. Prendergast

*Trinity Centre for Bioengineering, School of Engineering, Trinity College, Dublin 2, Ireland.*

*Email: [pender@tcd.ie](mailto:pender@tcd.ie)*

Computer simulations of the fracture environment are useful for testing hypotheses about fixation devices, loading, and interspecies variation. Two aspects to modeling are (i) the description of the spatial environment, and (ii) simulating temporal change of that spatial environment. Considering first the spatial environment. The load applied by through the bone and musculature determines the loading on the callus. Loading will vary and daily loading datasets are useful to get an average, or else patient-specific data may be used. The musculature can also determine the source of precursor cells that migrate into the callus. Within the callus itself, cells proliferate, migrate, and apoptose in response, in part, to mechanical stimuli such as mechanical strain, fluidic stimulation, and electric

potentials. Modelling cell activities can be done using lattice modeling, where an orthogonal array of lattice points is used, each lattice point being either vacant or occupied by a cell whose phenotype is mechanoregulated [1]. What happens over time can be modeled using finite element analysis to determine the mechanoregulatory stimuli at a point in time and then incorporating this into an iterative simulation. In this presentation a simulation of bone healing in the tibia is presented considering a patient-specific geometry and loading.

[1] Byrne, D.P., Lacroix, D., Prendergast, P.J., Simulation of fracture healing in the tibia: Mechanoregulation of fracture healing using a lattice modeling approach. *Journal of Orthopaedic Research* Vol. 29, pp. 1496-1503, 2011

## Alveolar bone resorption is triggered by sudden strain relaxation of gingival fibroblasts

N. Gadban<sup>1</sup>, N. Rudlich<sup>2</sup>, S. Moskovich<sup>2</sup>, N. Amariglio<sup>2</sup>, E. Weinberg<sup>1</sup>, A. Yaffe<sup>3</sup> and I. Binderman<sup>1</sup>.

<sup>1</sup>Department of Oral Biology, the Goldschleger School of Dental Medicine, Sackler Faculty of Medicine and <sup>2</sup>Department of Pediatric Hematology-Oncology, The Chaim Sheba Medical Center, Tel Aviv University, Tel Aviv 69978, Israel, <sup>3</sup>Department of Prosthodontics, Haddasah Faculty of Dentistry, Hebrew University, Jerusalem.

**INTRODUCTION:** In the mammalian adult, the teeth are anchored through a network of strained fibroblasts aligned on bundles of collagen fibers, connecting the root cementum to alveolar bone and to marginal gingiva. Our previous studies and others data have shown that separation of the gingiva from the tooth root that disrupts the dento-gingival and dento-periosteal fibers in a rat model, lead to an abrupt strain relaxation of local fibroblasts, release of ATP from cells, and an up-regulation of the purinergic receptor P2X4, which is a specific receptor of extracellular ATP. Our hypothesis is that sudden strain relaxation of gingival fibroblasts induces release of cellular ATP that through activation of P2X receptors may play a pivotal role in Ca<sup>+2</sup> influx and elevated expression of RANKL in fibroblasts and osteoblasts, that activate local osteoclasts, leading to alveolar bone resorption.

**METHODS:** In order to test this hypothesis we employed human gingival fibroblasts (HGF) that were derived from marginal gingiva explants of young patients. Subcultures of HGF were grown on collagen films during 4-6 days to reach subconfluent conditions.

**RESULTS:** The length of the cells grown on plastic dishes (group A) and on stretched collagen films (group B) was similar, 155± 47 µm and 147 ± 28 µm, respectively. By detaching the collagen films a significant reduction of 45% in cell length was measured, 83± 27 µm. (p< .001), implying that abrupt strain relaxation of fibroblasts induces changes in cell shape. ATP release from HGF cells

of group C increased more than 10 folds in comparison to strained cells grown on collagen films (group B) or on plastic culture dishes (group A). After 10 minutes the amount of extracellular ATP declined by 25% and returned to control levels 50 minutes later. Also, an increase of P2X7 but not P2X4 gene expression was found in human cells in response to detachment of collagen films (group C). When the collagen films were detached, this way reducing abruptly the cell strain, a high fluorescence of intracellular Ca<sup>+2</sup> appeared. It seems that extracellular ATP or strain relaxation of HGF cells induces influx of Ca<sup>+2</sup> into the cells. On the other hand, extracellular ATP release is also controlled by intracellular calcium levels. EGTA prevented the effect of ATP on influx of Ca<sup>+2</sup>. It was striking to find a significant up-regulation of stanniocalcin-1 (STC-1) in cells of group C, in response to abrupt drop of strain of HGF cells. STC-1 is a well known local regulator of Pi and calcium transport pathways.

**CONCLUSIONS:** Taken together, the *in vitro* results are in accord with the findings in the rat model, showing that strain relaxation of human gingival fibroblasts reducing HGF cell processes. At the same time release of ATP from these cells and sharp influx of calcium, , trigger molecular changes that propagate toward osteoclastic alveolar bone remodeling. Since, in periodontal diseases, degradation of collagen is dominant, strain relaxation of gingival fibroblasts that follows, may be considered as an important trigger of alveolar bone resorption.

## **"Composite biomaterials for bone repair and regeneration -reconstruction of orbital floor defects in an animal model- "**

Dirk Grijpma

*University of Twente, Netherlands*

In the treatment of orbital floor fractures, bone is ideally regenerated. The materials currently used for orbital floor reconstruction do not lead to the regeneration of bone. Our objective was to render polymeric materials based on poly(trimethylene carbonate) (PTMC) osteoinductive, and to evaluate their suitability for use in orbital floor reconstruction. For this purpose, osteoinductive biphasic calcium phosphate (BCP) particles were introduced into a polymeric PTMC matrix. Composite sheets containing 50 wt% BCP particles were prepared. Also laminates with poly(D,L-lactide) (PDLLA) were prepared by compression moulding PDLLA films onto the composite sheets. After sterilization by gamma irradiation, the sheets were used to reconstruct surgically-created orbital floor defects in sheep. The bone inducing potential of the different implants was assessed upon intramuscular implantation.

The performance of the implants as orbital floor reconstruction was assessed by cone beam computed tomography (CBCT). Histological evaluation revealed that in the orbital and intramuscular implantations of BCP containing specimens, bone formation could be seen after 3 and 9 months. Analysis of the CBCT scans showed that the composite PTMC sheets and the laminated composite sheets performed well in orbital floor reconstruction. It is concluded that PTMC/BCP composites and PTMC/BCP composites laminated with PDLLA have osteoinductive properties and seem suitable for use in orbital floor reconstruction.

## Resorption characteristics of Chronos™ inject in metaphyseal bone defects caused by distal radius fracture

CM Sprecher<sup>1</sup>, R Arora<sup>2</sup>, M Lutz<sup>2</sup>, I Sitte<sup>2</sup>, S Duda<sup>1,2</sup>, M Blauth<sup>2</sup>, S Milz<sup>1,3</sup>

<sup>1</sup> [AO Research Institute, AO Foundation, Davos, CH.](#) <sup>2</sup> [Dep. of Surgery and Sports Medicine, Medical University Innsbruck, Innsbruck, A.](#) <sup>3</sup> [Dep. of Anatomy, Ludwig-Maximilians University, München, D.](#)

**INTRODUCTION:** Resorbable calcium phosphate cement is frequently used to treat bone defects in human patients. An example is ChronOS™ Inject (Synthes, Switzerland) which can be used as a metaphyseal bone void filler for reconstruction of these defects. A resorption rate of up to 90% in 6 months has been reported in an animal model<sup>1</sup>. The purpose of this study was to investigate the resorption characteristic of ChronOS™ Inject in human patients. Here the cement was applied into the metaphyseal bone void in dorsally displaced distal radius fractures.

**METHODS:** Distal radius fractures (AO classification C1, C2, C3) of six elderly patients (average age 70 years) were treated with a volar locking plate system (2.4 mm LCP Distal Radius Plates, Synthes, Switzerland). The metaphyseal bone defect was filled with ChronOS™ Inject during surgery. During implant removal (6 - 15 months later) a biopsy Ø 2 mm was taken from the former defect zone, using a bone biopsy device. The study was conducted in accordance with the Declaration of Helsinki (1996 revision) and was approved by the ethics committee of the University of Innsbruck, Austria. Specific informed consent for participation in the study was obtained from all patients individually.

All biopsies were embedded in MMA, cut with a heavy duty microtome at 5 - 6µm and stained with Masson-Goldner's trichrom or Methylene blue stain. In all specimens' the area of bone and osteoid tissue were histomorphometrically measured using KS400 image analysis software (Zeiss, Germany). Two specimens were additionally investigated with µCT40 (Scanco Medical, Switzerland) prior to sectioning. Histological observations like cement particles, bone marrow fibrosis and signs of inflammation were recorded. The CT data were used to determine the volume fractions of ChronOS™ Inject and mineralized tissue and to generate a 3D model of their distribution.

**RESULTS:** In the histomorphometrical analysis, the amount of bone in the measured areas (i.e. the apparent bone density) varied between 6.9 and 36.2% in comparison to the amount of osteoid between 0.5 and 7.8%. Notably, patients receiving osteoporosis medication had a lower ratio between bone and osteoid compared to patients without that kind of treatment. Qualitative evaluation showed vital bone tissue, osteoid formation, mast cell occurrence and marrow fibrosis in most specimens. Varying amounts of inhomogeneously distributed granular material identified to be remainder of the injected cement were detected in all specimens. Bone tissue was found between the islands of granular material which were sometimes incorporated into trabecular bone. Newly formed osteoid in direct contact with the remaining cement was also observed. There was no solid cement agglomeration detectable in the specimens investigated. The inhomogeneous distribution of ChronOS™ Inject was quantified by micro CT measurements. The local ratio of bone and ChronOS™ Inject varied between 9.5 and 97.3.

**DISCUSSION & CONCLUSIONS:** The present study shows that ChronOS™ Inject is still present in elderly human patients 15 months after implantation into a bone defect in the distal radius. ChronOS™ Inject is integrated into the newly formed trabecular bone meshwork and certainly a larger proportion is resorbed during that time period. Results indicate that ChronOS™ Inject injection in metaphyseal bone voids of distal radius fractures may be an alternative to autologous bone grafting, especially in osteoporotic patients.

**REFERENCES:** <sup>1</sup> Apelt et al., *Biomaterials*, 2004, 25:1439-1451

**ACKNOWLEDGEMENTS:** The authors thank Andrea Tami and Vittoria Brighenti for their assistance by the µCT measurements and the data analysis.

## Bone void fillers: towards simplicity and low-cost

M Böhner<sup>1</sup>

<sup>1</sup> [RMS Foundation](#), Bettlach, CH.

**INTRODUCTION:** Bone defects for example resulting from trauma or diseases are generally treated with autologous bone, i.e. bone extracted from the patient via a second surgery. However, the high morbidity and costs associated with this procedure have been an incentive to find alternatives, such as synthetic bone void fillers. The first scientific studies devoted to these materials date from the early 1920's, but it is only with the Vietnam war that research efforts have soared [1]. In the last 40 years, hundreds of products have been proposed and tested, going from ceramics to metals via polymers [2]. Interestingly, most tested bone void fillers enhance bone formation suggesting that bone is a very permissive self-healing organ.

Despite this success, the yearly number of research articles in this field is still increasing going from 27 articles in 1981, to 66, 432 and 884 in 1991, 2001 and 2011, respectively. In fact, there are still several problems remaining such as the relatively poor mechanical properties of these materials or the absence of universal and cheap osteoinductive bone void filler [3]. A more recent trend is related to the cost pressure in the healthcare system: bone void fillers have to be cheap and allow a fast and easy application. In other words, production processes have to be simplified and optimized. Also, products have to be injectable, mouldable and/or without complicated handling [4]. The aim of the present talk is to describe this evolution and the current market needs.

**REFERENCES:** <sup>1</sup> L.L. Hench, J.W. Hench (2004) *J Australasian Ceram Soc* **40**:1-42. M. Böhner (2010) *Mater Today* **13**:24-30. <sup>3</sup> M. Böhner, L. Galea, N. Döbelin (2012) *J Eur Ceram Soc* doi:10.1016/j.jeurceramsoc.2012.02.028. <sup>4</sup> M. Böhner (2010) *Eur Cells Mater* **20**:1-12.

## An injectable *in situ* forming composite gel to guide bone regeneration: design and development of technology platform

R Dorati<sup>1</sup>, I Genta<sup>1</sup>, B Conti<sup>1</sup>, Holger Klöss<sup>2</sup>, Katja Martin<sup>2</sup>

<sup>1</sup> Dept. of Drug Sciences, University of Pavia, Via T.Taramelli 12, 27100 Pavia, Italy, <sup>2</sup> Geistlich Pharma AG, Wolhusen, Schweiz

**INTRODUCTION:** Various clinical situations such as augmentation of osteoporotic fractures, treatment of bone defects and specific indications in spine surgery can benefit of injectable composite gels with self-setting features [1]. The aims of this research project are i) to develop a novel injectable/mouldable bone graft substitute which consists of an approved bone graft substitute of natural origin with excellent biofunctionality suspended in a thermosensitive, biocompatible and biodegradable polymer solution and ii) to assess the feasibility of using the *in situ* forming composite gel (ISFcG) as filling or grafting material suitable to support tissue regeneration in dental/orthopaedic surgery.

**METHODS:** Several formulations of thermogelling polymer solution based on chitosan and glycerol phosphate disodium salt were prepared and tested as delivery vehicle for Orthoss<sup>®</sup> spongius granules (Geistlich Pharma AG, Wolhusen, Switzerland) to obtain the final ISFcG. All basic components of the polymer solution are of natural origin, biodegradable, biocompatible and already approved by regulatory agencies for human use. The final formulation was selected by determination of i) swelling and resistance, ii) mechanical and chemical stability, iii) cell seeding capacity and long-term cell growth and iv) long-term stability (6 months) of various polymer compositions.

**RESULTS:** All ISFcGs were rapidly (30 sec) and completely re-hydrated when KRH buffer was added. Samples were easy to handle by spatula with good adaptability and robustness (**Figure 1**). They successfully maintained the morphological and physical integrity during the mechanical and chemical stability studies, and they effectively entrapped the Orthoss<sup>®</sup> granules into the polymer network.

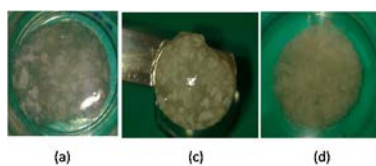


**Figure 1** Re-hydration performances of ISFcG: (a) after 30 sec, (c) 6 h and (d) 8 days.

Good cell seeding capacity was observed for all ISFcGs, ranging between 30-40%. Good cell proliferation was shown after 28 days in culture (**Figure 2**), demonstrating that the excellent bioconductive properties of Orthoss<sup>®</sup> granules were preserved when they were incorporated into chitosan polymer matrix.

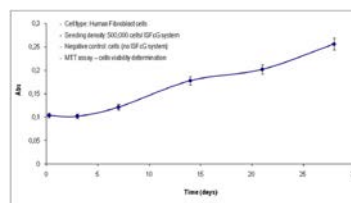


**Figure 2** Proliferation of adult fibroblasts in ISFcG over a period of 28 days, at 37°C, 5% CO<sub>2</sub> in DMEM supplemented with 10% FBS.

The final ISFcG presented optimal stability either in simulated media (KRH) or whole human blood for 8 days. Bone graft granules were entrapped and maintained within the polymer matrix for more than 8 days, no evidence of gel disaggregation was visible (**Figure 3**).

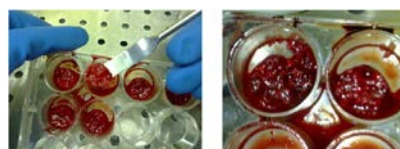


**Figure 3** ISFcG embedded into whole human blood after 8 days.

The long-term stability (6 months) of final ISFcGs performed at  $+5\pm 2^\circ\text{C}$  did not reveal any evidence of physical instability such as release of spongius granules or uncontrolled discharge of polymer matrix. The final ISFcG was developed both as a ready to use injectable formulation and in the freeze-dried form (solid form) which can be easily and promptly re-hydrated to a mouldable consistency.

**DISCUSSION & CONCLUSIONS:** The excellent stability and the good capacity to support cell growth in addition to its injectable/mouldable features make this system a promising candidate as scaffold for bone regeneration..

**REFERENCES:** <sup>1</sup>Sune Larsson, et al (2011) *Injury, Int. J Care Injured* 42 S30-S34.

## Low modulus novel bone substitutes for osteoporotic vertebral fracture management

HM Wong<sup>1</sup>, PK Chu<sup>2</sup>, KL Leung<sup>1</sup>, KDK Kuk<sup>1</sup>, KMC Cheung<sup>1#</sup>, KWK Yeung<sup>1#</sup>

<sup>1</sup> Department of Orthopaedics and Traumatology, Queen Mary Hospital, The University of Hong Kong, Hong Kong SAR, China. <sup>2</sup> Department of Physics and Materials Science, City University of Hong Kong, Hong Kong SAR, China (# Co-corresponding authors)

**INTRODUCTION:** Currently developed bone substitutes such as calcium-based bone cements have tried to overcome the clinical complications found in PMMA cement augmentation for osteoporotic spinal fracture<sup>1</sup>. However, lack of osteointegration and mismatched mechanical properties of PMMA potentially jeopardize surgical outcomes e.g. interfere bone healing and adjacent level fracture<sup>2</sup>. Hence, our group has fabricated a novel bone substitute comprised of polycaprolactone (PCL) and magnesium (Mg) with a wide range of compressive moduli and enhanced osteoblastic activity for vertebral cement augmentation. This paper aims to report the mechanical characteristics, *in-vitro* and *in-vivo* properties of the new bone substitute.

**METHODS:** The bone substitutes were prepared by incorporating 0.1g or 0.6g silane-treated Mg particles into 1g PCL. Their mechanical properties were evaluated by compression test, whereas the cytocompatibility and osteogenic differentiation properties were studied by direct cell culture, MTT and ALP assays, respectively. The *in-vivo* response was studied in rat model for 6 months. The animals were monitored and examined by Micro-CT at respective time points. Commercial PMMA and pure PCL were served as the controls.

**RESULTS:** The compressive moduli of the composites with 0.1g and 0.6g Mg were 1-fold and 3-fold higher than PCL, respectively (as shown in Figure 1). Also, they were about 5-fold and 2-fold lower than PMMA. The cell viabilities of all new composites were higher than 100% as compared to the control. The ALP activities of PMMA were significantly lower on days 3, 7 and 14 as compared to the new composites and pure PCL, whereas significantly higher ALP activities were found on day 14 of the new composites with 0.1g Mg. Figure 2 shows the percentage change of bone volume on all the samples during the implantation period. Significant more new bone formation was found on new composites with 0.1g Mg after 1 week of post-operation and up to 8 weeks as compared with the control.

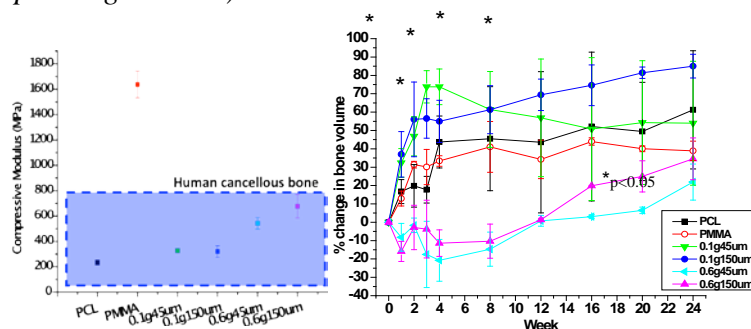


Fig. 1 (Left): Compressive moduli of the PCL-Mg composites as compared to PMMA & PCL (Blue box: range of human cancellous bone moduli). Fig. 2 (Right): The percentage change of bone volume during the implantation period.

**DISCUSSION & CONCLUSIONS:** The results of *in-vitro* tests suggested that the new composites were well tolerated by bone cells and osteoconductive. In *in-vivo* experiment, new bone formation found in the composite with 0.1g Mg was significantly higher than that of PMMA at the early time points. It indicated the new bone substitutes could promote fast bone healing as compared to the conventional PMMA. Additionally, various compressive moduli of the new composites can be adjusted by incorporating different amounts of Mg particles into the material matrix in which these new substitutes are mechanically similar to the cancellous bone (50-800MPa)<sup>3</sup>. Hence, they potentially help reduce the post-op complications while using PMMA. In summary, we prove that the mechanical properties of the newly developed bone substitutes can be individualized according to patient's need. Also, the new composites are radiopaque, biodegradable and injectable that benefit for clinical applications.

**REFERENCES:** <sup>1</sup> DK. Ahn et al (2009) J Korean Orthop Assoc **44**:386-90. <sup>2</sup> S. Larsson et al (2002) Clin Orthop Relat Res **395**:23-32. <sup>3</sup> X. Banse et al (2002) J Bone Miner Res **17**:1621-28.

**ACKNOWLEDGEMENTS:** This project is financially support by Hong Kong Research Grant Council Competitive Earmarked Research Grant (#718507); Hong Kong Seed Funding for Basic Research

## Type I collagen coating improves implant osteointegration in vivo

[S Cecconi](#), [M Mattioli-Belmonte](#), [S Manzotti](#), [A Gigante](#)

*Dipartimento di Scienze Cliniche e Molecolari, [Università Politecnica delle Marche](#), Ancona, Italy.*

**INTRODUCTION:** Titanium is the material of choice for load-bearing, bone-contacting devices [1]. Coating of orthopaedic or dental implants with extracellular bone matrix components is performed to enhance bone healing [2]. Type I collagen, the major structural protein in bone, plays an important role in osteoblast cells behaviour and it could enhance the osteointegration of titanium devices [3].

**METHODS:** Type I collagen coated and uncoated titanium implants 4 mm wide and 8.5 mm long were inserted into the extra-articular bone of the distal femur of twelve skeletally mature New Zealand White Rabbits. Labelling of bone formation was performed by sequential intraperitoneal administration of three stains. After 45 and 90 days, specimens were embedded in a glycol methacrylate resin. Blocks were sectioned along a plane parallel to the long axis of the implanted screws for the histomorphometric (Fig 1), scanning electron microscopy (SEM) (Fig 2) and energy dispersive X-ray (EDX) analysis. Bone implant contact (BIC), trabecular thickness (Tb.Th) and calcium-phosphorus ratio were measured. Statistical analysis was performed by Student's t-test.

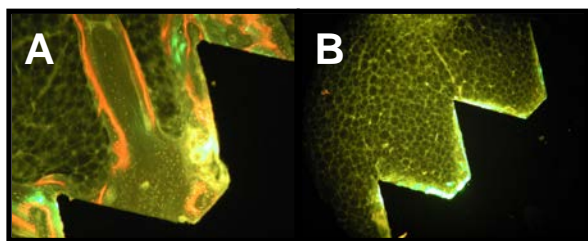


*Fig. 1: Fluorescence microscopy images at 40x magnification of representative titanium implants after 45 days of healing. A: Collagen I coated implant. B: Uncoated implant (control)*

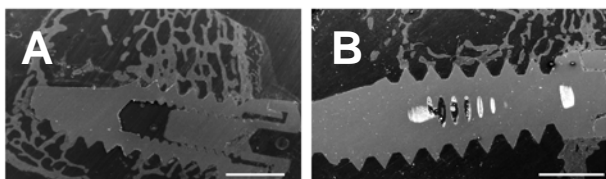


*Fig. 2: SEM images of representative titanium implants after 90 days of healing. A: Collagen I coated implant. B: Uncoated implant (control)*

**RESULTS:** All implants healed uneventfully without adverse reactions. After 45 days of implantation, significant differences ( $p < 0,05$ ) in BIC and Tb, Th were observed between the collagen-coated implants ( $55,6\% \pm 17,1$ ;  $108,7\mu\text{m} \pm 67,1$ ) and the uncoated implants ( $29,2\% \pm 20,1$ ;  $66,6\mu\text{m} \pm 48,6$ ). Also after 90 days of implantation, significant differences ( $p < 0,05$ ) in BIC and Tb, Th were observed between the collagen-coated implants ( $61,3\% \pm 2,1$ ;  $211,4\mu\text{m} \pm 80,8$ ) and the uncoated implants ( $35,7\% \pm 16,4$ ;  $150,9\mu\text{m} \pm 61,5$ ). No significant differences were measured in calcium-phosphorus ratio.

**DISCUSSION & CONCLUSIONS:** An accelerated stable fixation between bone and implant would allow early or immediate loading of the device, with significant implications in terms of decreased patient morbidity, patient psychology and health care costs [4]. These data indicate that titanium integration in trabecular or cortical bone can be enhanced by the surface collagen layer. Overall, this study confirms that biochemical modification of Ti surface can enhance the rate of bone healing due to an osteoconductive effect of the collagen itself.

**REFERENCES:** <sup>1</sup> OE. Pohler (2000) *Injury* **31**:7-13. <sup>2</sup> S Rammelt et al (2006) *Biomaterials* **27**:5561-5571. <sup>3</sup> M Mizuno et al (2000) *J Cell Physiol* **184**:207-213. <sup>4</sup> D Puleo et al (1999) *Biomaterials* **20**:2311-21.



## Bioactive PLGA/TCP/Icaritin composite scaffolds reduce incidence of joint collapse in steroid-associated osteonecrotic femoral head of bipedal emus

LZ Zheng<sup>1</sup>, G Zhang<sup>1</sup>, Z Liu<sup>1</sup>, M Lei<sup>2</sup>, XH Xie<sup>1</sup>, YX He<sup>1</sup>, L Huang<sup>1</sup>, DP Wang<sup>2</sup>, Y Chen<sup>2</sup>, L Qin<sup>1</sup>

<sup>1</sup> *Dept of Orthopaedics & Traumatology, the Chinese University of Hong Kong, HK.* <sup>2</sup> *Dept of Orthopaedics & Traumatology, Shenzhen Second People's Hospital, Shenzhen, China.*

**INTRODUCTION:** Bipedal emu is a desirable model for preclinical research of osteonecrosis and subsequent joint collapse because its hip joint biomechanics is similar to humans. Icaritin is a novel bioactive and osteogenic phyto molecule found in serum as a metabolite of phytoestrogenic herbal epimedium. This study is using emus to evaluate treatment efficacy of bioactive PLGA/TCP/Icaritin porous scaffolds implanted for repairing steroid-associated osteonecrosis (SAON) in emu femoral head after core decompression.

**METHODS:** Bioactive porous PLGA/TCP/Icaritin was fabricated using our established rapid prototyping technique [1]. Totally 15 adult male emus (30 hips) were used. SAON was induced by a combination of methylprednisolone (MPS) and Lipopolysaccharide (LPS)[2]. Twelve weeks after SAON induction, core decompression (bone tunnel) of a 6mm in diameter was created at proximal femur. A custom-made PLGA/TCP/Icaritin cylinder composite was implanted into the drill bone tunnel (P/T/I group, n=10) (Fig.1-A), respectively. PLGA/TCP was used as vehicle control (P/T group, n=10) and no scaffold implanted group was used as empty control (Control group, n=10). MRI test was performed to confirm the drill tunnel surgery (Fig.1-B). Twelve weeks after implantation, femora were collected and microCT was used to evaluate the femoral head collapse and local osteogenesis of the novel composite materials and its degradation in the bone tunnel.

**RESULTS:** No animal died after SAON induction. Femoral head collapse incidence was 70% in the Control group, 30% in the P/T group and 10% in the P/T/I group. Fisher's exact probability test showed that the collapse incidence in the P/T/I group was significantly lower than that in the Control group ( $p < 0.05$ ) (Fig.1-C). Within the bone tunnel, newly formed bone was found in P/T/I group and P/T group while almost no new bone formed in Control group in micro-CT images (Fig.2). Micro-CT quantitative analysis showed that the BMD and BV/TV of newly formed bone in tunnel in the P/T/I group were both significantly higher than those in the P/T group ( $p < 0.05$  for

both), indicating that PLGA/TCP/Icaritin composite scaffolds reduced incidence of the joint collapse in femoral head by enhancing the repair of SAON lesions in femoral head in bipedal emus. No pathological changes were observed macroscopically.

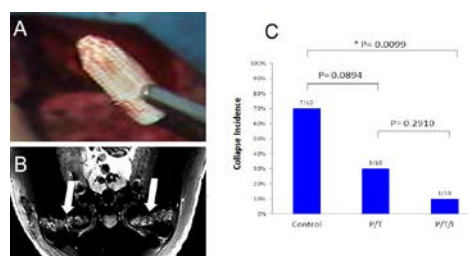


Fig. 1: Scaffold implantation (A), after its implantation (white arrow) (B) and collapse incidence in each group (C) (\* $P < 0.05$ ).

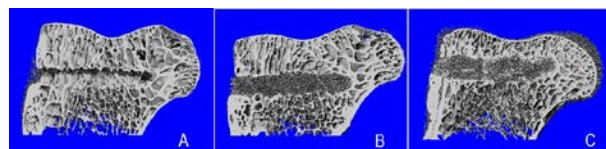


Fig. 2: Representative XtremeCT images of proximal femora. (A) Empty control group; (B) P/T group; and (C) P/T/I group.

**DISCUSSION & CONCLUSIONS:** This was the first efficacy study using bipedal emu model for prevention of joint collapse after core-decompression. Clinical trial registration is on the way before applying for SFDA approval for clinical research and applications. The innovative and bioactive PLGA/TCP/Icaritin porous scaffolds were able to reduce incidence of joint collapse in steroid-associated osteonecrotic femoral head of bipedal emus.

**REFERENCES:** <sup>1</sup>XH. Xie, XL. Wang, G. Zhang, et al (2010) *Biomed Mater* **5** 054109. <sup>2</sup>L. Qin, G. Zhang, J. Peng, et al (2010) *Bone* **47**:S352.

**ACKNOWLEDGEMENTS:** This work was supported by Hong Kong ITC (GHP/001/08 and ITF Tier 2 ITS/451/09FP).

## Biogenic hydroxyapatite from eggshell as bone formation material

K Balázs<sup>1</sup>, G Gergely<sup>1</sup>, C-H Chae<sup>2</sup>, H-Y Sim<sup>3</sup>, J-Y Choi<sup>4</sup>, S-G Kim<sup>5</sup>, C Balázs<sup>1</sup>

<sup>1</sup>Institute for Technical Physics and Materials Science, Research Centre for Natural Sciences, HAS, Budapest. <sup>2</sup>Department of Dentistry, Hallym University, 1 Hallymdaehak-gil, Gangwon-do, Korea. <sup>3</sup>Department of Orthodontics, SMG-SNU Boramae Medical Center, Korea <sup>4</sup>Department of Biochemistry and Cell Biology, Kyungpook National University, Jung-gu, Daegu. <sup>5</sup>Department of Oral and Maxillofacial Surgery, College of Dentistry, Gangneung-Wonju National University, Gangwondo, Korea

**INTRODUCTION:** One of perspective, non-expensive and environmental friendly material for Hap preparation is an eggshell. The eggshell is composed by calcium carbonate 94%, calcium phosphate 1%, organic matter 4% and magnesium carbonate 1% [1]. Bone replacements are frequently required to substitute damaged tissue due to any trauma, disease or surgery. Resorbable porous bioceramics, such as hydroxyapatite have been widely used as bone defect filling materials due to their remarkable biocompatibility and close chemical similarity to biological apatite present in bone tissues [2,3]. The aim of this work is to propose a simply method for producing HAp by mechanochemical activation from eggshells and study the bone regeneration of HAp successfully applied as bone graft for dental implants.

**METHODS:** The eggshells were collected and mechanically cleaned. The raw eggshells were calcinated at 900 oC in an air. The next 3 hours thermal treatment, calcium oxide formation from eggshells were obtained. To synthesize calcium phosphate powders, shells were crushed and milled by high efficient attritor mill (Union Process 01 HDDM) at 4000 rpm for 5 h. The shell : H<sub>3</sub>PO<sub>4</sub> ration was 50 : 50 wt%. The details of milling procedure is presenting in [4]. After milling, a small amount of HAp powders were heat treated at 900°C for 2 h in air atmosphere. For in vivo test, New Zealand white rabbits were used. This experiment was approved by the Institutional Animal Care and Use Committee of the Bioventure Incubation Center, Hanbat National University, Daejeon, Korea (No. 2009-NCT-003). Two 8-mm-diameter defects were created, one on each side of the midline. The graft – nHAp was placed on cavariial defects. Some defects were remained as empty as control at 4 and at 8 weeks.

**RESULTS:** Nanosized Hap (Fig. 1A) bioactivity was evaluated in animal (rabbit and mouse) models. After bilateral parietal bony defects formation (diameter: 8.0mm), nano-HAp was grafted. The control was unfilled defect. Results of bone regeneration evaluated by micro-computerized tomograms at 8 weeks are shown in Fig.1. HAp showed much more bone formation compared to unfilled control group in both micro tomographic and histomorphometric analysis.

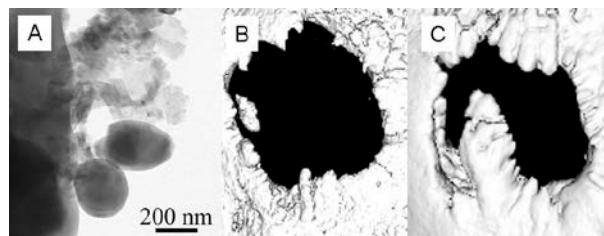


Fig. 1: A)TEM image of nano Hap, B Micro-computed tomography images of control grafted group and C)Hap grafted group at 8 weeks.

**DISCUSSION & CONCLUSIONS:** Nanosized hydroxyapatite was successfully produced from recycled eggshell and phosphoric acid by attritor milling. The study considering that the eggshell is easily available and cheap, nano-HAp from the eggshell can be good calcium source in tissue engineering.

**REFERENCES:** <sup>1</sup> E.M. Riviera et al. (1999) *Materials Letters* **41**: 128–34. <sup>2</sup> L.L Hench (1998) *J Am Ceram Soc* **81**:1705–28. <sup>3</sup> R. Cancedda, P. Giannoni, M. Mastrogiacomo (2007) *Biomaterials* **28**:4240–50. <sup>4</sup> G. Gergely, et al. (2010) *Ceram Inter* **36**: 803–6.

**ACKNOWLEDGEMENTS:** OTKA 76181, BioGreen21 (grant no. 200810FTH01 0103002 and 200810FTH010102001), by the János Bolyai Research Scholarship of the Hungarian Academy of Sciences and OTKA PD 101453.

## Angiogenesis and inosculation in bone tissue engineering

MW Laschke

*Institute for Clinical & Experimental Surgery, University of Saarland, 66421 Homburg/Saar, Germany*

One of the key challenges in bone tissue engineering is the establishment of an efficient vascularisation, because long-term survival and function of cells within bone constructs crucially depends on an adequate blood supply after their implantation. To achieve this goal, two principal vascularisation strategies have been pursued in the field of tissue engineering during the last years, i.e. angiogenesis and inosculation.

Angiogenesis, the development of new microvessels from pre-existing ones, is a multi-step process, which is well regulated by the close interaction of humoral and cellular mechanisms. Several approaches are currently under consideration, which may be suitable to stimulate this process after implantation of a tissue construct and, thus, to optimise the ingrowth of new blood vessels from the surrounding host tissue into the implant [1]. These include the modification of the chemical composition and architecture of scaffolds as well as their bioactivation by incorporation of growth factor delivery systems or by seeding them with different cell types.

However, a general problem of pro-angiogenic approaches is the fact that the development of new blood vessels underlies specific biological kinetics, which can only be accelerated to a limited extent. Accordingly, even highly effective approaches will not be able to prevent hypoxia-induced cell death in larger three-dimensional tissue constructs during the initial days after implantation.

Inosculation represents a promising strategy to overcome this problem. The basic principle of this strategy is the generation of a preformed microvascular network within a tissue construct prior to its implantation. This bears the advantage that the preformed network simply has to develop interconnections to the host microvasculature at the implantation site to get fully reperfused within a short period of time [2].

During the last years, we have established a novel approach, which allows for the *in vivo* analysis of angiogenesis and inosculation of implanted scaffolds for bone tissue engineering. For this purpose, nano-size hydroxyapatite particles /

poly(ester-urethane) scaffolds are implanted for 20 days into the flank of green fluorescent protein (GFP)-positive mice to generate *in situ* prevascularised tissue constructs with GFP-positive microvessels. Subsequently, the prevascularised constructs are carefully excised and transferred into the dorsal skinfold chamber of wild-type recipient mice to study their inosculation and vascularisation by means of intravital fluorescence microscopy and immunohistochemical techniques.

Using this approach, we could demonstrate that the establishment of blood perfusion in prevascularised constructs is markedly accelerated and improved by inosculation when compared to non-prevascularised controls. Moreover, we could show that the inosculation process can be further optimised by short-term precultivation of tissue constructs prior to their implantation [3] or by embedding them in a pro-angiogenic extracellular matrix [4]. However, we also found that even the strategy of inosculation cannot guarantee an adequate blood perfusion during the very first days after construct implantation. Accordingly, this approach may be combined in the future with preconditioning methods, which increase the ischemic tolerance of cells inside tissue constructs. In addition, it may be possible to generate prevascularised constructs with vascular pedicles, which can be microsurgically anastomosed to the blood vessels of the host defect site.

**REFERENCES:** <sup>1</sup> M.W. Laschke, Y. Harder, M. Amon, I. Martin, et al. (2006) *Tissue Eng* **12**:2093-104. <sup>2</sup> M.W. Laschke, B. Vollmar, M.D. Menger (2009) *Tissue Eng Part B Rev* **15**:455-65. <sup>3</sup> M.W. Laschke, H. Mussawy, S. Schuler, A. Kazakov, et al. (2011) *Tissue Eng Part A* **17**:841-53. <sup>4</sup> M.W. Laschke, H. Mussawy, S. Schuler, D. Eglin, et al. (2010) *Eur Cell Mater* **20**:356-66.

## Osteogenesis and angiogenesis coupling: the dialogue between human endothelial progenitor cells and mesenchymal stem cells

J. Amédée Vilamitjana

joelle.amedee@inserm.fr

*Inserm U1026, University Bordeaux Segalen, Tissue Bioengineering, Bordeaux, France*

**INTRODUCTION:** Members of the scientific community in the field of stem cell biology and tissue engineering have investigated the importance of the bone vasculature in osteogenesis. For ten years, data demonstrated that an intimate functional relationship exists between bone vascular endothelium and osteoblasts (OBs) and that this cell-to-cell communication could be crucial to the coordinated cell behavior necessary for bone development and remodeling. This hypothesis was substantiated by histological findings indicating that OBs are always located adjacent to endothelial cells (ECs) in blood vessels at the site of new bone formation. However, *in vivo*, communication between the bone forming cells and the ECs through direct cell contact remains unclear. This study discusses the mode of cross talk that could explain the observed cell coupling between the EC and OB lineages [1-3]. This cross talk leads to the hypothesis that bone vascular ECs might be essential in that they contribute to the intricate communication pathways that are operative in bone and that link different cell types via diffusible signaling molecules as well as by cell contact-mediated mechanisms. As extending this principle to bone tissue engineering, it appears crucial to establish a vascular network that temporally precedes new bone formation and provides a metabolically active bone graft. Then, the knowledge of the exchanges between the bone forming cells and the blood vessel forming cells appears fundamental for improving bone tissue engineering approaches.

**METHODS:** ECs (progenitors isolated from peripheral blood or differentiated endothelial cells i.e Human Umbilical Vein Endothelial cells) with human mesenchymal stem cells isolated from bone marrow or adipose tissue were co-cultured in two dimensional (2D) in plastic culture dishes or in matrices as three dimensional (3D) carriers for these stem cells. The production of soluble growth factors was quantified by ELISA, the presence of junctional proteins was analyzed by immunofluorescence and Western blot while their role in the coupling between angiogenesis and osteogenesis was demonstrated using blocking

antibodies against these junctional proteins or using specific inhibitory peptides against Cx43. The co-culture was performed from day 1 to day 12 in 2D or 3D.

**RESULTS:** Our co-culture models allow us to identify molecular actors required for controlling both osteogenesis and angiogenesis. The dialogue between endothelial and osteoprogenitor lineages, both in 2D and 3D co-cultures, is initiated by a migration of ECs, the production of uPA, VEGF165 and MMPs activities leading to a specific cell organization. This network contributes to cell interactions and formation of junctional activities between ECs, osteoprogenitor cells and between ECs and osteoprogenitor cells that regulate their respective activities. In 3D, the use of matrices that promotes these cellular interactions increases the kinetic of osteogenic differentiation and bone formation.

### DISCUSSION & CONCLUSIONS:

Understanding the course of angiogenesis and the relation with osteogenesis provides fundamental basis upon which we can build and optimize new vessel growth in a bone substitute. The development of 3D matrices that mimic tissue complexities and favor the cell communication should then provide a benefit for medical advancements in bone regenerative medicine.

**REFERENCES:** [1] Li H et al, *The role of vascular actors in two dimensional dialogue of human bone marrow stromal cell and endothelial cell for inducing self-assembled network.* PLoS One. 2011, 3;6(2):e16767. [2] Li H et al. *Role of neural-cadherin in early osteoblastic differentiation of human bone marrow stromal cells cocultured with human umbilical vein endothelial cells.* Am J Physiol Cell Physiol. 2010;299(2):C422-30. [3] Grellier M et al. *Cell-to-cell communication between osteogenic and endothelial lineages: implications for tissue engineering.* Trends Biotechnol. 2009;27(10):562-71.

**ACKNOWLEDGEMENTS:** Thanks to Inserm, to University Bordeaux Segalen and to the French National Research Agency for financial support.

**Co-seeding of EPC/MSC in 3D scaffolds (Endothelial Progenitor Cells / Mesenchymal Stem Cells) promotes implant's neovascularization: evidence of pericytes' participation.**

Verrier S<sup>1</sup>, Duttonhoefer F<sup>1,2</sup>; Egli S<sup>1</sup>; Benneker L<sup>3</sup>; Richards G<sup>1</sup>; Alini M<sup>1</sup>;

<sup>1</sup> [AO Research Institute](#), AO Foundation, Davos, CH. <sup>2</sup> Department of Oral and Maxillofacial Surgery, Albert-Ludwigs-University, Freiburg, Germany

<sup>3</sup> Department of Orthopaedic Surgery, Inselspital, University of Bern, Bern Switzerland

**INTRODUCTION:** Angiogenesis is a key factor in early stages of wound healing and is also crucial for tissue regeneration. In cases of large bone defect, to date most of the efforts have been focused on the filling of the gap with autologous bone grafts, or various bio-active materials associated or not with bone forming cells. However, vessels' ingrowth from nearby tissues and therefore implant neo-vascularization is insufficient in most large defect healing. In the present study we developed an in vitro pre-vascularized 3D polyurethane (PU) implant based on the association of Endothelial Progenitor Cells (CD34+ and CD133+) with Mesenchymal Stem Cells (MSC) both autologous.

**METHODS:**

MSCs were isolated by Ficoll-Paque density-gradient centrifugation from human bone marrow (KEK\_Bern126/03). EPCs (CD133+/CD34+) were isolated from MSC fractions using magnetic-activated cell sorting (MACS®). For 2D Matrigel® assays, MSC and EPCs were pre-stained using PKH26-red® and PKH67-green® respectively before seeded either alone or in combination. In 3D set-up, cells in different proportions were embedded in autologous growth factor rich gel (Platelet Rich Plasma) and seeded in PU scaffolds. Constructs were cultured in different media (osteogenic, angiogenic, or mixed), and after 7 days, some samples were analysed in histology (toluidine blue, endothelial-cell-, pericyte-specific antibodies), while other were implanted subcutaneously in nude mice and sacrificed at 8 weeks.

**RESULTS:**

On growth factor reduced Matrigel® we could observe rapid formation of cellular networks in which EPC and some of the MSC population participated. The MSC enrolled in these cells re-organizations showed positive staining with CD146 specific antibody.

In 3D scaffolds, the formation of luminal tubular structures in the co-seeded scaffolds as early as

day 7 in culture could be observed. These tubular structures were proven positive for endothelial markers vWF and PECAM-1. Of special significance in our constructs is the presence of CD146 positive cells, as a part of neo-vasculature scaffolding. These cells coming from the mesenchymal stem cells population (MSC or EPC-depleted-MSC) also expressed further markers of pericytes cells (NG2 and  $\alpha$ SMA), known to have a pivotal function in the stabilization of new formed pre-vascular network. In parallel, in co-cultures, osteogenic differentiation of MSC occurred earlier as in MSC monoculture, suggesting the close cooperation between the two cell populations in each other's differentiation and function.

**DISCUSSION & CONCLUSIONS:**

In conclusion, we were able to demonstrate the beneficial effect of MSC and EPC (CD34+ and CD133+) 3D co-culture on each other differentiation toward a functional osteoblastic- and endothelial phenotype respectively. The cell culture medium has proven to be as important as the cells co-seeding. The presence of angiogenic factors (from autologous platelet lysates) in association with osteogenic factors seems to be crucial for this synergy.

## Proposed evolution of bone tissue engineering strategies

I Martin, M Jakob, A Papadimitropoulos, C Scotti, D Wendt, A Scherberich

*University Hospital Basel, CH4031 Basel - Switzerland*

**INTRODUCTION:** Despite the large clinical needs in bone regeneration and the advances in scaffold production and regulation of osteoprogenitor cell function, the adoption of cell-based bone graft substitutes in the clinical practice is yet limited<sup>1</sup>. Indeed no study has yet convincingly demonstrated reproducible clinical performance of tissue engineered bone graft substitutes and at least equivalent cost-effectiveness as compared to the current treatment standards. This lecture will describe and discuss three alternative approaches currently pursued by the author's team to evolve classical tissue engineering paradigms towards possibly more effective products.

**1. BIOREACTOR-BASED CELLULAR GRAFT MANUFACTURE:** Bioreactors have been proposed as a possible tool to develop cell-based therapeutic approaches towards a broader clinical adoption<sup>2</sup>. The possibility of controlled culture conditions would improve the bio-process regulation and minimize the graft product variability. Monitoring systems would be instrumental to implement traceability and safety compliance, whereas process automation would target standardization, scaling-up and possibly cost-effectiveness. The latter represents the critical and ultimate target among the various criteria for reimbursement policies by healthcare systems. Moreover, the implementation of bioreactor technology could introduce changes in the manufacturing process to improve the cell quality as compared to current standards, possibly by generating more physiological 'niche' environments<sup>3</sup>

**2. INTRA-OPERATIVE CELLULAR GRAFT MANUFACTURE:** The approach derives from the attractive opportunity to eliminate the resource- and time-consuming in vitro expansion phase and to instead use the body of the patient as an in vivo bioreactor system to support the expansion and the differentiation of cells, freshly harvested and directly transplanted into the bone defect. In this context, the freshly-isolated stromal vascular fraction (SVF) of human adipose tissue might represent a suitable cell source for a one-step surgical procedure, thanks to an up to 100-fold higher number of clonogenic progenitors per

volume of tissue sample as compared to human bone marrow and the presence of endothelial lineage cells. The latter populations would play a crucial role in graft vascularization, instrumental for graft size scale-up.<sup>4</sup>

**3. 'DEVELOPMENTAL ENGINEERING':** The approach relies on the biological rationale of recapitulating normal bone regeneration, which typically follows the process of endochondral ossification. In a bone developmental engineering perspective, this means that the engineered graft would be a 'committed cartilage template', duplicating the critical stage of bone development by inducing the processes of vasculogenesis, remodeling and ultimately bone formation<sup>5</sup>.

**DISCUSSION & CONCLUSIONS:** The perspective highlights three of many possible other experimental strategies to evolve the classical tissue engineering paradigm into strategies of broader clinical adoption. The parallel pursue of different and possibly combined approaches, together with the understanding of their mechanisms of action, will be crucial to identify the necessary and sufficient set of signals that need to be delivered at the bone defect site. This should thus form the basis to define release criteria for reproducibly cost-effective engineered bone graft substitutes.

**REFERENCES:** <sup>1</sup>I Martin et al (2011) The survey on cellular and engineered tissue therapies in Europe in 2009. *Tiss Eng-A* **17**: 2221-2225. <sup>2</sup>I Martin et al (2009) Bioreactor-based roadmap for the translation of tissue engineering strategies into clinical products. *Trends Biotechnol.* **27**:495-502. <sup>3</sup>A Braccini, et al (2005) Three-dimensional perfusion culture of human adipose tissue-derived endothelial and osteoblastic progenitors generates osteogenic constructs with intrinsic vascularisation capacity. *Stem Cells* **25**:1823-1829. <sup>4</sup>AM Müller et al (2010) Towards an intraoperative engineering of osteogenic and vasculogenic grafts from the stromal vascular fraction of human adipose tissue. *Eur Cell Mater.* **19**:127-35. <sup>5</sup>C Scotti et al. (2010) Recapitulation of endochondral bone formation using human adult mesenchymal stem cells as a paradigm for developmental engineering. *Proc Natl Acad Sci U S A.* **107**:7251-7256

## Dental Pulp stem cells for bone tissue engineering

G Papaccio<sup>1</sup>

<sup>1</sup>Department of Experimental Medicine, Section of Histology and Embryology, School of Medicine, Second University of Naples, Naples, Italy

**INTRODUCTION:** Dental pulp stem cells (DPSCs), originating from neural crests, can be found within dental pulp. Up to now, it has been demonstrated that these cells are capable of producing bone tissue, both *in vitro* and *in vivo* and differentiate into adipocytes, endotheliocytes, melanocytes, neurons, glial cells, and can be easily cryopreserved and stored [1]. Moreover, recent attention has been focused on tissue engineering and on the properties of these cells [2]. In addition, adult bone tissue with good vascularisation has been obtained *in vivo* studies [3]. Their successful use in clinical trials for human mandible bone repair enforces the notion that DPSCs can be used successfully in patients [4].

**METHODS:** Dental pulp was digested in collagenase and dispase and DPSCs were isolated by CD34 and CD117 surface expression at cytometric sorting. At a different times of culture in DMEM at 20% FBS, DPSCs were analysed for both bone and endothelial differentiation markers including osteocalcin, osteopontin, Runx2, collagen and bone alkaline phosphatase and stained with Alizarin red S (bone markers), VEGF, PECAM-1, von-Willebrand and CD54 (endothelial markers). DPSCs were also cultured in adipogenic, chondrogenic, neural, muscle and melanocyte media for 21 days and then analysed for adiponectin, II Type collagen, Tuj-1, SMA, MART-1 and L-DOPA. In addition, DPSCs were loaded on PLGA, collagen sponges, titanium and biocoral scaffolds to evaluate the effect on these biomaterials on DPSCs differentiation. Moreover, DPSCs loaded with PLGA were also injected in murine models. Finally, DPSCs loaded on collagen sponges were used in regeneration of small mandible bone defects after extraction of third molar in consenting human patients according to Internal Ethical Committee Guidelines of Second University of Naples.

**RESULTS:** DPSCs cultured in DMEM at 20% FBS was able to differentiate in osteoblasts forming bone tissue after 30 days of culture. Tissue sections were positive for bone markers and Alizarin Red S. Under differentiation media, they differentiate in adipocytes, chondrocytes, neuronal cells, smooth muscle cells and melanocytes as confirmed by positivity for

adiponectin, II Type collagen, Tuj-1, SMA, MART-1 and L-DOPA. Loaded on scaffolds, DPSCs formed bone tissue well structured on microconcavity surface textures. In murine grafts, adult human bone tissue with good vascularization was obtained as confirmed by I Class HLA, osteocalcin, osteonectin, BSP, von-Willebrand and PECAM-1 positivities. Three months after autologous DPSC grafting, alveolar bone of patients had optimal vertical repair and complete restoration of periodontal tissue back to the second molars, as assessed by clinical probing and X-rays. Histological observations clearly demonstrated the complete regeneration of bone at the injury site. Optimal bone regeneration was evident one and three years after grafting also at the synchrotron observations.

**DISCUSSION & CONCLUSIONS:** DPSCs can be found within the “cell rich zone” of dental pulp. Their embryonic origin, from neural crests, explains their multipotency. On scaffolds, DPSCs show good adherence and bone tissue formation. In graft, DPSCs co-differentiate in bone tissue and endotheliocytes. The clinical study demonstrates that a DPSCs/collagen sponge biocomplex can completely restore human mandible bone defects and indicates that this cell population could be used for the repair and/or regeneration of tissues and organs. We are now studying epigenetic modifications involved in bone differentiation and evaluating the biologic behavior of DPSCs co-cultured with dental follicle stem cells, in collaboration with the Oral Biology of Zurich University: the results obtained up to now are of great interest.

**REFERENCES:** <sup>1</sup> F Paino, G Ricci, A De Rosa, et al (2010) Eur Cell Mater. 20:295-305. <sup>2</sup> C Mangano, A De Rosa, V Desiderio, et al. (2010) Biomaterials. 2010 31:3543-51. <sup>3</sup> R d'Aquino, A Graziano, M Sampaolesi, et al (2007) Cell Death Differ. 14:1162-71. <sup>4</sup> R d'Aquino, A De Rosa, V Lanza, et al. (2009) Eur Cell Mater.18:75-83.

### ACKNOWLEDGEMENTS:

Prof. Mauro Alini and prof. Thimios Mitsiadis are kindly acknowledged.

## Developmental engineering of a bone organ with human adult mesenchymal stem cells

C Scotti<sup>1</sup>, E Piccinini<sup>1</sup>, A Papadimitropoulos<sup>1</sup>, P Bourguine<sup>1</sup>, A Todorov<sup>1</sup>, A Barbero<sup>1</sup>, I Martin<sup>1</sup>

<sup>1</sup> *Departments of Surgery and of Biomedicine, University Hospital, Basel, Switzerland*

**INTRODUCTION:** Adult human Mesenchymal Stromal Cells (hMSC) have typically been used to engineer bone by a process resembling intramembranous ossification. However, most bones develop and repair through endochondral ossification. In addition, endochondral ossification presents several advantages for bone regeneration such as osteogenic performance, resistance to hypoxic environment, vasculogenic potential and, therefore, efficiency of engraftment. In this study, we aimed at developing an upscaled endochondral bone organ model by using hMSC.

**METHODS:** Human MSC were expanded for 2 passages, seeded onto 8mm diameter, 2 mm thick collagen sponges (Ultrafoam<sup>TM</sup>), cultured for 5 weeks *in vitro* under chondrogenic and hypertrophic conditions, implanted subcutaneously in nude mice and then retrieved after 5 and 12 weeks *in vivo*. Samples were analyzed by histology (Safranin-o; Alizarin red; H&E; TRAP), IHC (Collagen I, -II, -X, BSP; MMP9, MMP13, DIPEN), biochemistry (GAG; DNA; Calcium), ISH for human Alu sequences and quantitative  $\mu$ CT. Bone marrow was extracted from the samples after 12 weeks *in vivo* by mechanical crushing and cells were characterized by flow cytometry for phenotype, and cultured in methylcellulose (MethoCult<sup>®</sup>).

**RESULTS:** *In vitro*, samples showed a mineralized collar, rich in Collagen I and BSP, and a hypertrophic core, rich in proteoglycans and Collagen X. *In vivo*, extensive remodelling, with mature vessel ingrowth (CD31+, NG2+) and osteoclast (TRAP+ and MMP9+ multinucleated cells), took place. Bone formation displayed a peculiar topography: at the periphery of the samples, perichondral bone was formed, corresponding to the *in vitro* pre-mineralized outer ring; in the core of the samples, endochondral bone was formed, corresponding to the *in vitro* non-mineralized cartilaginous areas. Importantly, abundant presence of bone marrow was described. Human cells could be still detected after 12 weeks *in vivo*, mainly in the bone in the core of the samples (Fig.2). Bone marrow was characterized by presence of Lin-, Sca1+, c-Kit+ (LSK) cells,

and gave rise to colonies in methylcellulose culture, suggesting presence of host-derived hematopoietic progenitors within the engineered endochondral bone *in vivo*. Both percentage of LSK cells and number of colonies were comparable to those of the native bone marrow extracted from mice femurs.

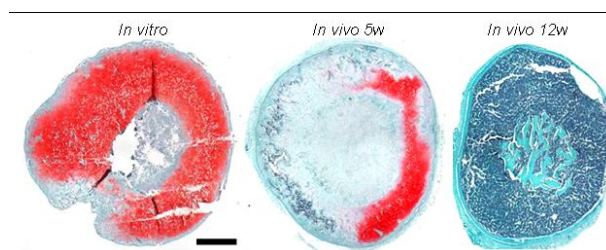


Fig. 1: Safranin-o/Fast Green staining showing remodeling of the cartilaginous template into bone with abundant bone marrow. Scale bar = 1mm.

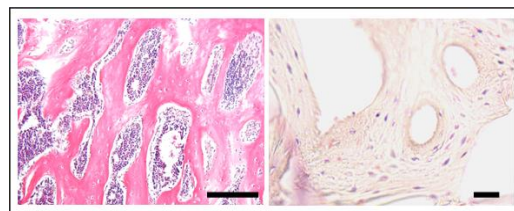


Fig. 2: H&E showing the trabecular structure of the endochondral bone (left) and ISH for human Alu sequences showing survival of human cells in the endochondral bone. Scale bar = 200 $\mu$ m.

**DISCUSSION & CONCLUSIONS:** This work demonstrates that hMSC can generate endochondral bone that has features of a “bone organ” in an upscaled, ceramic-free model. The engineered tissue was capable to host hematopoietic progenitors, suggesting the formation of a bone marrow niche. The findings are relevant towards (i) a clinically-sized endochondral grafts capable of enhanced bone repair and (ii) ectopic bone marrow niches to study hematopoiesis, also in pathologic conditions.

**REFERENCES:** <sup>1</sup>Scotti C, Tonnarelli B, Papadimitropoulos A, et al (2010) Recapitulation of endochondral bone formation using human adult mesenchymal stem cells as a paradigm for developmental engineering. *Proc Natl Acad Sci U S A* **107**(16):7251-6.



## A comparison of endochondral ossification by vessel derived stem cells and mesenchymal stem cells in wild type and ApoE<sup>-/-</sup> mice

Aleksandra Leszczynska<sup>1</sup>, Eric Farrell<sup>1</sup>, Aideen O'Doherty<sup>2</sup>, Fergal O'Brien<sup>3</sup>, Timothy O'Brien<sup>1</sup>, Mary Murphy<sup>1</sup>

<sup>1</sup>Regenerative Medicine Institute, <sup>2</sup>National Centre for Biomedical Engineering Science  
National University of Ireland, Galway, Ireland

<sup>3</sup>Department of Anatomy, Royal College of Surgeons in Ireland, Dublin Ireland

**INTRODUCTION:** Pericytes, although traditionally considered supporting cells, have recently been proposed to have a more active role in the repair and pathogenesis of various vascular diseases. There is growing body of research work indicating that the vessel wall contains a number of progenitor cell niches that remain as yet incompletely defined. In this study, we hypothesised that a pericyte-like stem cell population, termed vessel derived stem cells or VSCs with chondrogenic and osteogenic potential exist in the vessel wall and contribute, along with the circulating mesenchymal stem cells (MSCs), to the calcification of atherosclerotic plaques via endochondral ossification.

**METHODS:** VSCs from aortae of ApoE<sup>-/-</sup> mice and background C57BL/6 mice were isolated and characterised for cell surface markers by flow cytometry and immunocytochemistry. MSCs from bone marrow of these mice were also isolated and characterized. To assess the ability of VSCs and MSCs from normal and ApoE<sup>-/-</sup> mice to form bone, cells were seeded onto collagen-chondroitin sulphate scaffolds and primed chondrogenically *in vitro* followed by subcutaneous implantation for 8 weeks.

**RESULTS:** VSCs were strongly positive for Sca-1, CD44 and negative for CD31 and CD34. Immunocytochemistry for specific pericyte marker 3G5 revealed that a sub-population of VSCs expressed 3G5. Differentiation assays demonstrated the ability of the cells to differentiate into bone and cartilage. VSCs had significantly higher GAG/DNA ratio than MSCs indicating increased chondrogenesis. Chondrogenically primed constructs from both cell types (VSCs and MSCs) showed the ability to form bone by endochondral ossification *in vivo* in both ApoE<sup>-/-</sup> and C57BL/6 mice (Fig. 1).

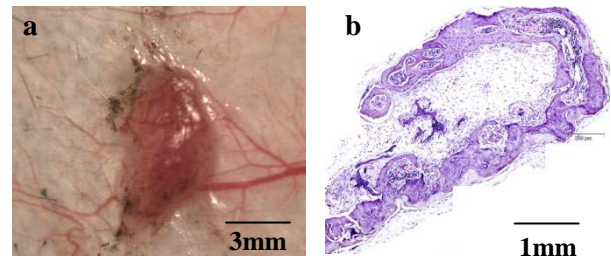


Fig. 1: Vascularised construct upon retrieval after 8 weeks (a) and representative H&E image showing endochondral bone formation (b) after 8 weeks *in vivo*.

**DISCUSSION & CONCLUSIONS:** That both MSCs and VSCs from the ApoE<sup>-/-</sup> atherosclerotic mice generate a more mature hypertrophic chondrocyte than cells from the C57BL/6 mice is interesting and suggests that the atherosclerotic environment may modulate the stem cell phenotype. Col-type II and aggrecan expression are being investigated to further test this hypothesis. Assessment of quantity and quality of bone formed is currently being performed.

**ACKNOWLEDGEMENTS:** This work was carried out with the support of the Irish Research Council for Science Engineering and Technology and Science Foundation Ireland.

## bone formation using autologous bone marrow derived mononuclear cells combined with $\beta$ -tricalcium phosphate ( $\beta$ -TCP) and absorbable atelocollagen for the treatment of aneurysmal bone cyst of the humerus in child

D Bulgin<sup>1</sup>, B Nemeč<sup>2</sup>, E Hodžić<sup>1</sup>

<sup>1</sup> [ME-DENT, The Center for Regenerative Medicine, Rovinj, Croatia.](#) <sup>2</sup> [Hip & Knee Clinic, Opatia, Croatia](#)

**INTRODUCTION:** Aneurysmal bone cyst (ABC) is a benign, locally destructive lesion of bone. Common methods of treatment vary considerably in the literature, particularly in children. After extensive curettage and surgical removal of pathologic tissue the healing stage of ABC might be triggered by introduction of an osteoinductive material into the cyst [1]. A large variety of bone substitutes have been used to fill the cystic lesions. To date there has been no graft material which can be regarded as completely satisfactory. Our experience with freshly isolated autologous bone marrow derived mononuclear cells (BMMNCs) combined with  $\beta$ -TCP and absorbable atelocollagen for bone formation is presented.

**METHODS:** The patient is 10-year old female after radiological evaluation and biopsy-proven aneurysmal bone cyst of the right humerus. The curettage and removal of pathologic tissue of the lesion associated with filling of the local bone defect by bone substitute scaffolds combined with autologous BMMNCs were performed under general anesthesia.

The bone substitute materials/scaffolds were:

- OSferion® (G1 type, Olympus Terumo Biomaterials Corp., Tokyo, Japan) is a white porous  $\beta$ -TCP granules with 75% porosity;
- the atelocollagen sponge Terudermis® (Terumo Corp., Tokyo, Japan), a cross-linked collagen material with large pores that permit cellular entry and is degraded *in vivo*.

Autologous bone marrow from patient used as a source for BMMNCs. Under general anesthesia 50.0 ml of the bone marrow was harvested from posterior iliac crest. BMMNCs were separated from autologous bone marrow according to Generic Volume Reduction Protocol by using Cell Separation System SEPAX S-100 (Biosafe Group SA, Switzerland). Postoperative follow-up was uneventful and no complications were observed. The final result was classified as healing according to clinical and radiographic criteria.

**RESULTS:** The ABC is demonstrating healing within the next 12 months post-operatively as documented by radiological examinations follow-

up (Fig. 1). The cyst enlargement ceased, a peripheral osseous shell appeared around the ABC within the first three months postoperatively, the bone substitute materials were gradually replaced by progressive ossification of the cyst, and lesion became nonpainful.



*Fig. 1: Healing period of the ABC. a, preoperative; b, 1 month postoperative; c, 3 months postoperative; d, 7 months postoperative; e, 12 months postoperative.*

**DISCUSSION & CONCLUSIONS:** Defect repair and bone ingrowth, maturation, and modeling are cell-mediated processes [2]. Most clinical trials report successful bone regeneration after the application of mixed cell populations from bone marrow. The autologous application of human bone marrow cells which are not expanded *ex vivo* has medico-legal advantages [3]. Scaffolding by  $\beta$ -TCP and collagen-based material combined with autologous BMMNCs has shown to be effective in bone regeneration. The concept of this treatment are based on stimulation of natural events continuously present in living bone appear to be a reasonable and beneficial alternative to promote healing of bone cysts and offering both osteoinduction and osteoconductive features.

**REFERENCES:** <sup>1</sup> K.F. Spence, K.W. Sell, R.H. Brown (1969) *J Bone Joint Surg Am* **51**:87-96. <sup>2</sup> P. Hinz, E. Wolf, et al (2002) *Orthopedics* **25**:597-600. <sup>3</sup> M. Jäger, P. Hernigou, C. Zilkens, et al (2010) *Orthop Rev* **2**:79-87.

**ACKNOWLEDGEMENTS:** The authors would like to thank Mr. Kazuhito Ikegami, and Mr. Toshihisa Iwanaga, for contribution to the case report.

## Pig as large animal model for cell therapy in bone tissue engineering

T Schubert<sup>1,2</sup>, D Xhema<sup>1</sup>, S Lafont<sup>2</sup>, G Beaurin<sup>2</sup>, P Gianello<sup>2</sup>, D Dufrane<sup>1</sup>.

<sup>1</sup> Centre of Tissue and Cell Therapy, Saint-Luc University Clinics, Université Catholique de Louvain, Brussels, Belgium.

<sup>2</sup> Laboratory of Experimental Surgery, Experimental and Clinical Research Institute, Université Catholique de Louvain, Brussels, Belgium.

### INTRODUCTION:

Autologous Adipose Mesenchymal Stem Cells (AMSCs) have been proposed for bone tissue engineering. We have demonstrated the feasibility of a Three Dimensional graft made of osteogenic differentiated AMSCs<sup>1</sup>. Two surgical models were developed in pigs to assess the potential of this autograft: (i) a multi-level spinal fusion and (ii) a femoral non-union.

### METHODS:

(i) Spine fusion (n=6): a 4 levels Anterior Lumbar Interbody Fusion procedure was achieved through a left lumbotomy. Intervertebral PEEK cages were inserted laterally. Four experimental groups were designed: 1 empty cage and 3 other spaces filled with freeze-dried (FD) irradiated cancellous bone graft, autologous bone graft or a 3D osteogenic differentiated AMSCs autograft, respectively. The spine model was designed to assess the early phase of ossification: 4 pigs were sacrificed at 8w and the two remaining at 12w post implantation.

(ii) Femoral non-union (n=4): a lateral approach was used to create a femoral defect of 1,5 folds the diameter of the femur stabilized by two 4,5mm titanium Locking Compression Plates (LCP). The non-union was assessed at 6 months post-surgery. All fibrous tissues were then removed, bone stumps were heightened and a 3D osteogenic differentiated AMSCs autograft was implanted.

CT-scans were performed every 4 weeks for in vivo follow-up. After sacrifice, explanted tissues were analyzed by micro CT-Scan ( $\mu$ CT), micro radiography ( $\mu$ RX), histomorphometry (Hemalun-Eosin, Masson's trichrom, Methylene Blue-Fuchsin) and immunohistochemistry for Osteocalcin and Vascular Endothelial Growth Factor (VEGF).

### RESULTS:

(i) Spine fusion: No spontaneous fusions were observed at 12w. FD grafts showed bone resorption between 8 and 12w as demonstrated by  $\mu$ CT ( $194.3 \pm 62.9$  mg/cm<sup>3</sup> vs  $141.1 \pm 53.3$

mg/cm<sup>3</sup>,  $P < 0.001$ ),  $\mu$ RX and histology. Similarly, autologous bone graft also demonstrated bone resorption ( $280.6 \pm 68$  mg/cm<sup>3</sup> vs  $248.8 \pm 88.7$  mg/cm<sup>3</sup>,  $P < 0.05$  at 8 vs 12w, respectively). Bone growth was observed within cages implanted with osteogenic differentiated AMSCs ( $\mu$ CT:  $149.5 \pm 23.2$  vs  $169.8 \pm 42.7$  mg/cm<sup>3</sup> at 8 vs 12w, respectively,  $P < 0.001$ ) in which histology showed bone ingrowth within the cage and  $\mu$ RX demonstrated the mineralization of the tissue.

(ii) Femoral non-union: intervention with 1 LCP led to a loss of stabilization before 8 weeks. With 2 plates, four non-unions of the femoral shaft were obtained at >6months, demonstrated by CT-scan and the presence of fibrotic tissue in the defect. In one pig, osteogenic differentiated AMSCs were implanted into the bone defect and bone fusion was observed at 5 months. Explanted tissue showed bone bridging on  $\mu$ CT and  $\mu$ RX. Bone and chondrocyte-like tissue found at the implantation site demonstrated endochondral ossification. Three pigs implanted with 3D differentiated autologous AMSCs are currently in progress of consolidation.

### DISCUSSION & CONCLUSIONS:

Two surgical models on pigs were developed to assess the potential of a 3D autologous AMSCs bone graft. No spontaneous fusion did occur in both models. Three-D differentiated AMSCs demonstrated bone formation at our implantation sites. Our femoral non-union model demonstrates the potential of our 3D engineered graft to induce bone fusion in a fibrotic unfavourable environment.

### REFERENCES:

1. Dufrane, D. & Delloye, C. Multi-dimensional biomaterial and method for producing the same. PCT/EP2010/057847 (2010).

**ACKNOWLEDGEMENTS:** This work was supported by grants of the Saint-Luc and Salus Sanguinis Foundations.

## Notch signalling regulates osteoblastogenesis and bone regeneration

MI Dishowitz<sup>1</sup>, F Zhu<sup>2</sup>, D Dopkin<sup>2</sup>, CB Bales<sup>3</sup>, KM Loomes<sup>3</sup>, J Ahn<sup>4</sup>, KD Hankenson<sup>1,2,4</sup>

<sup>1</sup>Graduate Program in Bioengineering, School of Engineering and Applied Sciences, <sup>2</sup>Department of Animal Biology, School of Veterinary Medicine, <sup>3</sup>Children's Hospital of Philadelphia and <sup>4</sup>Department of Orthopaedic Surgery, Perelman School of Medicine, University of Pennsylvania.

**INTRODUCTION:** Notch signaling is a ubiquitous, developmentally-conserved cell-to-cell signaling process that regulates stem cells. In particular, Notch intersects with BMP and Wnt signaling to regulate the terminal differentiation of various progenitors. Indeed, both Notch and BMP signaling activate the expression of the Hey family of transcription factors. Notch signaling is mediated by a ligand (DSL family) expressed on one cell interacting with a Notch receptor (Notch 1-4) on an adjacent cell.

In mouse models Notch signaling has been shown to regulate endochondral and intramembranous bone development by stimulating progenitor cell proliferation while inhibiting differentiation [1]. Notch signaling also inhibits osteoclast development. However, the roles of various Notch signaling components during skeletal development, remodeling, and bone repair are not well-described.

The Jagged1 (Jag1) ligand is highly expressed during skeletal development and by cells of the osteoblast lineage in both mice and humans [2]. Loss of function mutations in *JAG1* cause Alagille Syndrome (ALGS) in humans. The syndrome, which causes pediatric cholestatic liver disease, also results in various skeletal developmental defects including facial abnormalities, growth failure, butterfly vertebrae and radioulnar synostosis. In addition to skeletal development defects, patients experience significant morbidity as a consequence of recurring fractures that heal poorly [3]. This suggests that Jag1 plays an important role in regulating bone formation and regeneration. Jag1 has also been implicated in mediating the effects of parathyroid hormone (PTH) on bone. Jag1 levels are increased in osteoblasts with enhanced PTH signaling [4].

Our comprehensive work seeks to understand the significance of Notch signalling, mediated by the Jag1 ligand, in regulating osteoblastogenesis, bone formation, and bone regeneration.

**METHODS:** We have utilized a variety of in vitro approaches with mouse and human mesenchymal stem cells (MSC) and in vivo approaches with Cre-mediated conditionally regulated mice to

perturb Notch signalling during osteoblastogenesis, bone formation, and bone regeneration. **In vitro studies:** Primary mouse and human MSC were cultivated and plated onto Jag1 ligand to activate Notch signaling. Osteoblastogenesis was evaluated using gene expression analysis, Alk Phos activity, and Alizarin red S staining. **Bone regeneration models:** We utilized a guillotine tibial fracture model to evaluate long-bone healing, and a 3 mm calvarial defect to study craniofacial regeneration. **Jag1 conditional disruption:** Jag1 was selectively ablated in the developing mouse skeleton by breeding Jag1-loxP mice with mice expressing Cre recombinase in osteoblasts (Col2.3Cre/Jag1) and pre-osteoblasts (Prx1Cre/Jag1). **dnMAML overexpression:** Cre-regulated dominant negative Mastermind Like (dnMAML) mice were crossed with mice expressing Cre recombinase in osteoblasts (Col2.3Cre/Jag1) and pre-osteoblasts (Prx1Cre/Jag1), as well as with inducible Cre mice (Mx1-Cre). **Bone analysis:** To evaluate differences in bone, microcomputed tomography (microCT) was performed with a Scanco viva40 microCT. Bone was decalcified and embedded in paraffin for sectioning and subsequent evaluation using histomorphometry and IHC.

**DISCUSSION & CONCLUSIONS:** We have conducted extensive studies, characterizing the expression of Notch ligands, receptors, and target genes during bone regeneration and in MSC. Notch signalling is highly active during bone regeneration. Intriguingly, plating hMSC onto Jag1 has potent osteoblastogenic effects. The conditional disruption of Jag1 in bone results in alterations in trabecular bone mass. Overexpression of dnMAML similarly adversely affects bone mass and regeneration. The development of methodologies to deliver Jag1 ligand in vivo holds great promise as a potential therapeutic for enhancing bone regeneration.

**REFERENCES:** 1. Zanotti+ 2012 Calcif Tissue Int. 90(2):69-75. 2. Weber+ 2006 Bone 485-4935. 3. Bales+ J Ped Gastroenterol Nutr 2010 51(1):66-70. 4. Calvi+ 2003 Nature 841-6.

## A regenerative medicine approach to muscle, tendon, and ligament reconstruction

Stephen F. Badylak<sup>1,2</sup>

Corresponding Author: [badylaks@upmc.edu](mailto:badylaks@upmc.edu)

<sup>1</sup>University of Pittsburgh, Pittsburgh, Pennsylvania, USA, <sup>2</sup>McGowan Institute for Regenerative Medicine, Pittsburgh, Pennsylvania, USA

### INTRODUCTION:

Segmental musculotendinous and ligamentous defects, including volumetric muscle loss, have limited options for primary repair. Apposition of large tendon and ligament gaps can result in dysfunctional outcomes. Effective strategies to promote the formation of new muscle tendon units or functional bony insertion sites would provide a constructive option for the surgical repair of such lesions. A bioinductive scaffold composed of naturally occurring extracellular matrix (ECM) has been shown to promote constructive remodeling of numerous tissue types, including tissues with a smooth muscle component such as the urinary bladder and a skeletal muscle component such as the abdominal wall, esophagus, quadriceps muscle, and gastrocnemius muscle[1-5]. The mechanisms by which such scaffold materials promote a constructive host response include the recruitment of endogenous stem and progenitor cells, modulation of the innate immune response toward a “tissue repair” M2 phenotype, and scaffold degradation with the resultant generation of bioactive cryptic peptides that support tissue reconstruction.

### METHODS:

Preclinical studies in the rodent and dog in which functional skeletal muscle tissue has been generated de novo will be described. In addition, preliminary results in a human clinical trial will be presented showing constructive musculotendinous tissue reconstruction.

### RESULTS:

Site appropriate, functional, muscle and tendon tissue developed when biologic scaffolds are manufactured appropriately and when surgical techniques are combined with nonconventional aggressive rehabilitation.

### DISCUSSION & CONCLUSIONS:

The default healing response, specifically inflammation followed by scar tissue formation can be modified toward a more constructive outcome given the appropriate microenvironmental niche and biologic/mechanical signals. A discussion of constructive remodeling as mediated by biologic scaffolds, and mechanisms of tissue response will be the subject matter of this presentation.

### REFERENCES:

1. Valentin, J.E., et al., *Functional skeletal muscle formation with a biologic scaffold*. *Biomaterials*, 2010. **31**(29): p. 7475-84.
2. Derwin, K.A., et al., *Extracellular matrix scaffold devices for rotator cuff repair*. *J Shoulder Elbow Surg*, 2010. **19**(3): p. 467-76.
3. Turner, N.J., et al., *Xenogeneic extracellular matrix as an inductive scaffold for regeneration of a functioning musculotendinous junction*. *Tissue Eng Part A*, 2010. **16**(11): p. 3309-17.
4. Mase, V.J., Jr., et al., *Clinical application of an acellular biologic scaffold for surgical repair of a large, traumatic quadriceps femoris muscle defect*. *Orthopedics*, 2010. **33**(7): p. 511.
5. Boruch, A.V., et al., *Constructive remodeling of biologic scaffolds is dependent on early exposure to physiologic bladder filling in a canine partial cystectomy model*. *J Surg Res*, 2009. **161**(2): p. 217-25.

## IL-1 $\beta$ modulates *in vitro* remodeling and *in vivo* bone formation by endochondral primed human bone marrow mesenchymal stromal cells

<sup>1</sup>M Mumme, <sup>1</sup>C Scotti, <sup>1</sup>W Hoffmann, <sup>1</sup>A Papadimitropoulos, <sup>1</sup>A Todorov, <sup>1</sup>S Gueven, <sup>1</sup>M Jakob, <sup>1</sup>D Wendt, <sup>1</sup>I Martin, <sup>1</sup>A Barbero

<sup>1</sup>Departments of Biomedicine and Surgery, University of Basel, Switzerland

**INTRODUCTION:** The milieu of the fracture site contains many inflammatory cytokines during not only the initial healing phase but also the later remodeling phase. We aimed this study at investigating the influence IL-1 $\beta$  on endochondral bone formation by human bone marrow stromal cells (hBM-MSC), mimicking the remodeling of the cartilage callus into bone tissue.

**METHODS:** Human BM-MSC were expanded for 2 passages and cultured for 5 weeks in 3D collagen sponges (Ultrafoam<sup>TM</sup>, 8mm diameter, 2 mm thick) using a previously established protocol (3 weeks with chondrogenic medium and 2 weeks with a defined hypertrophic medium<sup>1</sup> with or without 50pg/ml IL-1 $\beta$ ) and then implanted ectopically in nude mice for 5 and 12 weeks. Constructs were analyzed biochemically (calcium, glycosaminoglycane, GAG) and histologically (Safranin-O, Alizarin red, TRAP, cryptic fragment of aggrecan, DIPEN) and with quantitative  $\mu$ CT (total bone volume).

**RESULTS:** As compared to controls, *in vitro* cartilaginous tissues exposed to IL-1 $\beta$  (i) accumulated 38% more calcium resulting in a thicker calcified bone collar, (ii) lost 12% more GAG and (iii) accumulated higher amounts of MMP-13 and DIPEN(Fig. 1).

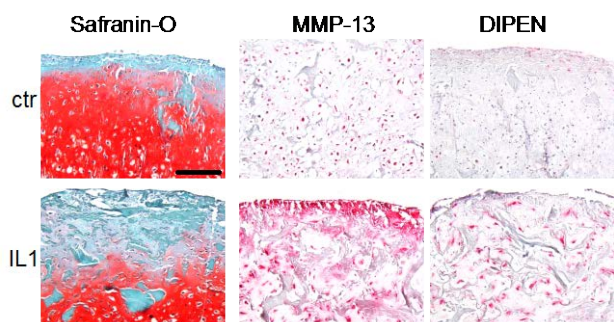


Fig.1 After 5 weeks *in vitro*, Safranin-O, MMP-13 and DIPEN stainings. Scale bar = 100 $\mu$ M

After 5 weeks *in vivo*, IL-1 $\beta$  treated samples contained (i) larger bone marrow areas and (ii) reduced cartilaginous areas (Fig.2) and (iii) higher amounts of TRAP positive cells. After 12 weeks *in vivo*, IL-1 $\beta$  treated samples showed a thicker outer

bone collar with increased, even though not statistically significant, total bone volume (Fig.3).

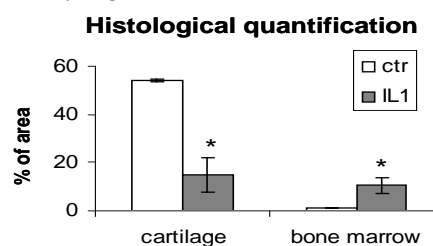


Fig.2: After 5 weeks *in vivo*, quantification of stained histology photos. \* =  $p < 0.05$  from ctr.

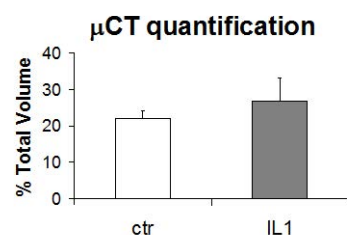
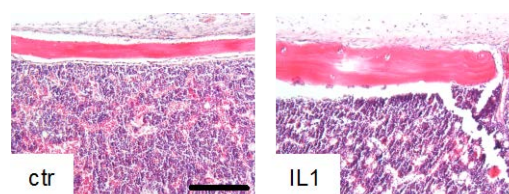


Fig.3: After 12 weeks *in vivo*, H&E staining shows (up) and quantitative  $\mu$ CT (bottom)

### DISCUSSION & CONCLUSIONS: IL-1 $\beta$ treatment during the *in vitro* endochondral priming of hBM-MSC resulted in an advanced degree of cartilage remodeling and subsequent more mature bone *in vivo*.

Controlling the inflammatory environment could enhance the success of therapeutic approaches for the treatment of fractures by resident MSC and as well improve the engineering of implantable tissues.

**REFERENCES:** <sup>1</sup>Scotti et al., *Proc Natl Acad Sci U S A* **107**(16):7251-6 (2010).

**ACKNOWLEDGEMENTS:** financial support by the European Union (OPHIS; #FP7-NMP-2009-SMALL-3-246373)

## Large bone healing defect- clinical need

Frankie Leung

*Department of Orthopaedics and Traumatology, the University of Hong Kong*

In considering the best treatment for large bone defect, one must appreciate there are different environments in which the healing may occur. The common indications include large cancellous void, long bone defect as well as spinal surgeries including interbody fusion and posterolateral fusion. The first two conditions will be discussed here.

Conditions regarding the mechanical stability and the vascularity of the surrounding tissues are crucial in deciding whether healing will occur. Large cancellous voids can occur after comminuted fractures or fractures in the presence of osteoporosis. It can also occur after treatment of benign bone lesions or bone infection. Compared to others, this is relatively easier to treat due to the presence of the cortical shell and the better vascularity in bone tumour conditions. Different materials including autologous bone grafting, demineralised bone matrix, bone graft substitutes including calcium phosphate, bone cement, etc have been used successfully. Surgeons may also apply a mixture of autograft with either allograft or artificial bone substitutes in larger defects.

Large cortical defects in long bones commonly occur after debridement of open fractures, especially in the presence of infection. As a result, the vascularity of the surrounding tissues is often compromised. At the same time there is no definite boundaries of the defect and even bone grafting may not be effective. Multiple cancellous bone grafting, vascularised bone grafting or bone transport have been used in the past few decades to treat massive defects in the long bone. Usually multiple surgeries and surgical expertise are needed to achieve successful treatment. Recently, surgeons turn to the interim use of bone cement to fill the defect in the primary surgery, the so called Masquelet technique. A vascularised fibrous capsule will be formed after a certain period and cancellous graft can be inserted to the defect in a contained manner.

Bone transport can deal with massive defect, bony deformity and infected conditions at the same time. Despite the common docking problems, the

long period of treatment and the discomfort of the patients, this is still the most reliable method and successes have been reported even in developing countries.

Besides developing the suitable biomaterials to be used in large bone defects, one must also consider improving the surgical techniques. There have been recent attempts to improve the effectiveness of bone graft harvesting, e.g. the use of a specialized reamer-irrigator-aspirator (RIA).

## Bone Repair in the Spine

Paul F. Heini, Klinik Sonnenhof, Bern, Switzerland

paulheini@sonnenhof.ch

### Introduction

Bone repair and bony healing in the spine are requested in order to get a durable stable situation of one or several motion segments; this so-called spinal fusion remains one of the most important procedures in spine surgery. Estimation go for about 2 Mio fusion procedures per year [1]. Since the first spinal fusion procedures that were performed 100 years ago [2] the principles remain the same, however several bone substitutes are used in order to provide and support spinal fusion [3,4]. The most potent mean for spinal fusion except autologous bone graft appears BMP II and to a lesser extend BMP 7. They are in clinical use for lumbar fusion for several years [5]. However its use shows also limitations and needs critical observation [6].

### Methods

This is not a scientific paper but a report on the experience of the use of different fusion materials at the lumbar spine focusing on lumbar interbody fusion.

### Results

Based on a case series of 32 cases with anterior interbody stabilization and fusion using the Synfix®-Cage in combination with autologous bone graft (23 cases) or demineralized bone matrix (DBM) 4 cases (or BMP II (5 cases) shows a reliable fusion within 6 months using autograft or BMP. Both materials show to be very potent for spinal fusion. The case series is including the L5-S1 level only and show a similar behavior. For DBM the time for fusion appears far longer, only after 2 years bone formation in the cage is visible.

Interbody fusion by the so-called extreme lateral approach (X-LIF) using a cage (ORACLE®) for the stabilization and different bone graft substitutes shows a more variable outcome. On the one hand one can recognize the impact of the mechanical stability with better fusion in a stable environment and on the other hand a longer fusion time with the

increasing number of levels treated. Again autologous bone and BMP show similar behavior in favor of BMP and DBM is not showing any bony reaction within a one year period.

### Conclusion

These observations are interesting as the monitoring of the interbody fusion (by CT) is more reliable and allows a more precise assessment of the bony healing. The limited availability of autologous bone graft and its donor site morbidity show a clear need for bone graft substitutes. DBM appears not an optimal solution as a stand-alone substitute, BMP II has shown to be very effective, however it is very expensive and side effects need to be taken into consideration. Other alternatives (CaP, Nanoparticles, etc.) need to be assessed carefully – the benchmark is set by the ALIF procedure with autologous bone graft and the Synfix-Cage.

### References

1. Giannoudis PV, Dinopoulos H, Tsiridis E. Bone substitutes: an update. *Injury* 2005;36 Suppl 3:S20-27
2. Hibbs RA. A report of fifty-nine cases of scoliosis treated by the fusion operation. By Russell A. Hibbs, 1924. *Clin Orthop Relat Res* 1988:4-19
3. Marchesi DG. Spinal fusions: bone and bone substitutes. *Eur Spine J* 2000; 9:372-378
4. Miyazaki M, Tsumura H, Wang JC, Alanay A. An update on bone substitutes for spinal fusion. *Eur Spine J* 2009;18:783-799
5. Agarwal R, Williams K, Umscheid CA, Welch WC. Osteoinductive bone graft substitutes for lumbar fusion: a systematic review. *J Neurosurg Spine* 2009;11:729-740
6. Carragee EJ, Hurwitz EL, Weiner BK. A critical review of recombinant human bone morphogenetic protein-2 trials in spinal surgery: emerging safety concerns and lessons learned. *Spine J* 2011; 11:471-491



### Jaw bone reconstruction using CAD and stem cell technology

R Kontio, C. Lindqvist, J. Törnwall, K Mesimäki Alini

Dept of Maxillofacial Surgery, Helsinki University Hospital, Helsinki, Finland

**INTRODUCTION:** Surgical repair of three-dimensional defects in facial skeleton is remarkable difficult and unpredictable. Particularly, complex bony defects are difficult to reconstruct accurately. Reconstruction of bony defect in the facial skeleton involves harvesting of bone flap. This causes considerable donor site morbidity and complications in the area of reconstruction are common. Reconstructive surgery should be evolved into a multidisciplinary field where surgeon works in collaboration with scientists and engineers. One such new technology is the autologous adipose stem cell isolation and transplantation to recipient area. The goal of this procedure is to achieve ectopic bone to be transferred into facial defect area. At the present, computerized modelling and computer aided design (CAD) is randomly used in neurosurgery, orthopaedics and maxillofacial surgery (Hassfeld S 2001, Gellrich 2002). Recent developments in CAD and RP have opened up new views. Opposite to traditional surgery, CAD and RP makes use of 3D data and enables any 3D virtual form to be manufactured into solid implants. In the present report, the authors introduce a new concept of a combined surgical technique in which the maxillary bone defect is repaired using CAD planning and implantation of CAM scaffold with adipose stem cells.

**DISCUSSION & CONCLUSIONS:** Traditionally, restoration of extensive palatomaxillary defects have been achieved by prosthetic restoration, often with suboptimal functional results. More recently, vascularized bone-containing free flaps have been used for this purpose. In this report a novel multidisciplinary approach to reconstruct a bony defect is introduced. To use stem cells as part of clinical treatment, a method of isolating the cells in large enough quantities is needed. Bone marrow mesenchymal stem cells (MSCs) are promising but are associated with disadvantages regarding bone regeneration. One is that in bone marrow aspiration the cell yield is usually low.

Adipose tissue can be considered an attractive alternative source.

Until today there is only one reported clinical case, where ectopic bone formation inside free flap using autoASCs has been performed to reconstruct a bony defect.

#### Patient case

31 years old male was referred to Dept. of OMFS, Helsinki University hospital early 2007. Clinical and radiological examination revealed a large infiltrative tumour in maxilla. It filled both maxillary sinus and was contact with the skull base. No obvious metastasis was noticed. Diagnosis of SCC was set after histologic examination. Radical tumour resection (class IV, Brown et al) was carried out with bilateral neck dissection. The defect was then reconstructed using soft tissue LD flap. This is with accordance with literature research and with authors own experience. Patient received postoperative radiotherapy, 65 Gy.

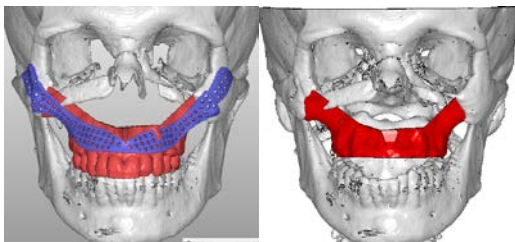


Fig. 1: Images of virtual models in this case – a) Original maxilla added to postoperative 3D virtual model b) Maxilla modified suitable for RP solid model manufacturing.



Fig.2.a) ALT tissue flap with ectopic bone raised, b) After 5 months of reconstruction dental implants are placed into neomaxilla (ectopic bone).

During the follow up, patient experienced a recurrency 1 year postoperatively. After additional radiotherapy the tumour disappeared. During the follow up of two years the patient remained disease free. 3 years after primary operation stem cells of abdominal fat were harvested and then isolated in GMP-class clean rooms according to Standard Operation Procedures at REGEA. Simultaneously, using CAD technique the neomaxilla was reconstructed exactly similar to patients own but now resected maxilla (fig.1.). Furthermore, the PSI reconstruction plate to fix the neomaxilla precisely was designed. After three weeks, the combination of stem cells, TCP $\beta$  and rhBMP-2 in a preformed polylactide cage was implanted cage carefully in a pouch prepared in the patient's left ALT. Three identified perforator islands were set around the cage. The final reconstructive operation took place 6 months later (fig 2.). Vital bone was detected to develop from stem cells, TCP $\beta$  combination. The microvascular operation and the follow up were uneventful.

#### Conclusions

The technique to grow ectopic bone based on stem cells and TCP $\beta$  is already available. However, the method seems not to be reliable. There are many open questions still related to growth of stem cells.

At the moment the carrier of stem cells is granular type TCP $\beta$ . This is difficult to shape. Without separate scaffold this technique is not usable.

Further studies are needed both related to stem cell biology and to mechanical/ biologic properties of carriers.

**REFERENCES:** Novel maxillary reconstruction with ectopic bone formation by GMP adipose stem cells. Mesimäki K, Lindroos B, et al. Int J Oral Maxillofac Surg. 2009 Mar;38(3):201-9.

Prefabrication of vascularized bioartificial bone grafts in vivo for segmental mandibular reconstruction: experimental pilot study in sheep and first clinical application. Kokemueller H, Spalthoff S, et al. Int J Oral Maxillofac Surg. 2010 Apr;39(4):379-87.

Mesenchymal stem cells and inorganic bovine bone mineral in sinus augmentation: comparison with augmentation by autologous bone in adult sheep. Gutwald R, Haberstroh J. Br J Oral Maxillofac Surg. 2010 Jun;48(4):285-90.

Reconstruction of defects of maxillary sinus wall after removal of a huge odontogenic lesion using pre-bended 3D titanium-mesh and CAD/CAM technique. Stoetzer M, Rana M, et al. Head Face Med. 2011 Nov 9;7:21.

CAD/CAM and rapid prototyped titanium for reconstruction of ramus defect and condylar fracture caused by mandibular reduction. Wang G, Li J, Khadka A, et al. Oral Surg Oral Med Oral Pathol Oral Radiol. 2012 Mar;113(3):356-61.

Custom-made, root-analogue direct laser metal forming implant: a case report. Mangano FG, Cirotti B, Sammons RL, Mangano C. Lasers Med Sci. 2012 Jun 15.

## The Clinical Relevance of Bone Oedema: The Bony Enigma

J. A. Fairclough<sup>1</sup>, C. W. Archer<sup>2</sup>, H. McCarthy<sup>2</sup>, I. Khan<sup>2</sup> and L. Nelson<sup>2</sup>

<sup>1</sup>Cardiff Metropolitan University, Cardiff, UK, South Glamorgan School of Biosciences, Cardiff University, Cardiff, <sup>2</sup>Cardiff Institute of Tissue Engineering and Repair, Cardiff University.

The finding of increased signal in the MRI T2 weighted imaging of bone is common and was initially described as “bone marrow oedema” by Wilson in 1986. The use of the Greek word οίδημα/oedema (swelling) is, however, inaccurate since in the confined space between the trabecular bones, swelling cannot occur. Consequently, Bone Marrow Lesion (BML) is more appropriate. The increased signal seen in BML is associated with pathophysiology in the subchondral bone is, however, diverse and it is important to differentiate between both location and associated conditions.

In trauma, damage to the trabecular bone either associated with fractures or compressive impact which is often seen in joint dislocation, as in ACL tears, where the subchondral change is often poorly defined and reticulated and often called bone bruising (Mink).<sup>1</sup> Chronic trauma produces a similar appearance of BML change without the stress lesions in the athlete and lacking radiological change. These are variable in site and size but significantly rarely involve joints. In a similar manner, diffuse changes in periarticular lesions are observed and may be associated with pain but, without any apparent long-term consequence.<sup>2</sup> This is termed regional migratory osteoporosis (RMO) where there is transient osteoporosis with migratory features with involvement of another joint, which occurs usually within 6 months of the onset of primary symptoms.<sup>3</sup> RMO typically migrates to adjacent joints and, most commonly, affects the knee and ankle.

It is in degenerative joint disease that the occurrence of bone marrow lesions are frequently noted and their presence has been suggested as indicating a pathophysiological process that is linked to both symptom complexes and clinical prognosis. The literature often lacks clarity when grouping dissimilar pathological conditions based purely on radiological findings without considering the subchondral and hyaline cartilage environment and disease processes associated with the signal change. Where histology has been performed, the fat cells are often observed to be abnormal with inflammatory vascular changes and variable changes to the trabecular bone structure being osteoporotic or in certain conditions, associated with avascular necrosis.

BML have been associated with increased pain in certain patients with degenerative joint conditions and there is some evidence that the pathophysiological changes in the subchondral region of these osteoarthritic joints may be strongly linked with disease progression. Felson described BML in 77.5% of patients with pain compared with 30% in those without pain.<sup>4,5</sup> The term transient bone marrow oedema syndrome has been used to describe the sudden onset of knee pain and MR findings of a typical large BML pattern without a specific cause.

In isolated condylar defects, where there is loss of hyaline cartilage, the underlying local area often has bone marrow changes that would appear to suggest the bone marrow is involved in a cross-talk with the hyaline cartilage.

In inflammatory disease, the BML may represent a cellular infiltrate within bone such as in rheumatoid arthritis where histopathological studies suggest that this cellular infiltrate and osteoclasts and lymphocytes may migrate through the

subchondral area the towards the joint surface being thus an aetiology of joint damage in rheumatoid arthritis.

BML in osteoarthritis, the subchondral bone has been demonstrated as being relative to normal tissue, such as fatty marrow in 53%, intact trabeculae in 16%, and blood vessels in 2% of tissue volume. Although in certain situations, this has been associated with osteoclastic activity and bone resorption.<sup>6</sup>

The Multicenter Osteoarthritis Study (MOST) concluded that BMLs with associated cartilage loss where 66% of the pre-existing BMLs showed a change in size over 30 months, and about 50% of BMLs at baseline decreased or disappeared.<sup>7</sup> These findings are not consistent, and in symptomatic OA, it has been observed that BMLs are unlikely to resolve and may even grow. Where BMLs are associated with mechanical alignment, progressive joint disease is frequent with associated hyaline cartilage loss.<sup>8</sup>

### REFERENCES:

- 1) Mink JH, Deutsch AL. Occult cartilage and bone injuries of the knee: Detection, classification and assessment with MR imaging. *Radiology* 1989; 170:823-9.
- 2) Hayes CW, Conway WF, Daniel WW. MR imaging of bone marrow edema pattern: transient osteoporosis, transient bone marrow edema syndrome, or osteonecrosis. *Radiographics* 1993. Sep;13(5):1001-1011, discussion 1012
- 3) Cahir JG, Toms AP. Regional migratory osteoporosis. *Eur J Radiol* 2008;67:2-10.
- 4) Felson D, McLaughlin S, Goggins J, et al. (2003) Bone marrow edema and its relation to progression of knee osteoarthritis. *Ann Intern Med* 139, 330–6.
- 5) Felson DT, Niu J, Guermazi A, Sack B, Aliabadi P. Defining radiographic incidence and progression of knee osteoarthritis: suggested modifications of the Kellgren and Lawrence scale. *Ann Rheum Dis*. 2011 Nov;70(11):1884-6. Epub 2011 Sep 8.
- 6) Zanetti M, Bruder E, Romero J, Hodler J (2000) Bone marrow edema pattern in osteoarthritic knees: correlation between mr imaging and histologic findings 1. *Radiology* 215, 835–40.
- 7) Roemer FW, Guermazi A, Javaid MK, MOST Study investigators (2009) Change in MRI-detected subchondral bone marrow lesions is associated with cartilage loss: the MOST Study. A longitudinal multicentre study of knee osteoarthritis. *Ann Rheum Dis* 68, 1461–5.
- 8) Phan CM, Link TM, Blumenkrantz G, et al. (2006) MR imaging findings in the follow-up of patients with different stages of knee osteoarthritis and the correlation with clinical symptoms. *Eur Radiol* 16, 608–18.
- 9) Hunter DJ, Zhang Y, Niu J, et al. (2006) Increase in bone marrow lesions associated with cartilage loss: a longitudinal magnetic resonance imaging study of knee osteoarthritis. *Arthritis Rheum* 54, 1529–35.

## Biogenic nanosized hydroxyapatite / cellulose acetate composites for tissue engineering

C Balázs<sup>1</sup>, G Gergely<sup>1</sup>, R Xue<sup>2</sup>, C Goldbeck<sup>3</sup>, P.L. Perrotta<sup>4</sup>, K Balázs<sup>1</sup>, P.I. Gouma<sup>2</sup>

<sup>1</sup> Institute for Technical Physics and Materials Science, Research Centre for Natural sciences, HAS, Budapest. <sup>2</sup> Dep. of Materials Science and Engineering, State University of New York at Stony Brook, New York. <sup>3</sup> Biological Nanostructures Facility at The Molecular Foundry, Lawrence Berkeley National Laboratory, Berkeley, CA. <sup>4</sup> Department of Pathology, West Virginia University, Morgantown, WV

**INTRODUCTION:** Huge amounts of by-products or rest of the raw materials are wasted, generating an undesirable environmental impact. The eggshell is a one of these by-products. Eggshells are rich in calcium and it is increasingly important for hydroxyapatite (HAp) preparation. Nanosized HAp is a popular material for use in bone regeneration for its excellent bio properties [1-3]. CA scaffolds have been used for growing “structurally mature” and “functionally competent” cardiac cell networks [4]. In this work, nanosized HAp and CA are combined to form novel hybrid 3D scaffolds mimicking the extracellular matrix (ECM) architecture by electrospinning.

**METHODS:** Nanostructured HAp powder was synthesized from raw materials [1]. The as-received n-HAp powder was added to acetic acid forming a 9.38% wt/vol solution. This solution was then mixed with CA solution, which was CA powder dissolved in acetone to form 15% wt/vol composition. The mixed solution 71/29 vol% acetone/acetic acid was introduced into a standard vertical electrospinning setup: flow rate 9.6 ml/hr, voltage 19 kV and distance from needle to collector 10 cm. SaOS<sub>2</sub> human osteoblast-like cells were grown at 37°C, 5% CO<sub>2</sub> in a humidified incubator in DMEM complete medium. The cells were trypsinized with 0.25% trypsin-EDTA [Sigma] and seeded on the scaffolds at a density of 50,000 cells per well in a volume of 1.5 ml. The cells were cultured for up to 14 days.

**RESULTS:** The continuous HAp /CA composite electrospun fibers with fiber diameters 300 nm was found. The uniform distribution of nano HAp clusters was observed. The average size of hydroxyapatite nanoclusters on the fibers is 35 nm. The detection of mineralization study confirmed that the scaffolds without cells showed only a slight background staining even though some of the scaffolds contained hydroxyapatite (Fig. 1). There was a clear increase in mineralization for all of the samples between day 1 and day 14. The

nano scaffolds showed the most intense staining at each time point with the day 14 samples being the most intense. Hexagonal mineral crystals were found to grow on n-HAp clusters along the CA fibers on elongated cells.

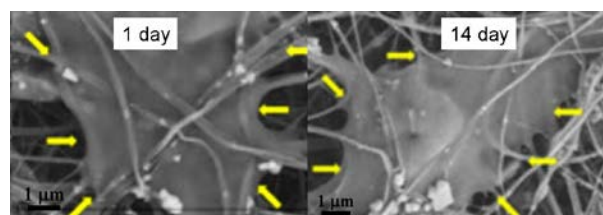


Fig. 1: Osteoblast cells grown on n-HAp containing CA fibers after 1 and 14 days.

**DISCUSSION & CONCLUSIONS:** Nanosized HAp/polymer composites were successfully manufactured by electrospinning and applied in bone tissue engineering. Our studies suggest that both the morphology and structure of the HAp-CA composite scaffolds play important roles in facilitating cell spreading and differentiation and enhance apatite mineralization. The electrospun nanosized HAp/CA scaffolds are considered as a promising candidate for bone tissue engineering application.

**REFERENCES:** <sup>1</sup> R. Murugan, S. Ramakrishna (2005) *Composites Sci & Technol* **65** : 2385-406. <sup>2</sup> L.L. Hench, J.M. Polak (2002) *Science* **295**: 1014-17. <sup>3</sup> L.L. Hench, (1991) *J. Am. Ceram. Soc.*, **74** : 1487-510. <sup>4</sup> E. Entcheva, H. Bien, L. Yin, C-Y. Chung, et al (2004) *Biomaterials* **25**: 5753-62. <sup>5</sup> C. Balázs, et.al. (2007) *J. Eur. Cer. Soc.* **27** 1601-6.

**ACKNOWLEDGEMENTS:** This work was supported by EPA STAR award, the Molecular Foundry at the LBNL and Hungarian National Research Program (OTKA 76181).

## Development of biocompatible TiC/a:C nanocomposite barrier coating for dental implants

K Balázs<sup>1</sup>, M Vandrovcová<sup>2</sup>, L Bačáková<sup>2</sup>, I Bertóti<sup>3</sup>, C Balázs<sup>1</sup>

<sup>1</sup> Institute for Technical Physics and Materials Science, Research Centre for Natural sciences, HAS, Budapest. <sup>2</sup> Institute of Physiology, Academy of Sciences of the Czech Republic, Prague. <sup>3</sup> Institute of Materials and Environmental Chemistry, Research Centre for Natural Sciences, HAS, Budapest.

**INTRODUCTION:** Titanium is preferred for dental implants for their good biocompatibility, corrosion resistance and strength [1]. Mosser et al. proved that the thickness of natural TiO<sub>2</sub> on Ti implant's surface is increased for 5 nm to 200 nm after 5 years implantation [2], representing that the implant material was endlessly oxidized in the organism and there was no defensive layer to prevent further oxidation for their porosity. The presence of fluoride ions in body may be detrimental to corrosion resistance of Ti or Ti alloys depending on the fluoride concentrations [3]. The alloying elements probably enhanced the diffusion of Ti ions leading to a thicker oxide film. The protectiveness of the TiO<sub>2</sub> based film on the Ti-6Al-4V in artificial saliva was already destroyed when the NaF concentration increased to 0.1% [4]. Ti and C are suitable elements to optimize surface chemistry and promote fast osteointegration [5]. TiC based coatings were developed as potential barrier coating for interfering of Ti ions from pure Ti or Ti alloy implants by dc magnetron sputtering. Correlation between structure and other properties was found.

**METHODS:** The TiC / a:C nanocomposite films were prepared by DC magnetron sputtering on silicon (001) substrates. Films were deposited at 25-800°C in argon at 0.25 Pa. The input power of the carbon target (C) was 150 W and 40 W for the titanium (Ti). The thickness of TiC/ a:C films are about 300 nm.

For the cell culture experiments, the sample deposited at 200°C was sterilized with 70% ethanol, inserted into 24-well polystyrene cell culture plates (TPP, Switzerland; internal well diameter 15.6 mm) and seeded with human osteoblast-like MG63 cells (European Collection of Cell Cultures, Salisbury, UK). The cells were cultured for 1, 3, and 7 days at 37°C in a humidified air atmosphere containing 5% CO<sub>2</sub>. For the cell culture experiments, glass slides and also the bottom of standard polystyrene cell culture dishes were used as reference materials.

**RESULTS:** The structural investigations of nanocomposites confirmed the columnar TiC crystallites embedded in thin amorphous matrix. In the case of film deposited at 200°C with extraordinary mechanical properties (H ~ 18 GPa, E ~ 205 GPa, wear resistance 0.25), MG63 osteoblast cells were used for in vitro study. The 7 day lasting tests showed a higher value of cells on TiC/a:C surface and the more spread morphology than the cells on control.

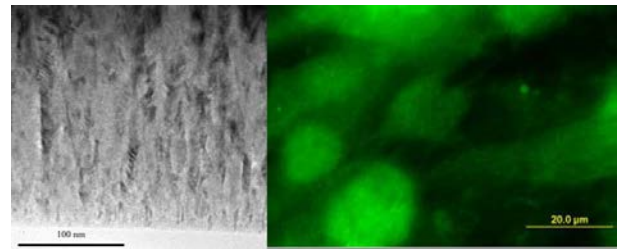


Fig. 1: Osteoblast cells cells grown on TiC/a:C after 7 days seeding.

**DISCUSSION & CONCLUSIONS:** Based on above results it can be concluded that thin nanocomposite TiC /a:C coating is biocompatible and may be applied as protective coating on Ti implants.

**REFERENCES:** <sup>1</sup> K. Lee et al. (2010) *Surf Coat Technol* **205**: S267–70. <sup>2</sup> A. Mosser, C. Speisser, et al (1992), in: D. Muster (Ed.), *Biomaterials-Hard Tissue Repair and Replacement*, Elsevier, Amsterdam, 143-52. <sup>3</sup> R.W.-W. Hsu, C.-C. Yang, C.-A. Huang, Y.-S. Chen (2004) *Mater. Sci. Eng. A*, **380**: 100–9. <sup>4</sup> H.-H. Huang, T.-H. Lee (2005) *Dental Mater.* **21**: 749–55. <sup>5</sup> D.V. Shtansky et al. (2006) *Surf Coat Technol* **201**: 4111–8.

**ACKNOWLEDGEMENTS:** This study was supported by OTKA Postdoctoral grant Nr. PD 101453, the János Bolyai Research Scholarship of the Hungarian Academy of Sciences, OTKA 76181 and by the Grant Agency of the Czech Republic (P108/10/1858). The authors thank to Dr. G. Sáfrán for tribological measurements.

## Neurogenic and angiogenic properties of bone marrow-derived mesenchymal stromal cell conditioned media

JJ Bara<sup>1</sup>, S Roberts<sup>1</sup>, G Griffiths<sup>2</sup>, R Benson<sup>2</sup>, KT Wright<sup>1</sup>

<sup>1</sup> RJAH Orthopaedic Hospital, Oswestry, UK, <sup>2</sup>Imagen Biotech, Manchester, UK

**INTRODUCTION:** Innervation and vascularisation are important considerations for the integration, survival and correct functioning of tissue engineered bone. Bone marrow-derived mesenchymal stromal cells (BMSCs) have previously been shown to stimulate neurogenesis<sup>1,2,3</sup> and angiogenesis<sup>4</sup> however, the molecular mechanisms regulating these processes are not fully understood. We investigated the neurogenic and angiogenic effects of BMSC secretomes by incorporating conditioned media into an *in vitro* model of nerve growth and by assessing the production of neurogenesis and angiogenesis-related proteins.

**METHODS:** Dorsal root ganglia (DRG) explants were cultured in 24-well plates coated with type I collagen as previously described<sup>3</sup>, with either human BMSC conditioned media (from 7 different patients), control conditioned media (that had not been incubated with cells) or standard DRG culture media for 48 hours at 37°C. DRG explants were fixed and immunolabelled using a monoclonal anti-neurofilament antibody (Clone NE14, Sigma, UK). BMSC conditioned media was screened for neurogenic and angiogenic factors using custom designed antibody array membranes (RayBiotech Inc, USA) and visualised by chemiluminescence. Levels of neurogenic and angiogenic factors were normalised to cell number and positive controls on each respective membrane.

**RESULTS:** BMSC conditioned media stimulated DRG neurite outgrowth compared to both control conditioned media and standard media (Figure 1).

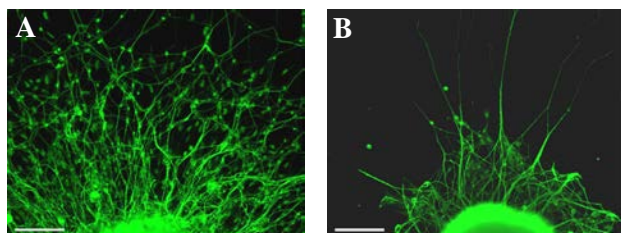


Fig. 1: Immunocytochemical detection of neurofilament in DRG cultures after application of (A) BMSC conditioned media and (B) control conditioned media. Scale bars 100µm.

Stimulation of neurite outgrowth was also associated with increased fibroblast-like outgrowth from DRGs. BMSC conditioned media contained a range of neurogenic and angiogenic factors (Figure 2). Specifically, high levels of BDNF, PDGF-AA, VEGF and FGF-4 were detected in all samples.

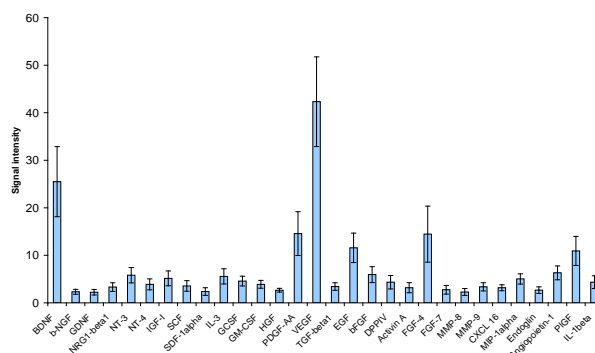


Fig. 2: Levels of neurogenic and angiogenic factors in BMSC conditioned media detected on antibody array membranes. Data normalised to positive controls and cell number. Data shown are means  $\pm$  standard error of the mean ( $n=7$ ).

**DISCUSSION & CONCLUSIONS:** BMSC conditioned media stimulated neurite outgrowth as previously described<sup>3</sup> and contained a multitude of neurogenic and angiogenic factors. The relationship between fibroblast-like and neurite outgrowth is not yet clear and requires further investigation. For future work, we plan to examine the effects of BMSC secretomes on *in vitro* angiogenesis tube formation assays and ascertain potential crosstalk between neurogenic and angiogenic secreted factors.

**REFERENCES:** <sup>1</sup> B. Neuberger, B.T. Himes, J.S. Shumsky et al (2005) *Brain Res* **1035**:73-85. <sup>2</sup> L. Crigler, Robey, R.C., A. Asawachicharn et al (2006) *Exp Neurol* **198**:54-64. <sup>3</sup> K.T. Wright, W.E. Masri, A. Osman et al (2007) *Biochem Biophys Res Comms* **354**:559-566. <sup>4</sup> T. Kinnaird, E. Stabile, M.S. Burnett et al (2004) *Circ Res* **94**:678-85.

**ACKNOWLEDGEMENTS:** This work was funded by the BBSRC Industry Interchange Programme.

## PLGA Dynamic Degradation and Mechanical Properties

Rainer Böhm, Michael Zaucha and Sandy Williams.

Bose Corporation, ElectroForce Systems Group, Eden Prairie, Minnesota, USA

### Introduction

The ElectroForce® BioDynamic® test instruments provide precise characterization of biomaterials and biological specimens within a closed saline or cell culture media environment. The instruments can be used for the evaluation of a variety of specimens, including biomaterials, acellular scaffolds and cell-seeded scaffolds, native tissue samples and tissue-engineered constructs. Their compact design makes them suitable for incubator use and long term experiments in a biomaterials or cell culture laboratory.

BioDynamic test instruments combine mechanical testing and specimen stimulation in one system. Single or multiple specimens can be mechanically loaded under tension/compression, torsion, cyclic hydrostatic pressure, and pulsatile or steady flow. Measurements include displacement, load, torque, rotation, pressure, strain, diameter, pH, dissolved oxygen, carbon dioxide, lactate/glucose, and temperature.



Application specific validation studies were performed to determine the capabilities of the BioDynamic test instrument to measure dynamic degradation rates of PLGA scaffolds. Innopol, an open porous PLGA scaffold, produced by InnoTech Medical, Inc. was subjected to cyclic mechanical loading for 8 days while in a PBS bath at 37°C. Throughout the experiment, load and displacement were intermittently measured and recorded. Significant degradation can be observed after the experimental period in all groups compared to controls. In addition, modulus changes over the course of the experiment when the sample is subjected to mechanical loading.

### Materials and Methods

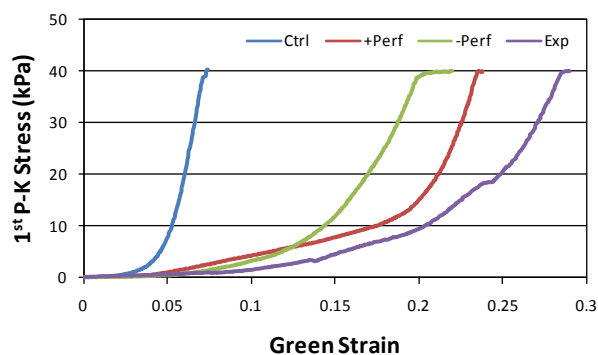
PLGA scaffolds were stimulated under dynamic loading conditions for 8 days while recording axial displacement, load, chamber pressure and outer diameter for 1 minute every hour. The chamber was perfused with PBS at a rate of 5mL/min. To serve as 3 control groups, scaffolds were kept in the original packaging (Ctrl), scaffolds were placed in the BioDynamic chamber but not subjected to mechanical loading (+Perf), and scaffolds were placed in PBS in a separate container without perfusion or mechanical loading (-Perf). Utilizing load control, the experimental PLGA scaffold was subjected to a sinusoidal load with a max compressive load of 30 grams and a minimum compressive load of 5 grams at a frequency of 1 Hz.

### Results and Discussion

End point testing was performed to compare the experimental sample to the three control samples. Due to geometrical differences at day 8, it would be of little value to compare the force-displacement curves of the four samples. Performing stress-strain analysis removes the bias from the geometrical differences and allows for comparison of the material response. The Green strain and 1<sup>st</sup> Piola-Kirchhoff stress, respectively,

$$E_{zz} = \frac{1}{2}(\lambda_z^2 - 1) \quad \text{and} \quad t_{zz} = \frac{F_z}{A_c}$$

are used where the stretch ratio,  $\lambda_z$ , is defined by  $\lambda_z = l/L_0$  where  $l$  is the loaded height and  $L_0$  is the unloaded height and  $F_z$  is the current force and  $A_c$  is the current area. The figure below (curves match captions from left to right) shows the material response of the 4 samples. Due to limitations imposed by the range of the load cell, all of the samples were still intact following the uniaxial test. All testing was performed in the BioDynamic chamber in PBS at 37°C.



Material response to a displacement ramp.

### Conclusion

This series of experiments demonstrate that the ElectroForce® 5100 BioDynamic test instrument is capable of accurately loading the test specimen at very small displacements while monitoring finite changes in the sample response and geometry. In addition, the BioDynamic device allows for stimulation proceeded by testing on the sample without the need for user exposure. This helps eliminate one variable during the experimentation process. With this data, researchers can generate reliable results without the need to constantly monitor an experiment.

Since the ElectroForce BioDynamic test instrument can be used to simulate in vivo conditions for the culture and testing of three-dimensional samples, it can be a valuable tool to bridge the gap between basic in vitro exploratory studies in culture dishes and in vivo animal experiments. It provides a controlled environment that mimics the in vivo conditions more closely compared to a Petri dish but does not have the complexity of an in vivo model. As such, cell types can be added one at a time to study cell-cell signaling, and cells can be seeded on different scaffolds to evaluate cell-extracellular matrix/substrate interactions. Cell differentiation, apoptosis, proliferation, and extracellular matrix protein production can be studied in response to mechanical loading and fluid flow conditioning.

## Design and fabrication of a 3D nanopatterned PEEK implant for cortical bone regeneration in a rabbit model

AS Brydone<sup>1</sup>, DSS Morrison<sup>1</sup>, J Stormonth-Darling<sup>1</sup>, RDM Meek<sup>2</sup>, KE Tanner<sup>1</sup>, N Gadegaard<sup>1</sup>

<sup>1</sup> *Bio-Interface Group, School of Engineering, University of Glasgow, UK,* <sup>2</sup> *Southern General Hospital, Glasgow, UK*

### INTRODUCTION:

The purpose of this project was to transfer electron beam lithography written nanotopography that has previously demonstrated osteoinductivity in vitro onto the surface of polymeric implants to investigate regeneration of a femoral gap defect in a rabbits.<sup>1</sup>

**METHODS:** Arrays of nano-pits were designed using L-edit CAD software, and written onto quartz wafers using a Vistec VB6 electron beam writer. A 50 micron layer of nickel was sputter-coated onto the quartz wafer, peeled away and used to line a rod shaped steel mould. LT1 poly-ether-ether-ketone (PEEK) was used to injection mould the nanopatterned rods using an Engel Victory Tech 28 injection moulder.

The nanopatterned rods were oxygen plasma etched to improve wettability and initial cell adhesion. Sessile drop water contact angle was assessed using comparative flat PEEK surfaces.

Proximal and distal intramedullary stems were machined from PEEK and fixed to the nanopatterned rods using cyanoacrylate. A 15mm mid-diaphyseal femoral osteotomy was created in two adult New Zealand white rabbit cadavers, the implants were inserted and secured using two proximal and two distal 1.5mm titanium cortical screws placed in an anterior to posterior direction. 3 point bending strength of the implants was calculated using a Dartec servohydraulic testing machine.

### RESULTS:

Nano-pits were 76.5nm deep and 90nm in diameter before plasma treatment. After 2 mins pits were 68nm deep and 113nm in diameter, after 5 mins pits were 66nm deep and 163nm in diameter, and after 10 mins pits were 35nm deep and 300nm in diameter. Centre-centre pit spacing was constantly 300nm (Fig. 1).

Sessile drop water contact angle was 87.2° on the planar surface and 92.5° on the nanopatterned

surface before oxygen plasma etching; after 2mins it was 29.2° and 24.3°, after 5mins it was 17.8° and 10.2°, and after 10mins it was 17.8° and 7.8° respectively.

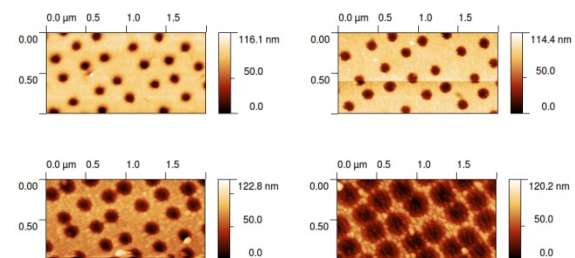


*Fig. 1: AFM images demonstrating the change in nanotopography after 0mins (top left), 2mins (top right), 5mins (bottom left), and 10mins (bottom right) of oxygen plasma treatment.*

Using SEM a 28.2µm wide pattern defect was observed and recognised as the seam between the two moulds. In the regions <50µm, 50-100µm and >100µm from the seam good pattern replication was observed. The most common defects were secondary to folding of the nanopatterned foil liner in the mould.

The mean load at failure of implants was 178.5N.

**DISCUSSION & CONCLUSIONS:** This project has resulted in the successful design and fabrication of a 3D nano-patterned implant with potential osteoinductivity for use in a femoral gap defect model in rabbits.

Future work will attempt to reduce the fold errors observed before in vivo implantation.

**REFERENCES:** <sup>1</sup>MJ Dalby, N Gadegaard, R Tare R, et al (2007) *Nat Mater* **6**: 997-1003.

### ACKNOWLEDGEMENTS:

A Khokhar, B Monahagh, B Robb.

This work is funded by NHS Scotland, Invibio, the AO Foundation.

### 3D co-cultures of osteoblasts and endothelial cells in DegraPol foam: Histological and high field MRI analyses of pre-engineered capillary networks in bone grafts

J Buschmann<sup>1</sup>, M Welti<sup>1</sup>, S Hemmi<sup>1</sup>, P Neuenschwander<sup>2</sup>, C Baltes<sup>3</sup>, P Giovanoli<sup>1</sup>, M Rudin<sup>3,4</sup>, M Calcagni<sup>1</sup>

<sup>1</sup> [University Hospital Zurich](#), Plastic and Hand Surgery, Zurich, CH. <sup>2</sup> [ab medica](#), Lainate (Milan), Italy. <sup>3</sup> [Institute for Biomedical Engineering](#), University of Zurich and ETH Zurich, CH. <sup>4</sup> [Institute of Pharmacology and Toxicology](#), University of Zurich, CH.

**INTRODUCTION:** There is a clinical need for bone grafts in order to treat bone defects after fracture, osteoporosis or after operation of malignant bone tumors [1]. A desirable and useful bone graft has a long implant life with complete tissue integration and similar mechanical properties compared to natural bone. However, up to date, available bone grafts are very limited with respect to size and appropriate 3D architecture, so that healthy bone has to be removed and used as autograft in bone reconstruction, which has the disadvantage of donor site morbidity and limited availability.

**METHODS:** Tissue engineering of bone grafts was addressed in a critical size model on the chick chorioallantoic membrane model (CAM assay), using DegraPol® (DP) foam as scaffold material. The scaffolds were seeded with cultures of human osteoblasts (OB) and human endothelial cells (EC), respectively, or with a co-culture of the two cell types (control: no cells). *In vitro* samples (7 days cultivation) and *ex vivo* CAM samples at incubation day 15 (ID 15) were analyzed by high field magnetic resonance imaging (MRI) and histology.

**RESULTS:** The co-culture system performed best with respect to perfusion, as assessed by contrast-enhanced MRI using Gd-DTPA. The scaffold seeded by the co-culture supported an increased vascular ingrowth, which was confirmed by histological analysis.

**DISCUSSION & CONCLUSIONS:** DP foam is a suitable scaffold for bone tissue engineering and the MRI technique allows for non-destructive and quantitative assessment of perfusion capability during early stages of bone forming constructs.

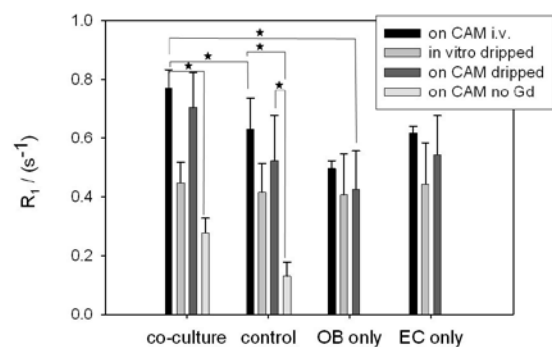


Fig. 1: Relaxation rates  $R_1$  in  $s^{-1}$  for co-culture, control, OB culture and EC culture, measured in the centre of the scaffold. Key of the legend: on CAM i.v. means Gd was applied i.v.; in vitro dripped means in vitro samples were dripped with Gd; on CAM dripped means the on CAM samples were dripped with Gd; on CAM no Gd means the on CAM samples were not treated with Gd. Error bars indicate standard deviations. One-way ANOVA was performed. Pairwise comparison probabilities,  $p$ , using the Fisher's PLSD post hoc test were considered significant if  $p < 0.05$  (\*) [2].

**REFERENCES:** <sup>1</sup> P.V. Giannoudis, C. Tzioupis, T. Almaki, and R. Buckley, (2007) *Injury*, **38S1** S90. <sup>2</sup> J. Buschmann, Welti M., Hemmi S., Neuenschwander P., Baltes C., Rudin M., Giovanoli P., and Calcagni M., (2011) *Tissue Engineering Part A* **17**(3-4): 291-299.

**ACKNOWLEDGEMENTS:** We thank Ms Pia Fuchs and Ms Silvia Behnke for their histological expertise and contribution and Dr. Dörthe Schmidt for providing the endothelial cells. We thank Dr. Yinghua Tian for performing the i.v. injections in the CAM assay. We received the DegraPol® foam as a gift from *ab medica*, Italy, and thank them for providing it.



## Biological tolerance and osseointegration of new bioceramics for arthroplasty applications

S. Cavalu<sup>1</sup>, V. Simon<sup>2</sup>, C. Ratiu<sup>1</sup>, O. Ponta<sup>2</sup>, I. Akin<sup>3</sup>, G. Goller<sup>3</sup>

<sup>1</sup>University of Oradea, Faculty of Medicine and Pharmacy, Romania, <sup>2</sup>Babes-Bolyai University, Faculty of Physics & Institute of Interdisciplinary Research in Bio-Nano-Sciences, Cluj-Napoca, Romania <sup>3</sup>Istanbul Technical University, Metallurgical and Materials Engineering Department, Istanbul, Turkey

**INTRODUCTION:** Al<sub>2</sub>O<sub>3</sub>, ZrO<sub>2</sub> and TiO<sub>2</sub> have been considered as bioinert ceramics since they cannot induce apatite formation in SBF. They do however support bone cell attachment, proliferation and differentiation [1]. The ideal ceramic is a high performance biocomposite that combines the excellent material properties of alumina in terms of chemical stability and low wear and of zirconia with its superior mechanical strength and fracture toughness. In this study, we assessed the *in vivo* performance of a new Al<sub>2</sub>O<sub>3</sub>-ZrO<sub>2</sub>-TiO<sub>2</sub> ceramic prepared by Spark Plasma Sintering, by using an animal model (Wistar rats).

**METHODS:** Investigation of the structural changes induced by TiO<sub>2</sub> addition to Al<sub>2</sub>O<sub>3</sub>/ZrO<sub>2</sub> was made by FTIR spectroscopy and X-ray diffraction (XRD) analysis. Scanning Electron Microscopy (SEM) and EDAX were used for microstructure and morphology investigation of the samples prior to *in vivo* tests. In order to perform *in vivo* tests, the rat model (Wistar) has been applied for biocompatibility evaluation. The ceramics were used as granular material, irregular shaped, filling the defects created in the femur of Wistar rats. SEM micrographs were recorded on the rat femur along with the elemental composition of the sheared implant surfaces at different time intervals after the surgery. Calcium/phosphate ratio was considered as an indicative of the surface implant coverage for a successful osseointegration [2]. In order to monitor the osseointegration process *in vivo*, radiographic images were recorded at different time intervals after the surgical procedure. Histological examination of the connective tissue was performed to detect any immunological or inflammatory responses.

**RESULTS:** Structural investigation of the proposed composites using XRD and FTIR spectroscopy confirmed the stability of the microstructure upon TiO<sub>2</sub> addition to alumina/zirconia matrix. Implanted material in critical size defect of the femur was well integrated in the original bone defects and covered

with a layer of soft tissue, as demonstrated by SEM. The details on the femur surface have shown a fibrinous and collagenous matrix extensively connected with the three-dimensional porous structure after the first 3 weeks (Fig.1). As shown by the EDAX spectra, calcium/phosphate ratio varies from 1.5 (after 3 weeks) to 2.1 (after 6 weeks). No signs of inflammatory reactions, such as necrosis or reddening suggesting implant rejection, were found upon histological examination. The periosteal and the endosteal regions were completely closed, with new blood capillaries around the implant site.

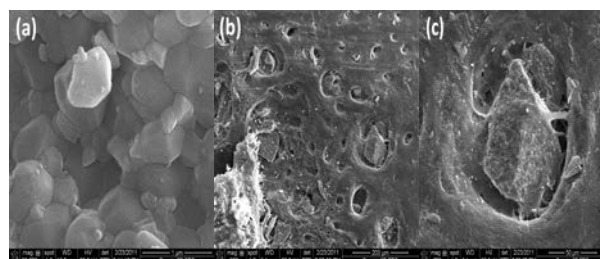


Fig. 1: SEM images recorded on the surfaces of (a) Al<sub>2</sub>O<sub>3</sub>-ZrO<sub>2</sub>-TiO<sub>2</sub> composite prior to the *in vivo* experiment; (b) and (c) rat femur 3 weeks after surgery showing the details of osseointegration.

**DISCUSSION & CONCLUSIONS:** The recently developed alumina-zirconia composites showed a good biological tolerance as demonstrated by *in vivo* test. These promising results recommend them for clinical applications in arthroplasty.

**REFERENCES:** <sup>1</sup> B. Ben Nissan, A.H. Choi, R. Cordingley (2008) 'Alumina ceramics' in *Bioceramics and their clinical applications* (ed T. Kokubo) Woodhead Publ, pp. 223-42. <sup>2</sup> S. Cavalu, V. Simon, C. Ratiu et al (2012) *Key Eng Mater* **493-494**:1-6.

**ACKNOWLEDGEMENTS:** This work was supported by the Romanian National Authority for Scientific Research CNCS-UEFISCDI, project nr. PNII-ID-PCE 2011-3-0441.

## BonyPid™: A lipid-and-polymer-based novel local drug delivery system Physicochemical aspects and therapy

N. Emanuel, D. Segal, Y. Rosenfeld, O. Cohen, Y.H. Applbaum and Y. Barenholz  
<http://www.polypid.com> PolyPid Ltd, Israel

Bacterial infection of bone may result in bone destruction which is difficult to cure due to poor accessibility to bone of systemically-administrated antibiotic and poor performance of currently available local antibacterial treatments. PolyPid Ltd developed a novel local drug delivery system based on self-assembly of pharmaceutically approved lipids and polymers that encapsulate doxycycline (Doxy). The formulation is self-assembled lipid matrix via the interaction of the lipids (cholesterol and synthetic phospholipids) and biocompatible - biodegradable polymer (poly-lactic-co-glycolic). The entrapped Doxy is located within the anhydrous environment and therefore fully protected from long-term water-exposure-related degradation. The fine coating of the tricalcium phosphate (TCP) bone filler by this Doxy-containing formulation (BonyPid™) is capable of releasing intact and active drug at zero-order kinetics for a predetermined period of up to 30 days.

The coating of the TCP granules with the polymer-lipids-Doxy formula (BonyPid™) did not change the granules' macroscopic shape, but altered its color from white to pale yellow, which resemble the color of the entrapped Doxy. The average sizes of the non-coated TCP granules and the coated granules BonyPid™ were similar, as determined by measuring the widest dimension of each granule ( $1135 \pm 241 \mu\text{m}$  and  $1072 \pm 242 \mu\text{m}$ , respectively,  $P=0.16$ ). The MIC for Doxy that was released from BonyPid™ at different time points was similar to the non-encapsulated Doxy, suggesting full bioavailability of the released drug. BonyPid™ formulation structure was characterized by different physical methods including X-ray diffraction, differential scanning calorimetric (DSC), SEM. The wide angle X-ray analyses (WAXS) of BonyPid™ samples show a strong signal in the range of  $1.3-1.8 \ 2\theta^\circ$ , suggesting that the polymer and lipid TCP coating is a highly organized substructure.

The principle lipid in BonyPid™ formulation is phosphatidylcholine, which constitutes more than 85% of the overall lipid mass. It was found that the length of the acyl chains (14, 16 and 18 carbons, respectively) can significantly alter the release rate of Doxy during the prolonged (30 days), zero-order release phase, a, but did not alter the release profile.

The anti-infection activity of BonyPid™ was tested in the rabbit tibia model contaminated with  $5 \times 10^5$  *S. aureus*. Both acute and chronic infection models were tested. Only BonyPid™ treatment demonstrated a statistically significant reduced bone absorption over the infected group ( $P < 0.04$  for day 7, 14 and 21) and significantly lower bacterial bone concentration ( $p > 0.05$ ) on day 21 following the bone grafting and the bacterial inoculation. In addition it was found that the antibiotic coating of the bone-filler in BonyPid did not reduce bone hilling as compared to free bone-filler.



Therefore a clinical evaluation is proposed for testing the efficacy and toxicity of BonyPid™ for therapy of both acute and chronic bacterial bone infections.

## Transcriptomic analysis of postnatal maturation in articular cartilage *in vitro*: evidence for subchondral bone – cartilage crosstalk

CR Fellows<sup>1</sup>, BA Evans<sup>2</sup>, IM Khan<sup>1</sup>, CW Archer<sup>1</sup>

<sup>1</sup> *Pathophysiology and repair division, School of Biosciences, Cardiff University, Wales.*

<sup>2</sup> *Department of Child Health, School of Medicine, Cardiff University, Wales*

**INTRODUCTION:** Postnatal articular cartilage is relatively unstructured; with a high chondrocyte density and cells distributed evenly throughout the tissue. In the months following birth, the articular cartilage starts the transformation to mature tissue, developing distinct zonal stratification and establishing high matrix to cell volume ratio. This forms a highly organised and specialised tissue capable of free articulation and able to withstand dynamic loading. We have previously shown that a combination of FGF-2 and TGF- $\beta$ 1 induces profound morphologic changes in immature articular cartilage, consistent with a highly accelerated postnatal maturational response<sup>1</sup>. Next generation transcriptome sequencing (NGS) of cartilage having undergone this process has identified key factors and pathways involved in regulating maturation progression. Here, we describe an increase in subchondral bone and cartilage intercommunication, shown to regulate matrix mineralization that ensures tissue homeostasis.

**METHODS:** Hyaline cartilage was harvested from the metacarpophalangeal joint of 7-day-old immature bovine steers. Eight mm full-depth biopsies were dissected and cultured in DMEM + insulin transferrin selenium (ITS) in the presence or absence of TGF- $\beta$ 1 (10 ngml<sup>-1</sup>) & FGF-2 (100 ngml<sup>-1</sup>) for 21 days. RNA was extracted and purified using RNeasy™ kit prior to processing for NGS on the SOLiD S4s platform. RNA-seq reads were aligned to the bovine genome using ‘Tophat’. The raw gene counts were normalized to ERCC spiked internal controls and then analysed using the ‘DeSeq’ package<sup>2</sup> in the ‘R’ statistical software, isolating statistically significant differentially expressed genes and calculating fold change. Pathway analysis of significant genes was executed using ‘David’ gene ontology software.

**RESULTS:** Analysis of NGS data evaluated through ‘DeSeq’ showed that transcript levels of many genes shown to affect osteoclast, osteoblast and osteocyte function were modulated during cartilage maturation. Osteoprotegerin, the RANKL decoy receptor, showed a 43-fold increase in expression during maturation. Osteoglycin,

implicated in ectopic bone formation, exhibited a 5-fold decrease during maturation. Matrix extracellular phosphoglycoprotein precursor (MEPE) was found to have a 9-fold decrease during maturation. MEPE is shown to induce bone growth and mineralization via action on osteoblasts and osteoclasts.

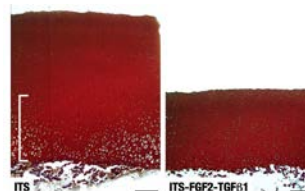


Fig. 1: Safranin-O staining of cartilage explants cultured for 21 days in DMEM +ITS (control) or in DMEM + ITS + FGF-2 & TGF- $\beta$ 1 (precocious maturation), showing ~50% reduction in thickness.

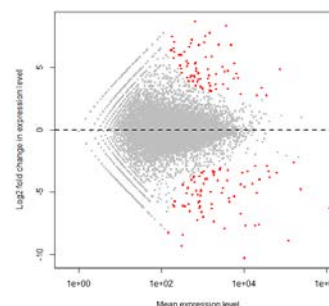


Fig. 2: Scatter plot of change in expression of genes in bovine articular cartilage after induction of maturation. Significant genes are shown in red.

**DISCUSSION & CONCLUSIONS:** During accelerated maturation of articular cartilage, factors regulating bone formation, mineralisation, resorption and mechanosensing are expressed. These factors may maintain a homeostatic border between the subchondral bone and cartilage matrix; preventing both ectopic bone formation and bone diminution during a period of dynamic tissue remodelling.

**REFERENCES:** <sup>1</sup>IM. Khan, SL. Evans, RD. Young et al. (2011) *Arth & Rheum* **63**:3417-27. <sup>2</sup>S. Anders and W. Huber (2010) *Genome Biology* **11**:R106-118 **ACKNOWLEDGEMENTS:** NGS was performed by the CGR, University of Liverpool. We are grateful to ARUK for funding (ARUK: 188771).

## In vivo evaluation of titanium macro-porous structures manufactured through an innovative powder metallurgy approach

[R. Ferro de Godoy<sup>1</sup>](#), [G. Blunn<sup>1</sup>](#), [M. Coathup<sup>1</sup>](#), [A. Goodship<sup>1</sup>](#)

[Institute of Orthopaedics and Musculoskeletal Science, University College London, Royal National Orthopaedic Hospital, Stanmore, UK;](#)

**INTRODUCTION:** Macroporous metal structures are emerging as a very powerful strategy to achieve a tough and time resistant bone fixation in orthopaedic components. This study explored the hypothesis that the osseointegration potential of two macroporous titanium surfaces obtained using an innovative powder metallurgy process suitable for manufacturing Functionally Graded Materials (FGM) devices was equivalent to osseointegration of conventional and new plasma sprayed surfaces.

**MATERIALS & METHODS:** Four different FGM specimens have been produced (Eurocoating Spa, Ita) by Spark Plasma Sintering (SPS) selectively coupling layers of: Ti macroporous structure with pores  $\varnothing$ : 400-600 $\mu$ m (TiMac400); Ti macroporous structure with pores  $\varnothing$ : 850-1000 $\mu$ m (TiMac850); fully dense Ti6Al4V; fully dense CoCrMo. Ti macropores are impregnated with Hydroxyapatite (HA). For comparative purposes two different clinically used Plasma Spray surfaces (Eurocoating Spa, Ita) were used: Ti-Growth<sup>®</sup>, an innovative macroporous Vacuum Plasma Spray coating and a Air Plasma Spray coating. For histological evaluation 4 groups of block implants (6x8x15mm) with different layer sequences from solid base to highly porous were used. Each surface was tested twice: once placed over a Ti-alloy substrate and once onto a CoCr bulk. For push out test 4 groups of cylindrical implants (4x8 mm) one for each different surface were used. Implants were placed in both medial femoral condyles in 24 sheep, two specimens per condyle (one for histology and one for push out test). Samples were explanted at four and eight weeks after surgery. Push-out loads were measured using a Material Testing System. Bone contact and ingrowth were measured by histomorphometry. Statistical analysis was performed.

**RESULTS:** Histological images showed early osteointegration for all the surfaces tested at 4 weeks. At 8 weeks both Ti macropores structures and Ti-Growth<sup>®</sup> allowed deep bone ingrowth and extended colonization by newly formed bone (Fig.1). The plasma spray surfaces had best performance regarding bone-implant contact. Among the SPS porous surfaces the TiMac400/Co-Cr dense and TiMac400/Ti-alloy dense had a better

bone contact and ingrowth. It was also observed a very good integration of newly formed bone and residual HA in deep Ti pores (Fig. 2). Bone Push-out test: all surfaces were well integrated with host tissue for both observation times.

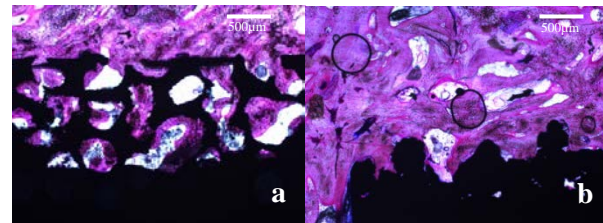


Fig. 1: Histology of a) TiMac400 and b) TiGrowth<sup>®</sup> macro porous surfaces with bone ingrowth at 8 w.

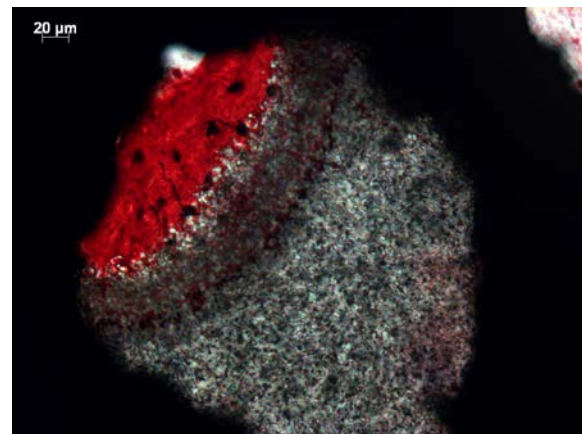


Fig.2: Bone (red)–HA (grey)–Ti (black) e.g. for bone integration inside SPS porous surfaces (TiMac400)

**DISCUSSION AND CONCLUSION:** It has been recognised that plasma spraying can also produce highly porous titanium surfaces with open and interconnected pores, which can vastly improve bone ingrowth characteristics [1, 2]. In this study, we could conclude that the plasma spray surfaces have a better bone-implant contact. Further more, the SPS porous surfaces HA impregnated allow a deeper integration bone-implant. Also the different metal substrates did not affect or delay bone colonization inside the applied porous structures.

**REFERENCES:** <sup>1</sup>D. Chen et al. (2011) *J Orthop Surg Res* 6: 56. <sup>2</sup>J. E. Biemond et al. (2012) *J Biomater Appl* 7: 26.

**ACKNOWLEDGEMENTS:** Study part of Space-Cups Project cosponsored by Prov. Aut. Trento, It.

## Porous metallic implants of Ti-13Nb-13Zr alloy

T S Goia<sup>1</sup>, K B Violin<sup>1</sup>, J C Bressiani<sup>1</sup>, A H A Bressiani<sup>1</sup>

<sup>1</sup> *Nuclear and Energy Research Institute, IPEN – CNEN/SP, São Paulo, Brazil*

**INTRODUCTION:** Biomaterials based on titanium and its alloys are widely used in dentistry and orthopaedics surgery due to their excellent mechanical properties and biological interaction. However, there are problems associated with the use of titanium as implant material. The high Young's modulus value when compared to the surrounding bone can cause problems of stress and subsequent dislocation of the implant<sup>1</sup>. To solve this problem have been developed osteoconductive porous materials for bone regeneration. One advantage in using materials with porous structure is the ability to allow a biological anchorage of surrounding tissues via bone ingrowth through the pores. Furthermore, the elastic modulus value can be adjusted between implant and trabecular bone values to match each other, thereby preventing bone resorption in the implant interface<sup>2</sup>. The Ti-13Nb-13Zr alloy studies has been developed due to its low elastic modulus combined with high values of mechanical strength and corrosion, compared to commercially pure titanium, besides its full biocompatibility<sup>3</sup>.

**METHODS:** The Ti-13Nb-Zr alloy was obtained by mixing metal powders of Ti (268496, Sigma-Aldrich), Nb (262722, Sigma-Aldrich) and Zr (403296, Sigma-Aldrich) in stoichiometric proportions of the alloy. Dense samples of Ti-13Nb-13Zr alloy were studied as a control group for comparative purposes. The technique used to obtain porosity involves mixing the metal powder suspension, consisting of water and natural polymers (starch from corn, potato, rice and gelatin). The ratio of polymer used was 16% by weight of the total solids in 1g/mL of hot water. Immediately after filling the mold with the formed slurry, it was frozen for 12 hours. After this stage, the samples were placed in a kiln (38 °C) prior to heat treatment (350 °C/1h) and sintering (1300 °C/3h). The samples were tested for cytotoxicity and for in vivo behaviour in rabbits (New Zealand White).

**RESULTS:** By X-Ray diffraction (XRD) analysis were observed the presence of  $\alpha$  and  $\beta$  phases and by scanning electron microscopy (SEM) were observed the homogeneity in the microstructure. The values for mean particle diameter of natural polymers and the final implants porosity are shown

in Table 1. No sample showed cytotoxicity in the test, enabling their use *in vivo*. After 7 weeks of repairing time, the rabbit's tibia with the implanted porous metallic material, showed good repair and penetration of bone tissue inside the pores.

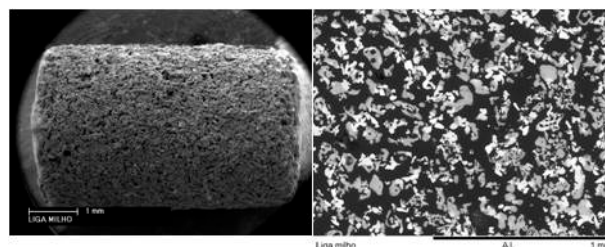


Fig. 1: Image of implant roughness surface, homogeneous microstructure and porosity.

Table 1. Mean particle diameter of the natural polymers and implants porosity.

	Particle size ( $\mu\text{m}$ )	Porosity (%)
Corn starch	16	61
Rice starch	11	62
Potato starch	55	64
Gelatin	225	68

**DISCUSSION & CONCLUSIONS:** Despite the high porosity, crystalline phases  $\alpha$  and  $\beta$  form the Widmanstätten structure proving the good diffusion of  $\beta$  stabilizing elements of the Ti-13Nb-13Zr alloy. The methodology provided materials with high porosity and no contamination from the process. The obtained interconnected porosity of the implants, by this process, allowed bone ingrowth into and through the pores.

**REFERENCES:** <sup>1</sup> J.P. St-Pierre, M. Gauthier, L.P. Lefebvre, et al (2005) *Biomaterials* **26**:7319-28. <sup>2</sup> J.P. Li, S.H. Li, C.A.V. Blitterswijk, et al (2005) *J Biomed Mat Research* **73A**: 223-33. <sup>3</sup> F.A. Müller, M.C. Bottino, L. Müller, et al (2008) *D Materials* **24**: 50-56.

**ACKNOWLEDGEMENTS:** CNPq (Conselho Nacional de Desenvolvimento Científico e Tecnológico) and FAPESP (Fundação de Amparo à Pesquisa do Estado de São Paulo).

## Osteogenic potential of ovine bone marrow stem cells

EM Haddouti<sup>1</sup>, TM Randau<sup>1</sup>, FA Schildberg<sup>2</sup>, DC Wirtz<sup>1</sup>, S Gravius<sup>1</sup>

<sup>1</sup> [Department of Orthopedics and Trauma Surgery, University of Bonn, Germany](#) <sup>2</sup> [Institutes of Molecular Medicine and Experimental Immunology, University of Bonn, Germany](#)

**INTRODUCTION:** Mesenchymal stem cells (MSCs) have significant potential for the development of cell-based therapeutics for tissue regeneration. Sheep have been used as a large animal models in orthopaedic research, for they are considered livestock animals, easy and cheap in their upkeep and suitable for biomechanical studies as well. Ovine MSCs, however, are poorly characterized and varying results have been reported. Therefore, the current study aimed to establish the isolation, cultivation and characterization of ovine bone marrow MSCs (oBMSCs), and to investigate their osteogenic differentiation potential.

**METHODS:** Animal experiments were approved by the local authorities. Full bone marrow was aspirated from the tuber ischiadicum of 3 young adult female merino sheep (2 to 3 years of age). Mono-nucleated cells were separated via Ficoll gradient centrifugation, and plated in DMEM containing 10% FCS. Non-adherent cells were removed after three days by washing. Adherent oBMSCs were cultured and expanded in DMEM and split and passaged upon confluence. oBMSCs were tested for their immunomodulatory capacity in a sheep lymphocyte proliferation assay. Cells of passage three or four were treated with standard osteogenic, chondrogenic and adipogenic induction media, and their differentiation potential was approved by the corresponding staining.

**RESULTS:** The isolated oBMSCs were proliferating and showed the typical MSCs phenotype. The proliferation of activated ovine lymphocytes was efficiently suppressed by oBMSCs in the lymphocyte proliferation assay. The adipogenic induction showed large fat vacuoles already after 10 days and was stained with Oil Red O. Chondrogenic differentiation in pellet culture showed positive but weak staining for glucosaminoglycans. The osteogenic differentiation was evaluated via positive ALP activity and Alizarin Red S staining.

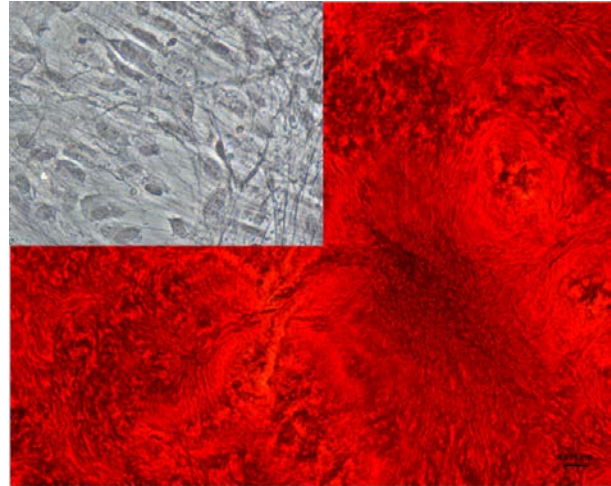


*Fig. 1: Alizarin Red Staining of osteogenic differentiated oBMSCs after 4 weeks of induction. Inset on the top left shows undifferentiated control. Scale bar represents 10  $\mu$ m.*

**DISCUSSION & CONCLUSIONS:** oBMSCs could be consistently isolated from full bone marrow of adult merino sheep with only slight modifications to standard protocols. The cells were able to differentiate into the three cell lineages and had immunomodulatory capacities. Further investigations, including FACS for surface markers and PCR are necessary to validate oBMSCs in comparison to the well characterized human and murine MSCs in order to further establish the ovine large animal model for cell based bone regeneration in orthopaedics.

**ACKNOWLEDGEMENTS:** This project was funded by the University of Bonn BONFOR grant and by industrial partners Peter Brehm GmbH, Weisendorf, Germany and Artoss GmbH, Warnemünde, Germany

## Histometry and histomorphology of bone reactions after human sinus floor augmentation with Bio-Oss® or Endobon®

D Hahn<sup>1</sup>, E Luvizuto<sup>2</sup>, H Plenk Jr<sup>1</sup>, M Weinlaender<sup>3</sup>

<sup>1</sup>Bone & Biomaterials Res., Medical University of Vienna, Austria. <sup>2</sup>Dept.Surgery & Integrated Clinic, Araçatuba Dental School, UNESP-Univ Estadual Paulista, Brazil. <sup>3</sup>Private Dental Practice, Vienna, Austria

**INTRODUCTION:** Augmentation of the atrophic maxillary sinus floor prior to endosseous dental implant placement is a well documented method. Over the last decade, deproteinized bovine bone mineral (Bio-Oss®, Geistlich Biomaterials) has emerged as the material of choice for most of the clinicians. The aim of this maxillary sinus augmentation mirror study was to compare the amounts of new bone generated with Bio-Oss® to another bovine bone-derived material (Endobon® - Biomet 3i), produced by a high-temperature sintering process.

**METHODS:** In a prospective and controlled multicenter study [1] a total number of 94 sinus augmentation procedures (38 unilateral/28 bilateral) were performed in 66 patients by the „lateral window technique”. One of the two bovine bone-derived bone substitute materials (Bio-Oss®, Geistlich Biomaterials, 0.25-1.0 mm granulate) or (Endobon®, Biomet 3i, 0.5-1mm granulate) was used according to randomization. After six months healing trephine biopsies (2 mm inner/3 mm outer diameter) were retrieved before implant placement. Only eight of the retrieved biopsies were processed in HP’s laboratory, and Giemsa-surface stained undecalcified ground sections were prepared for histomorphological and histometrical evaluation. For histometry digital micrographs were taken at 40x magnification and merged to overview images. Under microscopic control, new bone (NB) and bone substitute particles (BS) were identified, demarcated and false colour labelled, using Adobe Photoshop® CS5. On TIFF-images, the region of interest ROI (excluding the original sinus floor), area %NB and %BS per ROI, and BS surface% with NB contact were measured in NIS-Elements AR 3.2 (Nikon Laboratory Imaging Inc.), and calculations made with MSOffice Excel.

**RESULTS:** Light microscopy of Bio-Oss® shows orderly lamellar bone structures with osteons and clearly visible empty osteocyte lacunae. The Endobone® particles have a more “ceramic” granular structure, but also empty osteocyte lacunae and former Haversian canals are visible.

On both materials direct new bone apposition and growth into Haversian canals is visible (Fig.1), but no obvious signs of BS resorption.

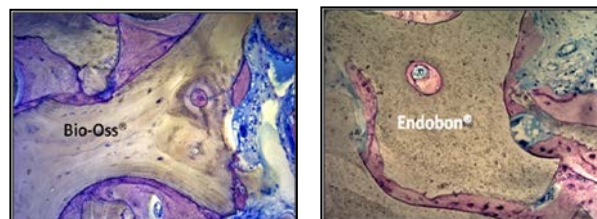
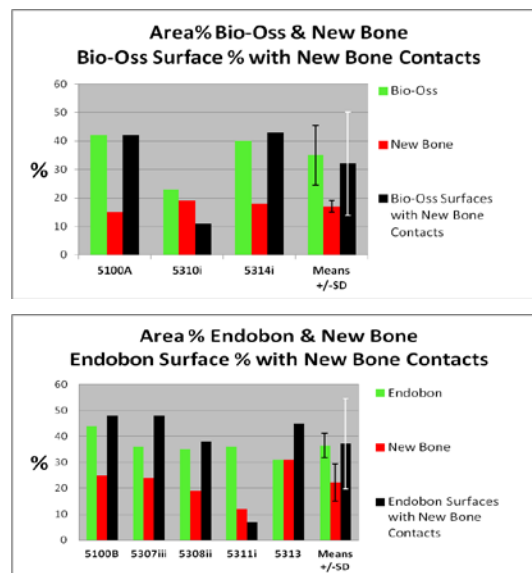


Fig.1: Details (100xmagn.) from Giemsa-surface stained ground sections show direct apposition of purple stained new bone to Bio-Oss® and Endobon® granulate surfaces.



**DISCUSSION & CONCLUSIONS:** Histometry demonstrated in this study that both bone substitute materials have similar “biological profiles” with regard to area% new bone formation and surface% contacts. However, histometric data varied greatly between biopsies of the same group, or even between sections of the same biopsy, making statistical significance calculations so far pointless.

**REFERENCES:** <sup>1</sup> M.Weinlaender, G.Krennmair, S.Schmidinger, W.Lill, H.Plenk Jr (2011) 20th Ann.Meet. EAO, Athens, P 341.

**ACKNOWLEDGEMENTS:** This study was sponsored by Biomet 3i, USA.

## Combined microCT, LM and BSE-SEM evaluation of a trephine bone biopsy after human extraction-socket filling with Bio-Oss-Collagen®

AN Herdina<sup>1</sup>, [B Metscher](#)<sup>1</sup>, D Gruber<sup>2</sup>, D Hahn<sup>3</sup>, J Lederer<sup>4</sup>, [H Plenk Jr](#)<sup>3</sup>

<sup>1</sup>Theoretical Biol. and <sup>2</sup>Cell Imaging & Ultrastruct., Univ. Vienna. <sup>3</sup>Bone & Biomaterials Res., Medical University of Vienna <sup>4</sup>Private Dental Practice, Vienna, AUSTRIA

**INTRODUCTION:** After tooth extraction, the alveolar bone bed for future dental implants can be preserved by augmenting socket healing with various bone substitute materials. The resulting bone reaction can be microscopically evaluated on trephine biopsies retrieved before dental implant insertion. Such biopsies should be processed undecalcified and preferably within the trephine drill to avoid fragmentation. This case study presents the combination of initial non-destructive microCT imaging with light and scanning electron microscopy of consecutive surface-stained ground sections of the biopsy and metallic drill for qualitative and quantitative evaluation of bone reactions to a deproteinized bovine bone mineral plus collagen substitute material.

**METHODS:** After root fracture, tooth #22 had been extracted in a human patient (f, 40 yrs) and the socket completely filled with blood-soaked Bio-Oss-Collagen® (Geistlich, Switzerland). At implant insertion after 8 months a biopsy was taken with a trephine drill (Ø 3mm), fixed in Schaffer's and embedded in PMMA. Top and bottom walls of the trephine drill were cut off (Buehler Isomet® diamond saw), leaving an about 2mm thick light and X-ray penetrable specimen block for further processing and evaluation. After high-resolution microCT imaging (Xradia MicroXCT), repeated grinding and polishing exposed consecutive layers for Giemsa-surface staining which were then evaluated by transmitted light microscopy (LM), and by backscattered electron scanning microscopy (BSE-SEM, Philips XL20®) after carbon-sputtering. New bone formation on and between bone substitute granulates was quantified by computerized histometry (Adobe Photoshop® CS5, NIS-Elements AR 3.2).

**RESULTS:** Despite artefact zones caused by the metallic trephine drill side walls, the microCT scan of the central core of the biopsy revealed images correlating well with the ground section surfaces in the LM and BSE-SEM evaluations (Fig.1, a-c). Based on this correspondence new bone and Bio-Oss® granulate signal intensities were manually

segmented in the microCT-images for more accurate representation and volumetry in the biopsy. Mainly lamellar new bone formation had started from the apical alveolar wall and partially infiltrated the augmented area (Fig.1d), but only 25% of the Bio-Oss® surfaces showed new bone contacts. The empty-appearing spaces on BSE-images (Fig.1c,d) were filled with a sparsely vascularised fibrous connective tissue.

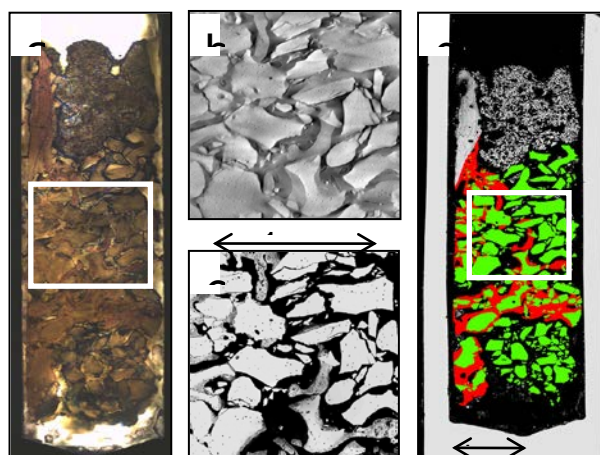


Fig. 1: a) Giemsa surface-stained ground section of the whole trephine biopsy. The white rectangles represent the area depicted by microCT(b) and BSE(c). On the BSE-overview image (d) Bio-Oss® is false-colour labelled in green, new bone in red.

**DISCUSSION and CONCLUSIONS:** MicroCT scanning before preparation of ground sections offers the advantage of 3D information about the new bone and bone substitute material contents of a trephine biopsy, which can be correlated with 2D information from conventional ground sections. The better structural preservation of the biopsy material within the trephine drill compensates for the minor impairment of microCT imaging by the metal. The Bio-Oss®-collagen in this case did not lead to an impressive augmentation of bone healing in the socket, which adds to the dispute about the merits of bone substitutes in this application.



## Nanofibrous scaffolds for bone tissue engineering

S-h Hsu<sup>1</sup>, Y-C Wang<sup>1</sup>, S Huang<sup>1</sup>

<sup>1</sup>*Polymer Science and Engineering, National Taiwan University, Taiwan, ROC*

**INTRODUCTION:** Extracellular matrix (ECM) plays an important role in cell attachment, growth, migration, and differentiation. Biofunctional materials that mimic the ECM are considered more favorable in tissue engineering. ECM-like collagen nanofibrous scaffolds that provide the structure of a native environment may improve the attachment, proliferation and compactness of mesenchymal stem cell (MSCs). A thermal-induced phase separation (TIPS) system with solvent exchange have been developed to prepare for nanofibrous scaffolds from poly(L-lactide) (PLLA) [1]. Here we described a novel system to fabricate nanofibrous membranes and scaffolds from poly(D,L-lactide) (PLA), poly( $\epsilon$ -caprolactone) (PCL), and poly(lactide-co-glycolide) (PLGA). The system may be applied to a wide type of general biodegradable polymers without heating the polymer solution. The mouse pre-osteoblasts (MC3T3-E1 cells) and human bone marrow-derived mesenchymal stem cells (hBM-MSCs) were utilized to examine the potential of these membranes and scaffolds to promote bone tissue engineering.

**METHODS:** A novel system that employed two solvents was developed to induce phase separation and fabricate PLA membranes with different nanostructures. PLA was dissolved in 1,4-dioxane and dimethylacetamide (DMAc) with a PLA/1,4-dioxane/DMAc weight ratio of 10/45/45 to form the polymer solution.

To make nanofibrous membranes or scaffolds with fiber diameter <100 nm, the solution was cast on the glass substrate or a mold immediately placed at -196°C (gelation temperature) to induce phase separation and then immersed into -20°C ethanol coagulant to achieve solvent exchange. Resulting membranes were washed with deionized water and lyophilized. The control microporous membrane was made by the dissolving PLA in 1,4-dioxane (10/90), cast and immersed into 25°C ethanol. Resulting membranes were washed and lyophilized.

The membranes and scaffolds (1.5 cm diameter, each 400  $\mu$ m and 3 mm thick) were examined by scanning electron microscopy. For cell studies, the membranes were seeded with mouse pre-

osteoblasts (MC3T3-E1 cells,  $5 \times 10^4$  cells per membrane) and scaffolds were seeded with Human bone marrow-derived mesenchymal stem cells (hBM-MSCs,  $1.5 \times 10^6$  cells per scaffold), in 24-well culture plates with  $\alpha$ -MEM containing 10% fetal bovine serum supplemented with 100 U penicillin and 1,000 U streptomycin at 37°C in a 5% CO<sub>2</sub> incubator. All culture medium used in this study was the basal medium without osteogenic induction additives. The culture medium was refreshed every two days before analyses of calcium and collagen deposition.

**RESULTS:** The structure of the scaffolds is shown in Figure 1 with the average fiber diameter ~67 nm. For membranes seeded with pre-osteoblasts for 14 days, the nanofibrous membranes had calcium ~0.15  $\mu$ g/cell vs. ~0.04  $\mu$ g/cell for microporous membranes. The total collagen was about 50% more for nanofibrous membranes. For scaffolds seeded with hBM-MSCs for 21 days, each nanofibrous scaffold had calcium ~29  $\mu$ g vs. ~11  $\mu$ g for each microporous scaffold. The total collagen was ~70% more for nanofibrous scaffolds. The expression of alkaline phosphatase, type I collagen and osteocalcin genes also confirmed the significantly greater extent of osteogenesis in the nanofibrous scaffolds.

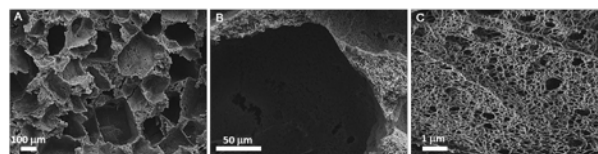


Fig. 1: Images of nanofibrous PLA scaffolds.

**DISCUSSION & CONCLUSIONS:** We have developed a new method to generate nanofibrous scaffolds from PLGA, PLA or PCL. The potential of PLA nanofibrous scaffolds in bone tissue engineering was tested. Results showed that these nanofibrous scaffolds could induce MSC osteogenesis in the absence of induction medium.

**REFERENCES:** <sup>1</sup> GB Wei, PX Ma (2009). Partially nanofibrous architecture of 3D tissue engineering scaffolds. *Biomaterials*. **30**:6426-34.

## Hydroxyapatite/pva-nocc bilayered scaffold for possible use in osteochondral Tissue-Engineering

T Kamarul<sup>1</sup>, M Hamdi<sup>2</sup>, A Amir<sup>1</sup>, W M Ng<sup>1</sup>, N Yusof<sup>3</sup>, L Selvaratnam<sup>4</sup> and G Krishnamurthy<sup>1</sup>

<sup>1</sup> Tissue engineering group (TEG), Department of Orthopaedic Surgery, Faculty of Medicine, University of Malaya, 50603 Kuala Lumpur. <sup>2</sup> Department of the Design and Manufacture, Faculty of Engineering, University of Malaya, 50603 Kuala Lumpur. <sup>3</sup> Malaysian Nuclear Agency, Ministry of Science, Technology & Innovation, Bangi, Malaysia. <sup>4</sup> School of Medicine and Health Sciences, Monash University Malaysia, Petaling Jaya, Malaysia.

**INTRODUCTION:** The use of biodegradable scaffolds has been suggested as an important option in the treatment of osteochondral defects. Earlier studies have shown that these materials provide a supportive matrix that encourages the in-growth of cells and tissues. However, scaffold materials must fulfill specific requirements with respect to the demands of mechanical stability and biocompatibility. Implants manufactured from hydroxyapatite are widely used in orthopaedic applications and seems to be appropriate for subchondral bone reconstruction in terms of their mechanical properties. The purpose of this study is to determine if a bi-layered scaffold containing hydroxyapatite (HA) and hydrogel (PVA/NOCC) can be used as a possible construct for treating osteochondral defects when used with mesenchymal stem cells *in vitro*.

**METHODS:** Bi-layered composite scaffolds were constructed from HA and PVA/NOCC using fibrin sealant. Biomechanical test was conducted by assessing the compression endurance of scaffolds. Human bone marrow derived MSCs (hMSC) were isolated, expanded and seeded on the designed bi-layered scaffold. Scaffolds without cells and cells without scaffold were used as controls. These groups were treated with osteogenic and chondrogenic condition medium respectively. Scanning Electron Microscopy was used to characterize the morphologies and microstructures of the scaffold and the attachment of cells on these scaffolds. Alkaline phosphatase (ALP) activity and Glycosaminoglycans (GAGs) concentration were performed at different time points (D3, D6, D9, D12, D15 and D21). Non-parametric analyses were conducted using the statistical software SPSS.

**RESULTS:** An average of 95N force was found as the upper limit for the deforming force of these novel bi-layered scaffolds. SEM images have showed that the cells were well attached onto the construct (figure 1). Significant differences in ALP

and GAG content were observed in controls and bi-layered construct ( $p < 0.05$ ).

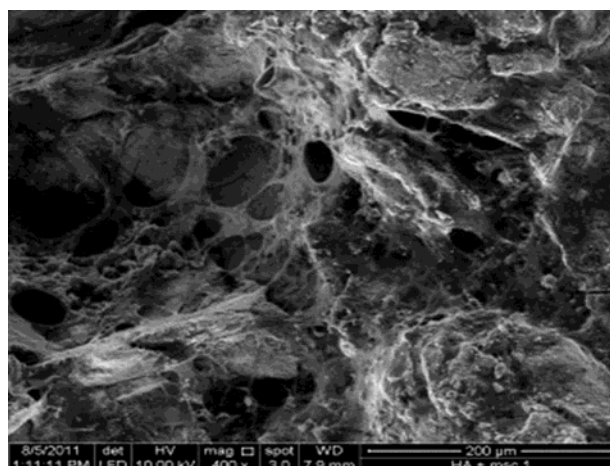


Fig. 1: SEM of osteocytes attached on HA scaffold.

**DISCUSSION & CONCLUSIONS:** HA and hydrogel appear to support cell attachment. ALP and GAG content shows that HA and Hydrogel maintain the phenotype of differentiated osteocytes and chondrocytes in condition media respectively. The ALP and GAGs content in un-supplemented media from construct also indicates differentiated osteocytes and chondrocytes maintain the phenotype. Therefore, the novel designed Bi-layered scaffold may be a suitable scaffold for use in clinical application in the treatment of osteochondral defects.

**REFERENCES:** <sup>1</sup> L. Le Guéhennec, P. Layrolle and G. Daculsi (2004) *European Cells and Materials* 8:1-11.

**ACKNOWLEDGEMENTS:** This research was funded by Fundamental Research Grant Scheme (FP026/2009), UM HIR-MOHE research grant initiative and University Malaya Research Grant (RG144/09HTM).

## Development of a nano-composite drug eluting bone plug enhancing fixation of screws in low quality bone

[U Kettenberger](#)<sup>1</sup>, J Bourgon<sup>1</sup>, R Obrist<sup>1</sup>, B Eng-Kämpfer<sup>2</sup>, S Höck<sup>2</sup>, V Luginbuehl<sup>2</sup>, P Procter<sup>3</sup>, J Arnoldi<sup>3</sup>, T Soerensen<sup>4</sup>, L Pfister<sup>5</sup>, [DP Pioletti](#)<sup>1</sup>

<sup>1</sup>Laboratory of Biomechanical Orthopedics, École Polytechnique Fédérale Lausanne (EPFL), CH.

<sup>2</sup>Institute of Biotechnology, Zürich University of Applied Sciences (ZHAW), CH.

<sup>3</sup>Stryker Trauma, Selzach, CH. <sup>4</sup>Stryker Trauma, Kiel, D. <sup>5</sup>Degradable Solutions, Schlieren, CH.

**INTRODUCTION:** Osteoporosis is a major public health problem in our aging population. Osteoporotic fractures are increasing both in number and severity and the disease also affects the treatment and outcomes. Screw cut-out due to low bone quality is a frequent complication leading to re-operation after fracture fixation<sup>1</sup>. During the last 3 decades, bisphosphonates have become the leading therapy for osteoporosis as this group of drugs is able to increase bone density in osteoporotic patients by inhibiting osteoclast activity<sup>2</sup>.

Our strategy to overcome the problem of insufficient screw anchorage is local delivery of Zoledronate, a potent bisphosphonate, to the bone stock around the screw. A tube shaped composite implant was made from microspheres containing Zoledronate-hydroxyapatite-nanoparticles. This was designed to be inserted into the pilot hole of the screw (Fig. 1). This approach targets improved primary stability of the screw by adding augmentation material and secondary stability due to the effect of the drug.

**METHODS:** Initially, Zoledronate (Enzo Life Sciences) was dissolved in water and absorbed to hydroxyapatite-nanoparticles (Sigma-Aldrich). Microspheres were then produced via a solvent evaporation technique that is described elsewhere<sup>3</sup>. In summary, a polylactide polymer (Resomer® R 203 S, Evonik) was dissolved in chloroform and mixed with the drug-loaded nanoparticles. This suspension was added to distilled water containing 1% polyvinyl alcohol (Sigma-Aldrich) as an emulsifier. After 15 hours of stirring, the resulting microspheres were filtered out of the solution and dried in vacuum. The microspheres were packed into moulds and then thermo-fused in an oven to obtain tube-shaped bone plug implants.

SEM was used to investigate the structure of the bone plugs. Handling and pull-out tests in artificial bone (Sawbones®) were performed to optimize the mechanical properties and the material composition of the bone plugs.

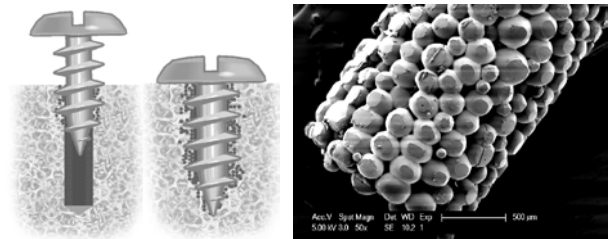


Fig. 1: Schematic illustration of the insertion of the screw into the bone plug in cancellous bone (left), SEM image of a composite bone plug with a diameter of 1.5 mm (right).

**RESULTS:** The SEM investigation showed good distribution of the nanoparticles in PLA and homogenous fusion of the microspheres (Fig 1). The heat-fusion technique allowed tailoring of the mechanical properties of the plugs. Through handling tests a balance was found between mechanical strength, which is necessary for plug insertion into bone, and fragility to enable distribution of the microspheres once the screw is inserted. Pull-out tests in artificial bone, with a structure similar to human bone, have shown that the presence of a bone plug improves the pull-out force of a screw by 16.4%.

**DISCUSSION & CONCLUSIONS:** The study demonstrates the feasibility of a new drug eluting nano-composite bone plug intended to improve both primary and secondary stability of bone screws in low quality bone. The next step will be an animal study using an established rat femur model. Dynamic histomorphometry based on micro-CT scans will provide information about drug release and the bisphosphonate effect *in vivo*.

**REFERENCES:** <sup>1</sup>Lobo-Escolar, A., E. Joven, et al., *Injury* **41**(12): 1312-1316. (2010). <sup>2</sup>Russell, R. G., *Pediatrics* **119** Suppl 2: S150-162 (2007). <sup>3</sup>Shi, X., Y. Wang, et al., *Pharm Res* **26**(2): 422-430 (2009).

**ACKNOWLEDGEMENTS:** This project is kindly supported by CTI (Commission for Technology and Innovation, Switzerland).

## Bone marrow multipotential stromal cell colonisation of natural bone substitute Orthoss® – Osteoconductivity, osteoinductivity and graft expander potential

Dimitrios Kouroupis<sup>1</sup>, Elena Jones<sup>1</sup>, Thomas Baboolal<sup>1</sup>, Peter V Giannoudis<sup>2</sup>

<sup>1</sup> Leeds Musculoskeletal Biomedical Research Unit, Leeds Institute of Molecular Medicine, University of Leeds, Leeds, United Kingdom <sup>2</sup> Academic Unit of Trauma and Orthopaedics, Leeds Institute of Molecular Medicine, Leeds General Infirmary, Leeds, United Kingdom

**INTRODUCTION:** In the Orthopaedic and Trauma discipline, both autografts and allografts have been used for the treatment of impaired fracture healing and the management of critical size bone defects<sup>1</sup>. In spite of its superiority, harvesting of autologous bone grafting has been associated with a number of comorbidities and limited volume availability<sup>2</sup>. For this reason, the concept of ‘graft expanders’ (combining grafts) has been recently popularised to increase the volume and potential biological activity of the implanted material. In addition, new strategies based on autologous multipotential stromal cells (MSCs) seeded on osteoinductive bone substitute scaffolds have been also developed<sup>3</sup>. The aim of this study was to test the properties of Orthoss® granules to support exogenously seeded MSCs as well as to attract neighboring host MSCs, thus serving as a potential graft expander for repairing large bone defects in trauma patients.

**METHODS:** Following ethics committee approval, bone marrow (BM) MSCs (passage 3, p3) harvested from 6 patients admitted for elective orthopaedic procedures were studied for their proliferative and differentiation capacities in 2-D cultures. Bone autograft was also harvested for the purpose of migration experiments. In 3-D cultures, Orthoss® granules (2-4 mm) were seeded dynamically with  $2 \times 10^5$  cells/granule p3 MSCs and further maintained either in MSC expansion or differentiation media for up to 21 days. In homing/migration experiments, bone autografts (size 4 mm) were placed in Matrigel in close proximity to Orthoss® to study cell egress from autografts and their penetration into the Orthoss®. Scaffold colonisation and MSC differentiation were assessed by confocal microscopy, standard electron microscopy, and energy-dispersive X-ray spectroscopy.

**RESULTS:** Cultured cells exhibited morphology, growth kinetics, phenotypic profile and tripotentiality consistent with MSCs. MSC attachment to Orthoss® was donor-independent showing excellent colonisation after both 4 and 7 days (Figure 1). Long-term incubation (21 days) resulted in formation of multiple cell-matrix layers lining the scaffold pores as well as outer surfaces.

MSC differentiation to osteoblasts was evident as strong deposition of Calcium and Phosphorus on the top of cell layers was detected (Figure 1). Importantly, high Orthoss® osteoinductivity was revealed following culture in both MSC expansion and osteogenic conditions. Cell egress experiments demonstrated the migration of cells from neighbouring autografts and their attachment and re-settlement on Orthoss®.

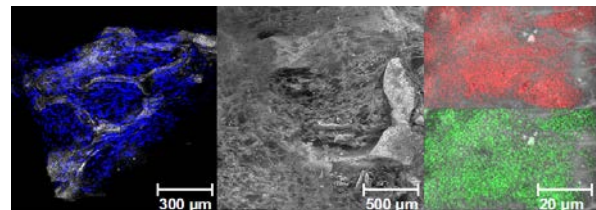


*Fig. 1: MSC colonisation of Orthoss® granules at days 7 (left) and 21 (middle). Calcium (upper right) and Phosphorus (bottom right) deposition by developed osteoblasts on day 21.*

**DISCUSSION & CONCLUSIONS:** Orthoss® scaffolds support MSC attachment, growth and osteogenic differentiation. Furthermore, our *in vitro* 3-D modelling experiments showed that resident bone subpopulations can rapidly migrate towards, attach, and expand on Orthoss® scaffolds. These results indicate that Orthoss® is not only an excellent natural bone substitute material but can be also used as graft expander in the discipline of trauma and orthopaedic surgery in cases where bone regeneration is desirable.

**REFERENCES:** <sup>1</sup> Kinney, R. C., Ziran, B. H., Hirshorn, K., et al. (2010) *Journal of Orthopaedic Trauma* **24**:S52-S55. <sup>2</sup> Giannoudis, P. V., Dinopoulos, H., and Tsiridis, E. (2005) *Injury* **36**:S20-S27. <sup>3</sup> Pittenger, M. F., Mackay, A. M., Beck, S. C., et al. (1999). *Science* **284**:143-147.

## Hydroxyapatite as a possible cell scaffold/ carrier that promotes osteogenic differentiation of adult bone marrow derived Mesenchymal stem cells (bMSCs)

Krishnamurithy<sup>1</sup>, M Hamdi<sup>2</sup>, A Amir<sup>1</sup>, W M Ng<sup>1</sup> and T Kamarul<sup>1</sup>

<sup>1</sup>Tissue engineering group (TEG), Department of Orthopaedic Surgery, Faculty of Medicine, University of Malaya, 50603 Kuala Lumpur. <sup>2</sup>Department of the Design and Manufacture, Faculty of Engineering, University of Malaya, 50603 Kuala Lumpur

**INTRODUCTION:** Hydroxyapatite (HA) has been widely used as a bio-ceramic for bone reconstruction. However, the interactions between HA with bone marrow stromal cells have not been previously elucidated. A study was thus conducted to evaluate the feasibility of using HA as a cell scaffold/carrier that will promote osteogenic differentiation of adult bone marrow derived MSCs for possible bone tissue engineering applications.

**METHODS:** Bovine derived HA scaffolds were prepared using previously described methods. Pore sizes and porosity of HA scaffolds was illustrated using 3-D construction of  $\mu$ -CT slices. Biomechanical tests were conducted to assess the compressive endurance of HA. Isolated bMSCs were seeded to HA scaffold and bone graft at the density of  $10^6$  cells/cm<sup>3</sup>. To compare, monolayered cell density of  $2 \times 10^2$  cells/cm<sup>2</sup> were used. Osteogenic induction was carried out using commercially prepared osteogenic medium. HA scaffold without cells in osteogenic medium served as a control. Scanning electron microscope (SEM) analysis was conducted to observe cell attachment in all the groups except monolayer on plastic surface. As for quantitative analysis, alkaline phosphatase activity was measured at the different time points (D3, D6, D9, D12 and D21). Non-parametric analyses were performed using SPSS software.

**RESULTS:** Pores distribution and 10-300 $\mu$ m pore sizes were observed using  $\mu$ -CT X-RAY images (figure 1). An average of 84N force was found as a deformation force of needed for compressive failure of HA. Significant levels of ALP were expressed from cells seeded on HA and bone graft and, monolayer compared to control group (HA without cells). However, no significant differences were noted between cells seeded on HA and bone graft ( $p > 0.05$ ).

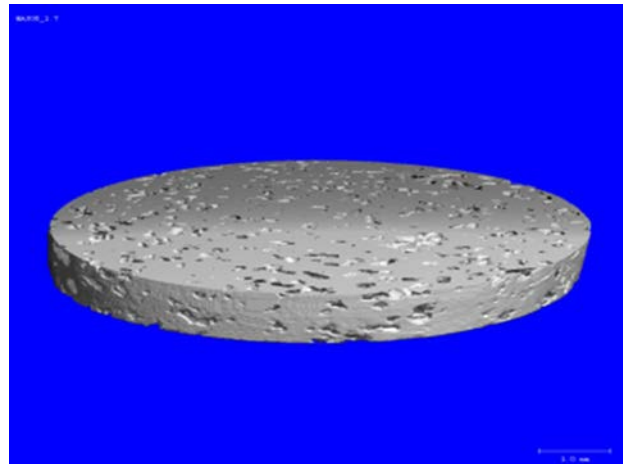


Fig. 1: 3-D  $\mu$ -CT X-RAY analysis to show the distribution of the pores on HA

**DISCUSSION & CONCLUSIONS:** We found that homogenous pores distribution may have allowed the diffusion of nutrient media and gases into the scaffold and excretion of waste by the cells, thereby making this scaffold comparable to natural bone grafts. Pore sizes ranging from 10-300 $\mu$ m provides large surface area for cell attachment and proliferation. SEM images showed excellent cells attachment onto HA, synthetic bone graft and plastic surface. Increase in ALP activity, osteogenic characteristics demonstrated that MSCs were differentiated into osteocytes when attached to the scaffold thereby making this material a potential scaffold for osteogenic differentiation of bMSCs.

**REFERENCES:** <sup>1</sup> C.Y.Ooi, M. Hamdi, S.Ramesh (2007) *Ceramics International* 33:1171-77. <sup>2</sup> J.P. Gleeson, N.A.Plunkett, and F.J. O'Brien (2010) *European Cells and Materials* 20:218-230.

**ACKNOWLEDGEMENTS:** This research was funded by University Of Malaya Postgraduate Research Fund (PS184/2009B & PS418/2010A), HIR-MOHE research grant initiative and University of Malaya Research Grant (RG144/09HTM).

## Response of gingival tissue to high-frequency traction at a rapid rate

[Chun Lei Li](#)<sup>1</sup>, [Hua Xiang Zhang](#)<sup>2</sup>, [Li Ma](#)<sup>2</sup>, [Lin Peng](#)<sup>2</sup>, [Lim Kwong Cheung](#)<sup>2</sup> and [Li Wu Zheng](#)<sup>1</sup>

<sup>1</sup>*Discipline of Oral Diagnosis & Polyclinics,* <sup>2</sup>*Discipline of Oral & Maxillofacial Surgery*

*Faculty of Dentistry, The University of Hong Kong, China*

**INTRODUCTION:** Distraction osteogenesis is an established surgical technique to correct severe bone deformities in orthopedics and maxillofacial regions. Continuous traction has been confirmed to create an optimal biological environment for bone healing.

During mandibular distraction, the attached gingival tissues are also affected by the stretching forces. Some studies have investigated the effect of continuous traction on osteogenesis, the response of gingival tissues to continuous mechanical traction remain unclear.

This study aimed to investigate the response of gingival tissue to continuous traction at a rapid rate using a rabbit model.

**METHODS:** Thirty adult New Zealand white rabbits weighting between 3.4kg to 4.0kg were randomly assigned into intermittent or continuous distraction group, 15 in each. 3-day after osteotomy, mandibular distraction was activated at a rate of 3.0mm/d for 4 days. The frequencies were eight times per second in continuous distraction while once per day in intermitted distraction. Five rabbits in each group were sacrificed at week 2, week 4 and week 12 of consolation period.

Gingival tissue overlying the distraction sites were harvested immediately after sacrifice. All samples were subjected to Hematoxylin and Eosin (HE) staining for histological examination

**RESULTS:** Distracted gingival tissue showed degenerative changes in both groups, characterized by disorganization and thinning of the epithelial layer, breakdown of keratin layer, vacuolation in the stratum granulosum, flattened or loss of rete ridges, cleaved and scattered collagen bundles and stretched blood vessels. Slight recovery by the reorganization of epithelial layer, increasing number and normal shape of rete ridges was observed in continuous group with time. Thickness of the epithelial layer was measured and compared between the two groups but no significant difference was found.

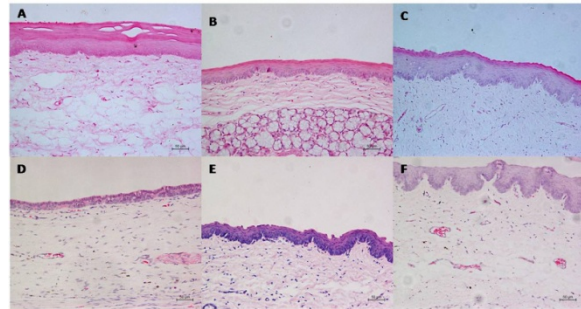


*Fig 1. Histological examination of the distracted gingival tissues (HE staining). A, B and C from continuous group while D, E and F from intermittent group at 2-, 4- and 12- week consolidation, respectively.*

*Table 1. Thickness of epithelial layer in continuous and intermittent distraction groups ( $\mu\text{m}$ ).*

	Continuous	Intermittent
<b>2-week</b>	62.24 $\pm$ 12.26	61.22 $\pm$ 33.60
<b>4-week</b>	67.21 $\pm$ 15.83	61.70 $\pm$ 16.35
<b>12- week</b>	89.69 $\pm$ 18.19	87.37 $\pm$ 12.64

**CONCLUSION:** Gingival tissue shows degenerative changes under rapid distraction. Continuous distraction may improve the regeneration of the attached gingival. Further studies with larger animals which are more similar to human are necessary to test its clinical potential.

**REFERENCE:** <sup>1</sup>K. Kentaro, M. Yutaka, S. Masaru et al (2007) *Oral Surg Oral Med Oral Pathol Oral Radiol Endod* **103(6)**:738-44. <sup>2</sup>B. Kruse-Losler, C. Floren, U. Stratmann et al (2005) *J Clin Peiodontol* **32**:98-103; <sup>3</sup>LW Zheng, L Ma, LK Cheung (2009) *Oral Surg Oral Med Oral Pathol Oral Radiol Endod* **108**:496-9.

**ACKNOWLEDGEMENT:** This project (S-07-76Z) is funded by AO Research Fund of AO Foundation.

## Skeletal site-specific responses to ovariectomy in a rat model

XL Liu<sup>1</sup>, WW Lu<sup>2</sup>, LK, Cheung<sup>1</sup>, LW Zheng<sup>1</sup>

<sup>1</sup>*Faculty of Dentistry, The University of Hong Kong, Hong Kong, China.* <sup>2</sup>*Department of orthopaedics and Traumatology, Faculty of Medicine, The University of Hong Kong, Hong Kong China.*

**INTRODUCTION:** The ovariectomized (OVX) rat is the most widely used animal model in osteoporosis research. The response of different skeletal structures to OVX varies, especially between calvarial bones, jaw bones and long bones.<sup>1, 2</sup> However, the site-specific response has not been fully investigated. This study aims to assess the quantitative and morphological changes of these important bone structures using an OVX induced rat model.

**METHODS:** Twenty-seven mature (age 24 weeks) female Sprague-Dawley rats were randomly assigned to OVX group (n=12) and sham operation group (n=12). Three animals in each group were sacrificed at week 2, week 4, week 12 and week 24 respectively. Three normal rats without any treatment were sacrificed at week 0 to serve as base line. The bone samples of parietal bone, interparietal bone, maxilla, mandible, femur and tibia were collected and subjected to micro-computed tomography (micro-CT) examination. Quantitative analysis and the 3D morphological reconstruction were performed to evaluate the micro-trabeculae.

**RESULTS:** Different skeletal structures showed varied responses to OVX (Fig 1). Noticeable bone loss was observed as early as week 2 in proximal tibia and week 4 in distal femur in OVX group, following with a continuous bone loss till week 24. The trend of bone loss was observed at week 2 in maxilla as well as in mandible, then the bone volume tended to rise to the previous level. In both interparietal bone and parietal bone, the bone volume level was relatively stable during the 24-week observation period.

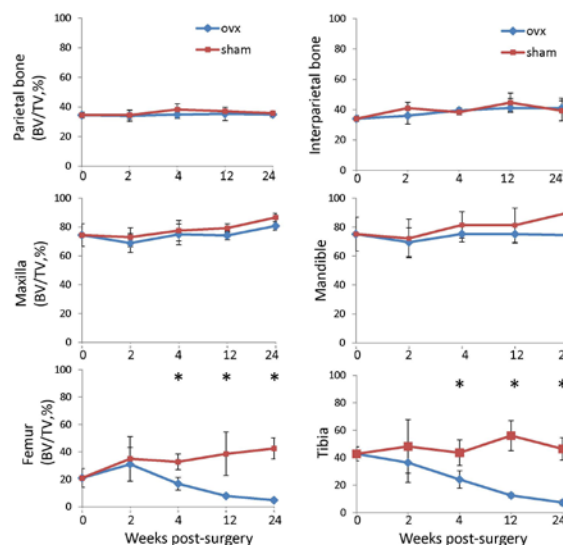


Fig. 1: Bone volume ratio (BV/TV, %) at the parietal bone, interparietal bone, maxilla, mandible, distal femur and proximal tibia. Error bars indicate SD. \*denotes significant difference from sham group (two-sample t test,  $p < 0.05$ )

**DISCUSSION & CONCLUSIONS:** Different skeletal structures demonstrated various responses to OVX in the Sprague-Dawley rat model. The bone structure changes in long bones were much more sensitive to OVX than that in calvarial bones and jaw bones. The present study may provide valuable site-specific index for the selection of appropriate anatomical structure in osteoporotic study.

**REFERENCES:** <sup>1</sup>J.I. Francisco, Y. Yu, R.A. Oliver, and W.R. Walsh (2011) *Relationship between age, skeletal site, and time post-ovariectomy on bone mineral and trabecular microarchitecture in rats.* J Orthop Res 29: 189-196. <sup>2</sup>M. Tanaka, E. Toyooka, S. Kohno, H. Ozawa, and S. Ejiri (2003) *Long-term changes in trabecular structure of aged rat alveolar bone after ovariectomy.* Oral Surg Oral Med Oral Pathol Oral Radiol Endod 95: 495-502.

**ACKNOWLEDGEMENTS:** Seed Funding Programme for Basic Research, The University of Hong Kong.

## Mandibular distraction osteogenesis: Continuous distraction at a rapid rate in the rabbit model

[XL Liu](#)<sup>1</sup>, [HX Zhang](#)<sup>1,2</sup>, [L Ma](#)<sup>1</sup>, [L Peng](#)<sup>1</sup>, [LK Cheung](#)<sup>1</sup>, [LW Zheng](#)<sup>1</sup>

<sup>1</sup>*Faculty of Dentistry, Prince Philip Dental Hospital, The University of Hong Kong, Hong Kong, China.* <sup>2</sup>*Department of Periodontology, School of Stomatology, Wuhan University, Wuhan, China.*

**INTRODUCTION:** Distraction osteogenesis is a widely accepted method of bone lengthening by gradual distraction.<sup>1</sup> Continuous traction is able to promote bone healing by enhancing angiogenesis and osteogenesis at a normal rate.<sup>2</sup> This study was designed to evaluate the response of distraction callus to continuous distraction at a rapid rate using a rabbit model of mandibular lengthening.

**METHODS:** Thirty adult New Zealand white rabbits were randomly assigned to the intermittent and continuous distraction group, with 15 in each. Osteotomy was performed on one side of the mandible. Manual-driven or auto-driven distractor was adopted accordingly afterwards. The distraction was activated at a rate of 3.0 mm per day for 4 days. Five rabbits in each group were sacrificed at week 2, week 4 and week 12 of consolidation, respectively. Plain radiography, micro-computed tomography (micro-CT) and histology examinations were used to evaluate the bone regeneration status.

**RESULTS:** Plain x-ray and histological studies (Fig. 1.) showed more advanced bone healing in continuous distraction group than that in the intermittent distraction group at all the examined time points. Quantitative micro-CT analysis showed significantly higher bone volume in continuous distraction group at week 2 ( $p < 0.01$ ) and week 4 ( $p < 0.05$ ) of consolidation.

**DISCUSSION & CONCLUSIONS:** This study showed that the bone regenerate was remarkably enhanced by continuous distraction, especially at week 2 and week 4 of consolidation. Auto-driven distractor could be a promising clinical alternative to shorten the treatment course of distraction osteogenesis. Further studies to test its clinical potential using large animals which have similar metabolic rate and muscular resistance with human being are necessary.

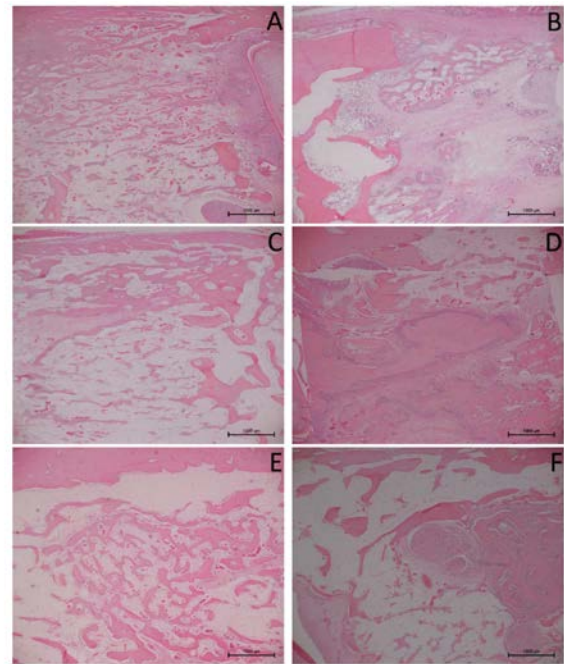


*Fig. 1: Histological section of the distracted regenerates in rabbit mandible (H&E stain). A: continuous distraction group at week 2 of consolidation; B: intermittent distraction group at week 2 of consolidation; C: continuous distraction group at week 4 of consolidation; D: intermittent distraction group at week 4 of consolidation; E: continuous distraction group at week 12 of consolidation; F: intermittent distraction group at week 12 of consolidation.*

**REFERENCES:** <sup>1</sup>G.A. Ilizarov (1989) *The tension-stress effect on the genesis and growth of tissues: Part II. The influence of the rate and frequency of distraction.* Clin Orthop Relat Res: 263-285. <sup>2</sup>L.W. Zheng, L Ma, L.K. Cheung (2009) *Comparison of gene expression of osteogenic factors between continuous and intermittent distraction osteogenesis in rabbit mandibular lengthening.* Oral Surg Oral Med Oral Pathol Oral Radiol Endod 108: 496-499.

**ACKNOWLEDGEMENTS:** Project no. S-07-76Z was supported by the AO Research Fund of the AO foundation.